Charles University in Prague
Faculty of Mathematics and Physics

DOCTORAL THESIS

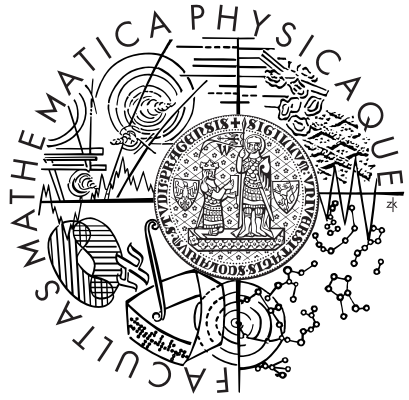

Hana Kouřilová

The study of Dynamic Behaviour and Interactions During the Temperature-Induced Phase Separation in Polymer Solutions

Department of Macromolecular Physics, Faculty of Mathematics and Physics, Charles University in Prague

Supervisor: doc. RNDr. Lenka Hanyková, Dr.

4F 4: Biophysics, Chemical and Macromolecular Physics

Prague 2011

Acknowledgement

I would like to express gratitude to doc. RNDr. Lenka Hanyková, Dr. for her supervision, for the time that she devoted to me and for her open and personal attitude, to doc. Jan Lang, Ph.D. for his valuable and inspiring advices, to Mgr. Pavel Srb who was always willing to help, to all colleagues in the NMR lab for their attitude and creating a friendly atmosphere, to Mgr. Julie Šťastná and RNDr. Jiří Spěváček, DrSc. for their cooperation, to all people in the Department of Macromolecular Physics, to my mum Hana Drápalová who was always encouraging me to follow my dreams and to my uncle Radomír Drápal without whose devoted help it would not be possible, to my friends who are keeping me sane and to Mgr. Karel Kouřil, my dear husband, for his inspiring ideas concerning NMR and for his limitless patience.

This work was supported by the Grant Agency of the Czech Republic (Project 202/09/1281) and the Ministry of Education of the Czech Republic (Project MSM0021620835).

To My Dear Grandparents
Anežka and Radomír
R.I.P.

The treasure lies not in the goal but in the journey itself
— Confucius

I declare that I carried out this doctoral thesis independently, and only with the cited sources, literature and other professional sources.

I understand that my work relates to the rights and obligations under the Act No. 121/2000 Coll., the Copyright Act, as amended, in particular the fact that the Charles University in Prague has the right to conclude a license agreement on the use of this work as a school work pursuant to Section 60 paragraph 1 of the Copyright Act.

In Prague .....

Název práce: Studium dynamického chování a interakcí během teplotně indukované fázové separace v polymerních roztocích

Autor: Hana Kouřilová

Katedra / Ústav: Katedra makromolekulární fyziky, Matematicko-fyzikální fakulta, Univerzita Karlova v Praze

Vedoucí doktorské práce: doc. RNDr. Lenka Hanyková, Dr., Katedra makromolekulární fyziky, Matematicko-fyzikální fakulta, Univerzita Karlova v Praze

Abstrakt: Fázová separace v polymerních roztocích byla studována ^{1}H and ^{13}C spektroskopií NMR vysokého rozlišení na 3 typech polymerních roztoků: i) poly(*N*-isopropylmetakrylamid)/D_2O/ethanol za/bez přítomnosti negativně nabitého komonomeru metakrylátu sodného, ii) statistický kopolymer poly(*N*-isopropylmetakrylamid-*co*-akrylamid) v D_2O, D_2O/ethanolu a D_2O/acetonu a iii) D_2O roztoky polymerních směsí poly(*N*-isopropylmetakrylamid)/poly(*N*-vinylkaprolaktam). V prvním případě jsme studovali tzv. efekt cononsolvency a vliv teploty na fázovou separaci. Byly nalezeny rozdíly mezi mesoglobulemi vzniklými vlivem složení rozpouštědla a teploty. V mesoglobulích vzniklých cononsolvency efektem nebyly detekovány molekuly ethanolu, u teplotně indukované fázové separace kromě molekul vody zůstávají v mesoglobulích navázané i molekuly ethanolu. V případě nabitých polymerů náboj v řetězci zesiluje interakce mezi polymerem a rozpouštědlem. Ve druhém polymerním systému poly(*N*-isopropylmetakrylamid-*co*-akrylamid) bylo zjištěno, že mesoglobule jsou dost porézní a neuspořádané. Sekvence akrylamidových jednotek obklopené sekvencemi isopropylmetakrylamidových jednotek jsou hydratované a pohyblivé, zatímco dostatečně dlouhé isopropylmetakrylamidové sekvence jsou dehydratované a se sníženou pohyblivostí. V případě polymerních směsí byly detekovány fázové přechody obou polymerů. Fázově separovaný poly(*N*-vinylkaprolaktam) v čase ($\approx$ hodiny) sedimentoval. Dolní kritická rozpouštěcí teplota poly(*N*-vinylkaprolaktamu) se posunuje k nižším teplotám jak se vzrůstající polymerní koncentrací, tak s obsahem poly(*N*-vinylkaprolaktamu). T_2 rozpouštědla se zkracuje po fázové separaci poly(*N*-vinylkaprolaktamu), po separaci poly(*N*-isopropylmetakrylamidu) nebylo další zkrácení pozorováno.

Klíčová slova: fázová separace, polymerní roztok, cononsolvency, ^{1}H a ^{13}C NMR spektroskopie

Title: The Study of Dynamic Behaviour and Interactions During the Temperature-Induced Phase Separation in Polymer Solutions

Author: Hana Kouřilová

Department / Institute: Charles University in Prague, Faculty of Mathematics and Physics, Department of Macromolecular Physics

Supervisor of the doctoral thesis: doc. RNDr. Lenka Hanyková, Dr.

Abstract: ^{1}H and ^{13}C high-resolution NMR spectroscopies were used for the phase separation investigation in three types of polymer solutions: i) poly(*N*-isopropylmethacrylamide)/D_2O/ethanol with or without negatively charged comonomer sodium methacrylate, ii) random copolymers poly(*N*-isopropylmethacrylamide-*co*-acrylamide) in D_2O, D_2O/ethanol and D_2O/acetone and iii) D_2O solutions of polymer mixtures poly(*N*-isopropylmethacrylamide)/poly(*N*-vinylcaprolactam). For i) cononsolvency effect and influence of temperature on the phase separation was studied. Differences between mesoglobules formed as a consequence of cononsolvency effect and of temperature were found. While inside the cononsolvency-induced mesoglobules no bound ethanol molecules were detected, in the mesoglobules formed by the effect of temperature ethanol molecules were present. The charge introduced into the polymer chains strenghtens polymer–solvent interactions. For ii) mesoglobules were found to be rather porous and disordered. Acrylamide sequences and surrounding short isopropylmethacrylamide sequences are hydrated and mobile, while sufficiently long isopropylmethacrylamide sequences are dehydrated with reduced mobility. For iii) phase transitions of both polymers were detected. The phase-separated poly(*N*-vinylcaprolactam) was sedimenting in the order of hours. Lower critical solution temperature of poly(*N*-vinylcaprolactam) shifts to lower temperatures with both the increasing polymer concentration and poly(*N*-vinylcaprolactam) content. Solvent T_2 shortens after the poly(*N*-vinylcaprolactam) phase separation, after the poly(*N*-isopropylmethacrylamide) separation no further shortening was observed.

Keywords: Phase Separation, Polymer Solution, Cononsolvency, ^{1}H and ^{13}C NMR Spectroscopy

Contents

Chapter 1

A Short Introduction

When Toyoichi Tanaka in 1979 observed the phase transition in polyacrylamide gels [95], the era of "smart gels" was triggered. These materials exhibit rapid changes in their properties as a response to small changes in external conditions. They can change their volume by a factor of 1000 upon change of temperature by 1 K (so called swelling/collapse of the gel). Such behaviour can be used in a wide range of applications from drug release/drug delivery systems over DNA separation and sequencing to oil spills cleaning.

This thesis deals with results on the phase separation in polymer solutions. In polymer solutions the polymer chains are not chemically crosslinked in comparison with gels. They behave very similarly to gels but are more simple and thus very convenient for experimental methods such as nuclear magnetic resonance which allows us to study its behaviour on molecular level. The phase separation can be induced by many factors (e.g. change of temperature, solvent composition, electric field, ionic strength etc.) and it means the transition between a system when the polymer is dissolved in the solvent, its chains are extended and are floating in the solvent (such polymer structure is called a "coil") and a system when the polymer becomes a dense compact "globule" (polymer–polymer and solvent–solvent interactions prevail over polymer–solvent interactions). It is a reversible process. After reaching the initial external conditions the polymer gets its original structure (see Chapter 2.2.2).

NMR is a powerful tool widely used in the molecular structure elucidation, dynamic properties of both large and small molecules, physiological processes exploration, in food industry to measure moisture content or to determine region of origin, in petroleum exploration, to detect ground water even at depths of hundreds of meters [76], in textile industry [13], to study flow of liquids in pipes

in industrial processes, in material research and many other fields [7]. In more than 60 years of the NMR existence, a large number of various techniques was developed.

The aim of our work is to improve understanding of phase separation on molecular level which can be useful in designing materials with specific properties for applications.

In the Theoretical Part of this thesis (Chapter 2) basics of the NMR method and of the phase separation phenomenon are described. In the second half of this chapter overview of publications on studied polymer solutions, water–ethanol solutions and cononsolvency effect can be found. In the Experimental Part (Chapter 3) description of the samples preparation and experimental techniques that we used is noted. Aims of this thesis can be found in Chapter 4 followed by Results and Discussion (Chapter 5) devoted to our own experimental results: first part summarizes results on poly(*N*-isopropylmethacrylamide)/water/ethanol solutions, second part deals with solutions of copolymers poly(*N*-isopropylmethacrylamide-*co*-acrylamide) and the last one is about solutions of polymer mixtures of poly(*N*-isopropylmethacrylamide) with poly(*N*-vinylcaprolactam). The thesis is ended by the conclusions and the lists of cited bibliography, tables, figures and abbreviations and also by the list of articles and presentations of results related to this thesis and presented on various conferences.

Chapter 2

Theoretical Part

2.1 Nuclear Magnetic Resonance

2.1.1 NMR Basics

Nuclear magnetic resonance spectroscopy is a powerful tool used for structure elucidation, for the exploration of various processes and for the study of material properties through magnetic properties of certain nuclei. In contrast to most of the methods widely used, NMR is a local method. It is based on the interaction of the nuclear magnetic moment $\hat{\vec{\mu}}$ of a nucleus with a static external magnetic field of induction $\vec{B}_0$, so called Zeeman interaction. Such a nucleus must have a non-zero spin angular momentum $\hat{\vec{I}}$ to be able to interact with $\vec{B}_0$. The **relation between the nuclear magnetic moment μ and the spin angular momentum $\hat{\vec{I}}$** [69] is given by

$$\hat{\vec{\mu}} = \gamma\hbar\hat{\vec{I}} \tag{2.1}$$

where γ is the gyromagnetic ratio of the respective nucleus and $\hbar$ is the reduced Planck constant.

The **Hamiltonian of the Zeeman interaction** is [69]

$$\hat{H}_{\mathrm{Z}} = -\hat{\vec{\mu}}.\vec{B}_0 = -\gamma\hbar\hat{\vec{I}}.\vec{B}_0 \tag{2.2}$$

In NMR the static external field $\vec{B}_0$ is assumed to define the laboratory-frame $+z$-axis. Then $\vec{B}_0 = (0, 0, B_0)$ and the Hamiltonian of the Zeeman interaction simplifies into the equation:

$$\hat{H}_{\mathrm{Z}} = -\mu_{\mathrm{Z}}.B_0 = -\gamma\hbar I_{\mathrm{Z}}.B_0 \tag{2.3}$$

where I_Z is the z-component of the nuclear spin operator.

The solution of the Schrödinger equation with $\hat{H}_\mathrm{Z}$ reveals that the **Zeeman interaction leads to energy level splitting** – see Fig. 2.1. The magnetic energy of the nucleus is thus restricted to $2I + 1$ certain discrete values E_m (eigenvalues of $\hat{H}_\mathrm{Z}$):

$$E_m = -\gamma\hbar B_0 m \tag{2.4}$$

where m is the magnetic quantum number.

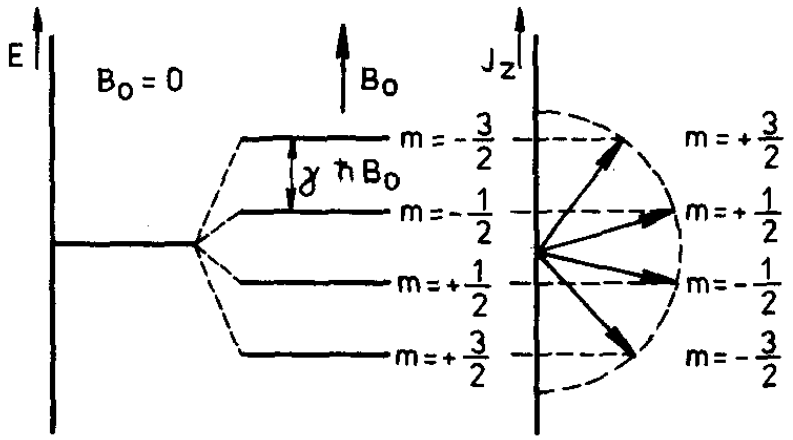

Figure 2.1: Energy levels of the Zeeman multiplet for $I = 3/2$. This picture was taken from [69].

These energy levels E_m in the so called Zeeman multiplet are equidistant with the distance ΔE

$$\Delta E = |\gamma|\hbar B_0. \tag{2.5}$$

Different energy levels correspond to different orientations of $\hat{\vec{\mu}}$ with respect to $\vec{B}_0$. Eigenstates are associated with the eigenvalues E_m. Eigenstates are the only states that are stationary [47] which means that when a quantum system is prepared in an energy eigenstate, it does not change into some other state unless the Hamiltonian changes. But generally a particle can be in a state which is a superposition of the eigenstates. The **superposition state** is a nonstacionary state, it evolves in time and it is fundamental in the NMR theory.

We cannot obtain information on properties of the spin neighbourhood when the spins are in the equilibrium state in the external static magnetic field $\vec{B}_0$. Such information can be extracted from their response upon a perturbation of the spin system. So we need a tool to introduce such a perturbation into our

spin system. In modern NMR spectrometers this is accomplished by applying a **radiofrequency pulse** of a frequency corresponding to the difference between the energy eigenstates. So let us add a small time-dependent magnetic field $\vec{B}_1(t)$ to the external magnetic field $\vec{B}_0$. The amplitude of the field $\vec{B}_1(t)$ is constant and its vector rotates with angular frequency ω_z in the xy-plane. Then the total magnetic field acting on the spin is [69]:

$$\vec{B} = B_1[\vec{\mathrm{i}}\cos(\omega_z \mathrm{t}) + \vec{\mathrm{j}}\sin(\omega_z \mathrm{t})] + B_0\vec{\mathrm{k}} \tag{2.6}$$

where $\vec{\mathrm{i}}$, $\vec{\mathrm{j}}$ and $\vec{\mathrm{k}}$ are unit vectors in the directions of x-, y- and z-axes, respectively.

Then the corresponding Hamiltonian of the spin particle can be expressed as a sum of two components:

$$\hat{H} = \hat{H}_{\mathrm{Z}} + \hat{H}_1(t) \tag{2.7}$$

where $\hat{H}_{\mathrm{Z}}$ is the Hamiltonian of the Zeeman interaction (see Eq. 2.3) and $H_1(t)$ describes influence of the field $\vec{B}_1$ and has the following form:

$$\begin{aligned} H_1(t) &= -\hat{\vec{\mu}}.B_1 && (2.8)\\ &= -\gamma\hbar B_1[\hat{I}_x\cos(\omega_z \mathrm{t}) + \hat{I}_y\sin(\omega_z \mathrm{t})] && (2.9)\\ &= -\frac{B_1}{2}\gamma\hbar[\exp(\mathrm{i}\omega_z \mathrm{t})\hat{I}^- + \exp(-\mathrm{i}\omega_z \mathrm{t})\hat{I}^+] && (2.10)\\ & && (2.11) \end{aligned}$$

where $\hat{I}^- = \hat{I}_x - i\hat{I}_y$ and $\hat{I}^+ = \hat{I}_x + i\hat{I}_y$ are ladder operators, which increment and decrement, respectively, the magnetic quantum number m by 1 when acting on the $\hat{I}_z$ eigenfunction.

If $B_1 << B_0$ then the influence of $\hat{H}_1(t)$ can be studied using the time-dependent perturbation theory [35, 69] which says that a small time-dependent perturbation can induce transitions between stacionary states of an unperturbed system. The probability of a transition $P_{m'_J,m_J}$ between states described by magnetic quantum numbers m'_J, m_J is proportional to the perturbed matrix element squared [14]:

$$P_{m'_J,m_J} \sim |< m'_J|\hat{H}_1|m_J >|^2 \tag{2.12}$$

From (2.11) and (2.12) it follows that the only non-zero matrix elements are those that fulfill the condition:

$$m'_J = m_J \pm 1 \tag{2.13}$$

It means that $\vec{B}_1$ can induce transitions only between neighbouring energy levels in the Zeeman multiplet. The matrix elements are symmetric, thus absorptions and emissions have the same probabilities. The distance between Zeeman multiplet levels given by 2.5 and a relation $\Delta E = \hbar\omega_0$ gives a condition for the **frequency of Larmour precession** [26, 69]:

$$\omega_0 = \gamma|\vec{B}_0| \tag{2.14}$$

This condition for the frequency of $\vec{B}_1$ must be satisfied so that $\vec{B}_1$ could induce transitions in the Zeeman multiplet and it is a fundamental condition for the magnetic resonance to occur. The absorption of energy can then be detected and converted into a spectral line using the Fourier transform.

2.1.2 Bloch Equations

All that was said until now concerned a single spin in the magnetic field. Now let us switch to the ensemble of spins.[1] Let us consider quantum mechanical expectation values of magnetic moment and angular momentum operators to be classical vector quantities. For the macroscopic description of a sample (containing for example ^{1}H nuclei) we use the macroscopic net magnetization vector $\vec{M}$ (of magnitude M_0) [26, 69]

$$\vec{M} = \sum_{i=1}^{n} \vec{\mu}_i \tag{2.15}$$

where $\vec{\mu}_i$ are magnetic moment vectors of all n nuclei of one type (^{1}H in our case).

In the equilibrium state $\vec{M}$ is parralel to $\vec{B}_0$. This direction will be labelled as the $+z$-direction. A transition to the state of higher energy[2] can be stimulated by the radiofrequency field fulfilling the resonance condition (2.14).

[1] Here we deal with an ensemble of non-interacting spins in the thermal equilibrium. In reality the spins interact with each other, however the non-interacting-spins approach is reasonable in isotropic liquids in particular cases.

[2] Magnetic nuclei in a macroscopic sample are distributed between their energy states and the difference in the population of protons between the ground state and the excited state at thermal equilibrium is given by the Boltzmann relation [26]:

$$\frac{\mathrm{N}_\alpha}{\mathrm{N}_\beta} = \exp(\frac{\Delta\mathrm{E}}{k_\mathrm{B}\mathrm{T}}) = \exp(\frac{\gamma\hbar B_0}{k_\mathrm{B}\mathrm{T}}) \approx 1 + \frac{\gamma\hbar B_0}{k_\mathrm{B}\mathrm{T}} \tag{2.16}$$

where N_α, N_β are the numbers of nuclei in the ground and excited states, respectively, ΔE is the energy difference between them, k_B is the Boltzmann constant and T is the absolute temperature. When the system is ruled by the Boltzmann distribution, the lower energy eigenstates are more populated than the higher ones. At thermal equilibrium the difference in the population of these two states depends on the energy difference between them in comparison with the avail-

As was said earlier, an application of a short strong radiofrequency pulse excites all nuclei of the corresponding frequency in the sample. The magnetic field changes to $\vec{B}_0 + \vec{B}_1(t)$, $|\vec{B}_1(t)| << |\vec{B}_0|$. During the resonance the pulse tips the magnetization $\vec{M}$ from $+z$-direction and the length of pulse duration determines the angle between $\vec{M}$ and $+z$-direction. Components of $\vec{M}$ in the xy-plane appear (transverse magnetization). After $\vec{B}_1(t)$ ceases, only $\vec{B}_0$ acts upon $\vec{M}$ and $\vec{M}$ starts its precession around the z-axis with the Larmor frequency characteristic of the particular nucleus and returns to its equilibrium position in $+z$-direction. The precessional motion of the x- and y-components of $\vec{M}$ induces an oscillating current in the receiver coil. During the return to equilibrium, the components of $\vec{M}$ in the xy-plane decay to zero through relaxation. Since the magnetization vector $\vec{M}$ is a macroscopic quantity, we can apply classical physics for the description of its motion. The motion of $\vec{M}$ is described by the phenomenological **Bloch equations**:

$$\frac{dM_x}{dt} = \gamma(\vec{M} \times \vec{B})_x - \frac{M_x}{\mathrm{T}_2} \tag{2.17}$$

$$\frac{dM_y}{dt} = \gamma(\vec{M} \times \vec{B})_y - \frac{M_y}{\mathrm{T}_2} \tag{2.18}$$

$$\frac{dM_z}{dt} = \gamma(\vec{M} \times \vec{B})_z - \frac{M_z - M_0}{\mathrm{T}_1} \tag{2.19}$$

where M_x, M_y, M_z are x-, y- and z-components of $\vec{M}$, M_0 is the equilibrium value of M_z, T_2 is the transverse (spin–spin) relaxation time (see chapter 2.1.4) and T_1 is the longitudinal (spin–lattice) relaxation time.

Bloch equations (2.17) and (2.18) describe the motion of the transverse components M_x and M_y of $\vec{M}$. The first term corresponds to the coherent motion of $\vec{M}$ in the rotating frame while the latter term predicts the exponencial decay of the magnetization in the xy-plane (M_x, M_y) to its equilibrium zero value. This decay is described by the spin–spin (transversal) relaxation time T_2. (2.19) pictures the motion of M_z, the longitudinal component of the magnetization. The second term in (2.19) describes the exponential relaxation of M_z ($M_z \parallel \vec{B}_0$) to its equilibrium value M_0. The time constant T_1 for this process is called the

able thermal energy of the sample [47]. We can easily calculate that at a room temperature, the available thermal energy is $k_\mathrm{B}\mathrm{T} \cong 4.14 \times 10^{-21}\mathrm{J}$. For protons at room temperature and at the field strength 11.7 T the difference between the Zeeman states $|\Delta\mathrm{E}| \cong 3.3 \times 10^{-25}\mathrm{J}$ which is four orders of magnitude smaller than the available thermal energy so the population difference is very small, $\frac{\mathrm{N}_\alpha}{\mathrm{N}_\beta} = 1 + 0.00008$. Thus, compared to other spectroscopic methods, NMR is not very sensitive.

spin–lattice (longitudinal) relaxation time (see Chapter 2.1.4).

During the return of $\vec{M}$ to the equilibrium the time signal called **free induction decay** (FID) is acquired, it is a representation of the NMR spectrum in the time domain. **Fourier transformation** of the FID provides the standard NMR spectrum in the frequency domain. This NMR method is called the pulse Fourier transform (PFT) NMR spectroscopy and is used nowadays. Method used earlier is the continuous wave (CW) NMR spectroscopy, where the perturbation was caused by a weak radiofrequency transmitter, whose frequency was varied continuously during the recording of the NMR spectrum. The main reason why the PFT method replaced the CW method is that in PFT the complete NMR spectrum can be excited with a single pulse and the corresponding time signal recorded within a second, while for the CW method each signal in the spectrum has to be measured separately [26].

2.1.3 NMR Interactions and Parameters

Until now the description did not involve the interactions of nuclear spins among each other. The interactions allow us to extract a lot of information about the spin neighbourhoods.

Chemical Shielding and Chemical Shift

The great advantage of NMR is the ability to distinguish between nuclei of the same isotope that have different neighbourhood in the molecule (chemical environment). The external magnetic field $\vec{B}_0$ causes electron currents in a molecule. These electron currents are responsible for the $\vec{B}_0$ field shielding and changing its value to $\vec{B}_{\text{local}}$. This phenomenon is called the **chemical shielding**. The local field $\vec{B}_{\text{local}}$ is given by:

$$\vec{B}_{\text{local}} = \vec{B}_0(1- \overleftrightarrow{\sigma}) \tag{2.20}$$

where $\overleftrightarrow{\sigma}$ is called the chemical shielding tensor.

The chemical shielding Hamiltonian for a single spin I in the Cartesian coordinates is as follows:

$$\hat{H}_{\text{CS}} = \gamma_I \hat{I}. \overleftrightarrow{\sigma} .\vec{B}_0 \tag{2.21}$$

In general the magnetic shielding tensor components can be both positive or negative. The situation in molecules is complex since the electronic cirulation must be considered within the whole molecule. From the fact that it is necessary to use a tensor for the magnetic shielding description it follows that the induced

magnetic field does not have to be parralel to $\vec{B}_0$. The presence of other nuclei reduces the diamagnetic effect due to the perturbation of the spherical symmetry of the electron distribution. This diminution can be treated as a contribution to the paramagnetic moment that strenghtens the external field $\vec{B}_0$. The magnetic shielding constant σ in molecules can be written as follows:

$$\sigma = \overset{\leftrightarrow}{\sigma}^{\text{local}}_{\text{dia}} + \overset{\leftrightarrow}{\sigma}^{\text{local}}_{\text{para}} + \overset{\leftrightarrow}{\sigma}' \tag{2.22}$$

where $\overset{\leftrightarrow}{\sigma}^{\text{local}}_{\text{dia}}$ is the diamagnetic component of the induced electronic motion which originates in the magnetic field created by electrons is s-orbitals, $\overset{\leftrightarrow}{\sigma}^{\text{local}}_{\text{para}}$ is the paramagnetic component generated by electrons in p-orbitals and $\overset{\leftrightarrow}{\sigma}'$ reflects the influence of neighbouring atoms and groups and can be both positive or negative. The last term is responsible for the fact that nuclei of one type exhibit different chemical shifts in different molecules.

Since the resonance frequency of an individual nucleus is proportional to the magnetic field, it is affected by the distribution of electrons in chemical bonds of the molecules. Thus value of the resonance frequency of a particular nucleus is dependent on molecular structure. This effect when the chemical environment causes a slight[3] shift of the resonance frequency is called the **chemical shift**.

In liquids the thermal motion causes averaging of chemical shielding interaction and thus only isotropic component of the chemical shielding tensor σ_{iso} matters:

$$\sigma_{\text{iso}} = \frac{1}{3}(\sigma_{11} + \sigma_{22} + \sigma_{33}) \tag{2.23}$$

It is useful to define the chemical shift independent of the magnetic field strength since NMR spectrometers operate at different B_0 fields and the resonance frequency varies with field strength (see Eq. 2.14). Therefore, a dimensionless quantity δ for the chemical shift was introduced:

$$\delta = \frac{\omega_{\text{substance}} - \omega_{\text{reference}}}{\omega_{\text{reference}}}.10^6 \tag{2.24}$$

where $\omega_{\text{substance}}$ is the resonance frequency of the signal under examination and $\omega_{\text{reference}}$ is the resonance frequency of a reference compound or a standard. The units used for the δ scale are parts per milion (ppm). This was chosen because $B_{loc} \ll B_0$.

[3]In diamagnetic liquids the resonance frequency shift is in the order of 0.001‰. This fact enables us to use pulses with a resonance frequency value corresponding to a particular nucleus as an isolated one during the experiment.

Integrated Intensities of NMR Spectral Lines

The NMR signals differ in their intensities. The area under the resonance signal is proportional to the number of protons that gives rise to that signal. But only the relative number of protons to the other signals can be determined by this operation. Integration is produced by the spectrometer integration software.

Direct Dipole–Dipole Interaction

The direct dipole–dipole interaction is the interaction between two nuclear magnetic moments or magnetic dipoles $\vec{\mu_1}$ and $\vec{\mu_2}$ through the space. For $\frac{1}{2}$-spins this is the most important interaction. A magnetic dipole $\vec{\mu_2}$ generates a local magnetic field $\vec{B}_{\text{local}}$ felt by a dipole $\vec{\mu_1}$ (and by other dipoles)

$$\vec{B}_{\text{local}} = -\frac{\mu_0}{4\pi r^3}(\vec{\mu}_2 - 3\frac{\vec{\mu}_2\vec{r}}{r^2}.\vec{r}) \tag{2.25}$$

where μ_0 is the vacuum permeability and $\vec{r}$ is the position vector of the $\vec{\mu}_2$ dipole.

If $\vec{\mu}_1 = \gamma_1\hbar\hat{\vec{I}}$ and $\vec{\mu}_2 = \gamma_2\hbar\hat{\vec{S}}$, then the dipole–dipole interaction Hamiltonian for the two spins I and S can be written in the following form:

$$\hat{H}_{\text{DD}} = -\frac{\mu_0\gamma_I\gamma_S\hbar}{4\pi r^3}(3\hat{\vec{I}}.\frac{\vec{r}\vec{r}}{r^2}.\hat{\vec{S}} - \hat{\vec{I}}.\hat{\vec{S}}) = b_{IS}\hat{\vec{I}}.\overleftrightarrow{D}.\hat{\vec{S}} \tag{2.26}$$

where $\overleftrightarrow{D}$ is the dipolar tensor.

For a constant distance r between two spins equal to r_{IS}, the dipole–dipole coupling constant b_{IS} is given by

$$b_{IS} = -\frac{\mu_0\gamma_I\gamma_S\hbar}{4\pi r_{IS}^3} \tag{2.27}$$

In isotropic liquids the dipole–dipole interaction cancels out due to molecular tumbling when the IS-spin axis changes its orientation very fast in comparison with the dipole–dipole coupling. However, it does not mean that the dipole–dipole interaction cannot be effective as a mechanism of relaxation.

Indirect Dipole–Dipole Interaction (J-Coupling, Scalar Interaction)

This interaction takes place between two spins and is mediated by electrons of the chemical bond. It is not averaged to zero in isotropic liquids. The Hamiltonian

of the J-coupling for two interacting spins I and S can be written as

$$\hat{H}_J = 2\pi \hat{\vec{I}}. \overset{\leftrightarrow}{J} .\hat{\vec{S}} \tag{2.28}$$

where $\overset{\leftrightarrow}{J}$ is the J-coupling Cartesian tensor.

The manifestation of the J-coupling in spectra is a signal splitting into multiplets. The splitting gives information about chemical bonds. J-coupling is mostly intramolecular since this interaction has an effect within a few bonds. However, for example when hydrogen bonds are involved, also intermolecular J-coupling can be observed.

Spin–Rotational Interaction

Spin–rotational interaction is the interaction between nuclear spins and the magnetic field. It is generated by the rotational motion of the molecule. This interaction is important only in the gaseous state NMR or in low-molecular substances. It is averaged to zero in isotropic liquids due to random fluctuations of the molecular motion.

Nuclear Quadrupolar Interaction

Electron quadrupolar interaction plays a role only for $> \frac{1}{2}$-spin nuclei. It is the interaction between nuclear quadrupoles and the electric field gradient on the nucleus.

Chemical Exchange Process

Generally, chemical exchange is a process when spins in a molecule change their magnetic environment. Molecules can exchange atoms physically (for example after mixing C_2H_5OH and D_2O an exchange of ethanol protons H for deuteria D takes place, chemical reactions, etc.) or they can change their magnetic environment only (conformational changes, isomerization, molecular complex formation, etc.). When signals of the exchanging species have different chemical shifts, they are in the so called "slow regime" when for the exchange rate k_{ex} and the difference between resonating frequencies of the exchanging species A and B $\Delta\omega$ the condition $k_{\mathrm{ex}} \ll \Delta\omega$ is fulfilled. In the "fast regime" the peaks of the exchanging species coalesce into a single one and $k_{\mathrm{ex}} \approx \Delta\omega$ (see Figure 2.2).

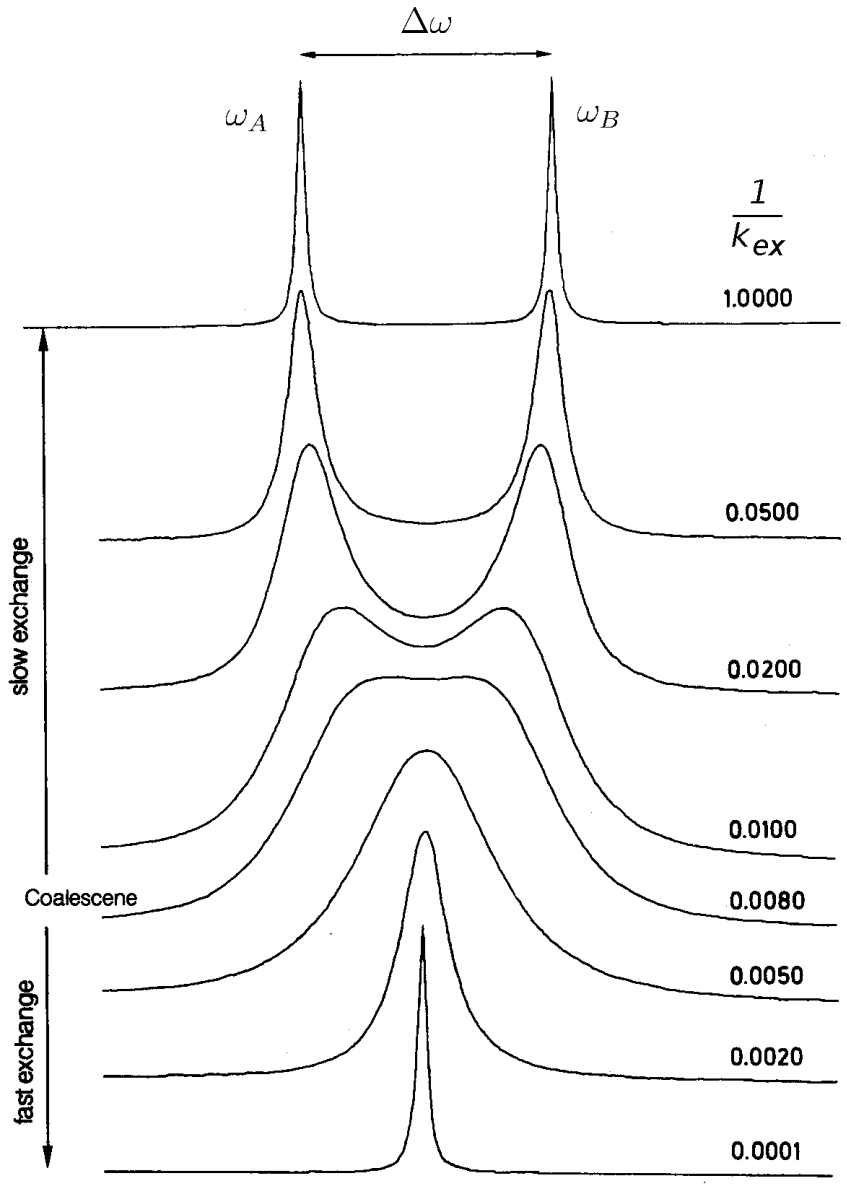

Figure 2.2: Theoretical NMR spectra for an exchange process A$\rightleftarrows$B as a function of parameter $\frac{1}{k_{\mathrm{ex}}}$. This picture was taken from [26] and modified.

2.1.4 NMR Relaxation

After an application of the pulse, when the sample has absorbed the radiofrequency radiation, the macroscopic magnetization starts to return to its equilibrium position which is parralel to $\vec{B}_0$. It means that the spins revert to the lower energy spin state. This process by which equilibrium is regained and the dissipating energy is absorbed into the lattice (i.e. the thermal molecular environment) is called the relaxation. The relaxation process allows us to perform NMR experiments. If there was no relaxation in our spin systems, the energy levels corresponding to the spins in the ground state and in the excited state would become equally populated after a short while after the irradiation and the system would neither absorb nor emit radiofrequency energy anymore.

Besides the interaction between spins with the surrounding environment there is another relaxation phenomenon which does not include energy exchange — random variations of the spin Larmor frequencies lead to phase decoherence between the spins in time.

NMR relaxation depends on the mobility of the NMR active species. As the molecule undergoes random thermal motion, there arise fluctuating magnetic fields from interactions with the lattice and from mutual interactions between spins. When these fluctuating magnetic fields have the proper frequency, they can lead to the nuclear magnetic relaxation. The magnetic field fluctuations can be induced by various mechanisms such as dipole–dipole interactions with other nuclei of the same or a different kind, chemical shift anisotropy, spin–rotation interaction, scalar interactions, chemical exchange, etc. For $\frac{1}{2}$-spins, the most important factors are the direct dipole–dipole interaction and the chemical shift anisotropy. For $> \frac{1}{2}$-spins, electric quadrupolar interactions also play a role.

These molecular-motion-induced fluctuations of the magnetic field in time have a zero mean value $< \vec{B}_{\text{fluct}}(t) > = 0$ and a non-zero mean-square $< \vec{B}^2_{\text{fluct}}(t) > \neq 0$. Then the magnetic field on the nucleus consists of the external static magnetic field $\vec{B}_0$ and the time-dependent component $\vec{B}_{\text{fluct}}(t)$:

$$\vec{B}_0(t) = \vec{B}_0 + \vec{B}_{\text{fluct}}(t) \tag{2.29}$$

The measure of how much the fluctuations $\vec{B}_{\text{fluct}}$ (and thus the positions of a nucleus) are related at two time moments is described by the time autocorrelation

function $\mathcal{A}(\tau)$:

$$\mathcal{A}(\tau) =< \vec{B}_{\text{fluct}}(t).\vec{B}_{\text{fluct}}(t+\tau) >= \frac{1}{T}\int_T \vec{B}_{\text{fluct}}(t).\vec{B}_{\text{fluct}}(t+\tau)dt \tag{2.30}$$

For long time intervals $\lim_{\tau\to\infty}\mathcal{A}(\tau) = 0$ so it is convenient to express the time autocorrelation function as an exponentially decaying one in the following form:

$$\mathcal{A}(\tau) = \mathcal{A}(0)\exp(-\frac{\tau}{\tau_c}) \tag{2.31}$$

where τ_c is the correlation time which can be interpreted as a measure of the time scale of random fluctuations' oscillations.

The Fourier transform of the autocorrelation function gives us the spectral density function $\mathcal{J}(\omega)$

$$\mathcal{J}(\omega) = \int_{-\infty}^{\infty}\mathcal{A}(\tau)\exp(-i\omega\tau)d\tau \tag{2.32}$$

which represents how much radiofrequency power the fluctuating local magnetic fields generate at a particular frequency. For the time autocorrelation function 2.31 the spectral density function is the Lorentzian function:

$$\mathcal{J}(\omega) = \mathcal{A}(0)\frac{2\tau_c}{1+\omega^2\tau_c^2} \tag{2.33}$$

The relaxation of populations (connected with the longitudinal magnetization) differs principially from the relaxation of the spin coherence (associated with the transverse magnetization) so two phenomenogical components of macroscopic magnetization are distinguished in NMR spectroscopy: the longitudinal magnetization along the z-axis and the transverse magnetization in the xy-plane (see Eq. 2.17–2.19). Both are subjects to the relaxation phenomena. The relaxation processes then may be divided roughly into two types: **spin–lattice (longitudinal) relaxation** characterized by the spin–lattice relaxation time constant T_1 and **spin–spin (transversal) relaxation** characterized by the spin–spin relaxation time constant T_2 [26, 47]. T_1 describes the equilibration of populations of spins in energy levels and T_2 the decay of single-quantum coherences between spins (see further).

For T_1 only fluctuations at the resonance frequency ω_0 play a role:

$$\frac{1}{\mathrm{T}_1} \sim \mathcal{J}(\omega_0) \tag{2.34}$$

while for T_2 both fluctuations at ω_0 and zero-frequency fluctuations (slow fluctuations that induce phase decoherence) are important:

$$\frac{1}{\mathrm{T}_2} \sim \text{const.}\mathcal{J}(0) + \mathcal{J}(\omega_0) \tag{2.35}$$

Thus, as a function of mobility, T_1 and T_2 behave differently (see Fig. 2.3). While T_1 has a minimum, T_2 exhibits a monotonic decrease with increasing correlation time (decreasing mobility).

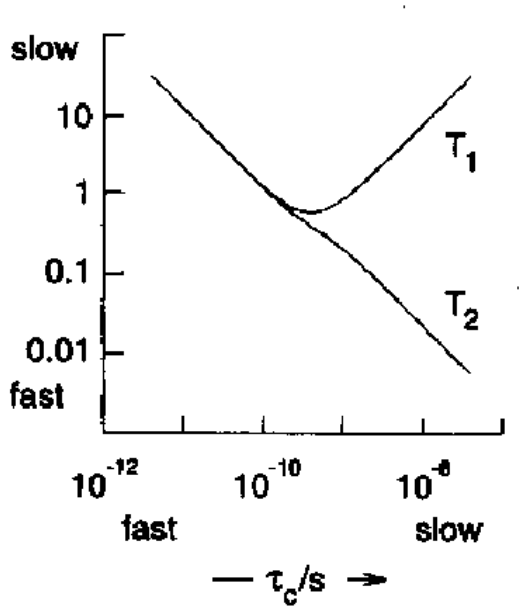

Figure 2.3: Dependence of relaxation times T_1 and T_2 on correlation time τ_c. This picture was taken from [31].

Longitudinal (Spin–Lattice) Relaxation

Immediately after exposing the spins in the sample to the external magnetic field $\vec{B}_1$ the spins are in a non-equilibrium state and the z-component of the macroscopic magnetization $M_z = 0$. Afterwards a build-up of M_0 takes place and the variation of M_z is governed by this first-order differential equation [26]:

$$\frac{dM_z}{dt} = \frac{M_0 - M_z}{\mathrm{T}_1} \tag{2.36}$$

where $\dfrac{1}{\mathrm{T}_1}$ is the transition rate constant of the perturbed system to the equilibrium state.

T_1 is the longitudinal (spin–lattice) relaxation time. During this time energy is transferred from the spins to the environment until the Boltzmann distribution of the populations is restored and $M_z = M_0$.

The basic experiment for T_1 measurements is the **inversion recovery** experiment. It consists of a 180° pulse followed by a 90° pulse with a variable delay τ_{mix} between the pulses.

$$180° \text{ — } \tau_{\text{mix}} \text{ — } 90° \text{ — acquisition}$$

One can obtain T_1 from the dependence of the signal on the mixing time τ_{mix}:

$$\text{Signal Intensity} \sim 1 - 2\exp(-\frac{\tau_{\text{mix}}}{T_1}) \tag{2.37}$$

Transverse (Spin–Spin) Relaxation

As was said earlier, T_2 is connected with the loss of the spin system coherence with time. The spins dephase because of two mechanisms: static inhomogeneities (nuclei have different local chemical environment and thus their resonance frequencies slightly differ) and spin dephasing caused by fluctuations (spin–spin relaxation). The first inhomogeneity can be eliminated by the use of a proper pulse sequence. The latter one is responsible for the intensity decrease of the echoes in comparison with the FID signal (see further) and it is the undisposable one. T_2 also contains a contribution from the process of return of the macroscopic magnetization to the equilibrium (T_1). There is a relation between the transverse relaxation and the spectral signal lineshape [26]:

$$\Delta = \frac{2}{T_2^*} \tag{2.38}$$

where

$$\frac{1}{T_2^*} = \frac{1}{T_2} + \frac{1}{T_{2n}^*} \tag{2.39}$$

Δ is the halfwidth (width at half-height) of the resonance signal in rad.s^{-1} units, $\frac{1}{T_2}$ is the homogeneous line broadening and $\frac{1}{T_{2n}^*}$ is the inhomogeneous line broadening. For the NMR absorption signal and its parameters see Fig. 2.4.

The decay of the FID is governed by T_2^*. We try to get rid of the inhomogeneous line broadening by a proper adjustment of experimental conditions.

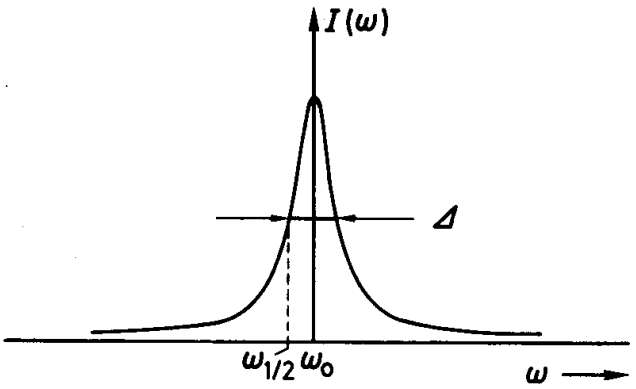

Figure 2.4: The NMR absorption signal (Lorentz curve). This picture was taken from [26].

But since we cannot dispose of the inhomogeneous line broadening totally, it is not convenient to determine T_2 from the line halfwidth. A **spin echo** experiment can be used for T_2 measurements:

$$90^\circ_x \text{ — } t_d \text{ — } 180^\circ_x \text{ — } t_d \text{ — acquisition (FID)}$$

First, a 90°_x pulse is applied which tilts the magnetization vector $\vec{M}$ into the y-direction. Then, during the delay t_d the nuclear spins start to defocus (because their speeds of precession differ) due to the magnetic field inhomogeneities. After the delay t_d a 180°_x pulse is applied which turns $\vec{M}$ along the $-y$-axis. The spins start to refocus and after time $2t_d$ they all end up in the $-y$-direction. This refocused signal is called a spin echo. Its signal intensity $I \sim \exp(-2t_d/T_2)$. Since the process of diffusion can significantly influence the spin echo experiment (it causes an increase of the distribution of Larmor frequencies), sequences based on **Carr-Purcell-Meiboom-Gill (CPMG) sequence** were developed to eliminate the influence of diffusion. In the CPMG sequence the delays t_d are kept constant while n, the number of repetitions of the $[t_d \text{ — } 180^\circ \text{ — } t_d \text{ —}]$ segment, is varied. The scheme of the CPMG sequence is as follows:

$$90^\circ \text{ — } [\ t_d \text{ — } 180^\circ \text{ — } t_d \text{ — }]_n \text{ — acquisition (FID)}$$

2.1.5 Liquid State NMR

There is a big difference between NMR spectra of isotropic liquids (solutions) and those of solids. In solids the nuclei orientation is rigid with respect to $\vec{B}_0$ and to the neighbouring nuclei. It causes a strong line broadening [26]. For example the

variation ΔB in the local magnetic field caused by the interaction between two nuclear magnetic moments at a mutual distance r and at an angle Θ with $\vec{B}_0$ is given by

$$\Delta B = \pm\frac{3}{2}\mu(3\cos^2\Theta - 1)r^{-3}\frac{\mu_0}{4\pi} \tag{2.40}$$

where μ_0 is the permeability in free space.

Thus the magnetic field in the solid changes with the position in the sample and then the typical linewidths are several kHz.

The Hamilton operator for solids is defined by the following expression [26]:

$$\hat{H_{\text{solid}}} = \hat{H}_{\text{Z}} + \hat{H}_{\text{CS}} + \hat{H}_{\text{S}} + \hat{H}_{\text{DD}} + \hat{H}_{\text{Q}} \tag{2.41}$$

where $\hat{H}_{\text{Z}}$ is the Hamiltonian of the Zeeman interaction of the nucleus with the external field $\vec{B}_0$, $\hat{H}_{\text{CS}}$ is the Hamiltonian of the chemical shielding, $\hat{H}_{\text{S}}$ is the Hamiltonian of the scalar spin–spin interaction, $\hat{H}_{\text{DD}}$ is the Hamiltonian of the dipole–dipole interactions and $\hat{H}_{\text{Q}}$ is the Hamiltonian of the quadrupolar interactions.

In isotropic liquids dipole–dipole and quadrupolar interactions do not play a role and both the chemical shielding and scalar coupling are isotropic. The **Hamilton operator for an isotropic liquid** has the following form [26]:

$$\hat{H_{\text{liquid}}} = \hat{H}_{\text{Z}} + \hat{H}^{\text{iso}}_{\text{CS}} + \hat{H}^{\text{iso}}_{\text{S}} \tag{2.42}$$

where $\hat{H}_{\text{Z}}$ is the Hamiltonian of the Zeeman interaction with the external field $\vec{B}_0$, $\hat{H}^{\text{iso}}_{\text{CS}}$ is the isotropic Hamiltonian of the chemical shielding, $\hat{H}^{\text{iso}}_{\text{S}}$ is the isotropic Hamiltonian of the scalar spin-spin interaction.

For isotropic liquids the random thermal translational and rotational motions make the factor $(3\cos^2\Theta - 1)$ in Eq. 2.40 equal to zero.[4] This fact can be derived when the time average over $(3\cos^2\Theta - 1)$ is replaced by the ensemble average obtained from $\Sigma(3\cos^2\Theta - 1)/3$. Therefore the dipolar interactions between nuclei cancel. The characteristic linewidths for spectral lines of liquid samples are up to several Hz, often less than 1 Hz. Therefore this spectroscopic method is called high-resolution NMR.

The shielding tensor $\overleftrightarrow{\sigma}$ can be generally brought into diagonal form through

[4]The term $(3\cos^2\Theta - 1)$ equals zero also when $\Theta = 54.7°$ (so called magic angle). A powerful technique called magic angle spinning (MAS) using rotation of a solid sample (mostly a crystalline powder) under this condition has developed [26].

a suitable coordinate transformation:

$$\overleftrightarrow{\sigma} = \begin{vmatrix} \sigma_{11} & 0 & 0 \\ 0 & \sigma_{22} & 0 \\ 0 & 0 & \sigma_{33} \end{vmatrix} \tag{2.43}$$

For solids $\sigma_{11} \neq \sigma_{22} \neq \sigma_{33}$ and for axially symmetric molecules $\sigma_{11} = \sigma_{22} \neq \sigma_{33}$. In liquids the chemical shift is measured as the trace of the symmetric matrix:

$$\mathrm{Tr}\,(\overleftrightarrow{\sigma}) = \frac{1}{3}(\sigma_{11} + \sigma_{22} + \sigma_{33}) \tag{2.44}$$

In the case of powders different σ–values are observed depending on the orientation of the individual microcrystals relative to $\vec{B}_0$.

A small preview into polymer solutions: The NMR lines of a bulk polymer would be much wider than the spectrum that we obtain during our experiments. The lines of the polymer dissolved in a solution are much more narrow (although still much wider than those of liquids) and thus are detectable by high-resolution NMR spectroscopy. When the phase separation (see Section 2.2.2) occurs, the polymer lines behave like those of a solid and become wider than the experimental window so they are hidden under the baseline and thus are decreasing the integrated intensities of the lines of the rigid parts of the polymer. This effect of integrated intensity decrease enables us to detect the phase separation in polymer solutions and to determine its extent and properties.

2.2 Phase Transition in Polymer Systems

2.2.1 Liquid-Liquid Phase Separation

Let me analyze a case of the phase transition in a mixture of liquids first. A system consisting of two partially miscible liquids (i.e. liquids that do not mix in all proportions and at all temperatures) can exhibit critical solution temperature behaviour. Assume that a liquid B is gradually added into another liquid A at a temperature T′ (see Fig. 2.5). Upon addition of a small amount of B, B dissolves in A completely. After further addition of B, a stage is reached where no more B dissolves and the system now consists of two phases in equilibrium with each other. When more and more B is added, A gradually dissolves in it. The relative abundances of the two phases are given by the lever rule. When a stage in which

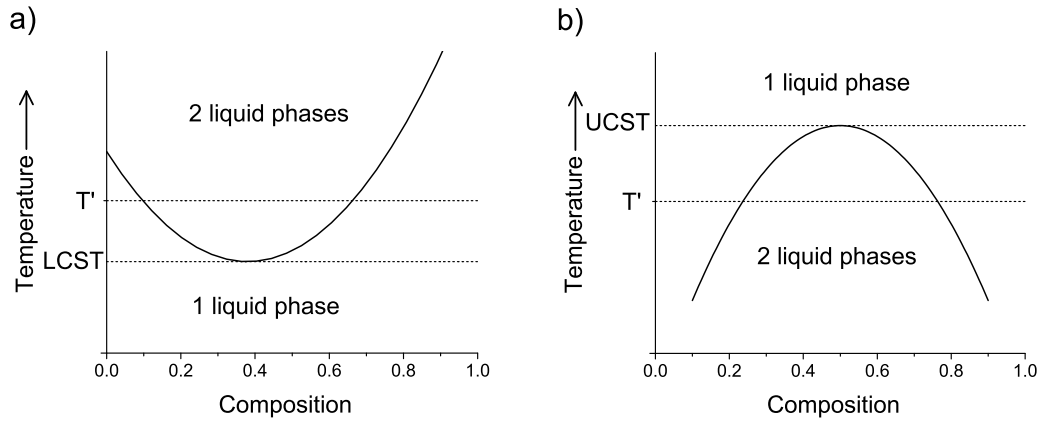

Figure 2.5: Schematic temperature–composition phase diagrams of two partially miscible solvents exhibiting lower critical solution temperature (a) and upper critical solution temperature (b), respectively.

so much B is present that dissolution of all A is achieved, the system reverts to a single phase. After further addition of B, B simply dilutes A and the single phase remains [6, 58].

As can be seen from the temperature–composition phase diagrams in Fig. 2.5, the composition of the two phases at equilibrium varies with the temperature. In the case of systems showing **lower critical solution temperature** (LCST) behaviour (Fig. 2.5a) the miscibility decreases with increasing temperature. Below the LCST the components mix in all proportions, above the LCST they form two phases. The LCST exists due to the fact that at low temperatures the two components are more miscible because they form a weak complex (e.g. stabilized by amphiphilic interactions, hydrogen bonding, van der Waals interactions, etc.). At higher temperatures the thermal motion disrupts the complexes which leads to the lower miscibility of the two components. An example of low molecular systems exhibiting LCST behaviour is a water/triethylamin system [63].

There are systems exhibiting **upper critical solution temperature** (UCST) (Fig. 2.5b) as well. In that case the UCST is the highest temperature at which phase separation occurs. Above this temperature the components are fully miscible. With increasing temperature the greater thermal motion overcomes any potential advantage of molecules of one type originating from being close together. UCST is shown by nitrobenzene/hexane system [6, 63].

Some systems (water/nicotine) show both LCST and UCST behaviour [6, 63].

2.2.2 Phase Transition in Polymer Systems

In this thesis, we will be dealing with polymer solutions showing the LCST behaviour. As was said in the previous text, the solubility of such systems decreases with increasing temperature; a complete miscibility is attained under the LCST while above the LCST they undergo the phase separation. These LCSTs are found in solutions in which both components are highly polar,[5] and are related to the decrease in entropy associated with the formation of hydrogen bonds at temperatures under the LCST. The miscibility decreases upon heating as the hydrogen bonds are broken by the motion of the molecules. These LCSTs are therefore at low temperatures, that is, at temperatures that are usually below the boiling point of the solvent [22, 81, 88]. Above the LCST polymer chains contract because polymer–polymer interactions are preferred to polymer–solvent interactions and the contraction increases number of monomer–monomer contacts. Such behaviour is not common for polymer solutions since the point of intramolecular condensation is rather close to the point of intermolecular condensation at which the polymer aggregates. In the case of **polymer solutions** the loose polymer structure under the LCST is called a **coil**. Above the LCST the polymers form compact **globules**. For typical conformations of a polymer coil and a polymer globule see Fig. 2.6.

In the case of **polymer networks** (also called gels), where the polymer chains are permanently crosslinked by chemical bonds, the phase transition from the expanded coil state under the LCST to the compact globular state above the LCST is called a **collapse** while the globule–coil transition is **swelling**. From the analysis of the classical Flory-Huggins equation of swelling equilibrium it follows that in a network two polymeric phases may coexist under certain conditions. These phases have a different conformation of chains and concentration of segments. A small change in the polymer–solvent interactions, which can be induced by a change of the external parameters (e.g. temperature or solvent composition), leads to a significant change in the degree of swelling of the gel (and thus the volume) – see Fig. 2.7. This phenomenon shows the character of the first-order phase transition [17, 18, 32]. The collapse was first found experimentally by Tanaka [95] for polyacrylamide (PAAm) gels in water–acetone mixtures upon changing the

[5] The polarity, however, is not a necessary feature of such systems. The LCST behaviour can occur in solutions of two components of very different molecular sizes and energies. Then the LCST is close to the gas–liquid critical point of the more volatile component. The first known example of a system of this kind was an ethane/ethanol solution [41], in which the LCST is at 32 °C, the same temperature as the gas-liquid critical temperature of pure ethane.

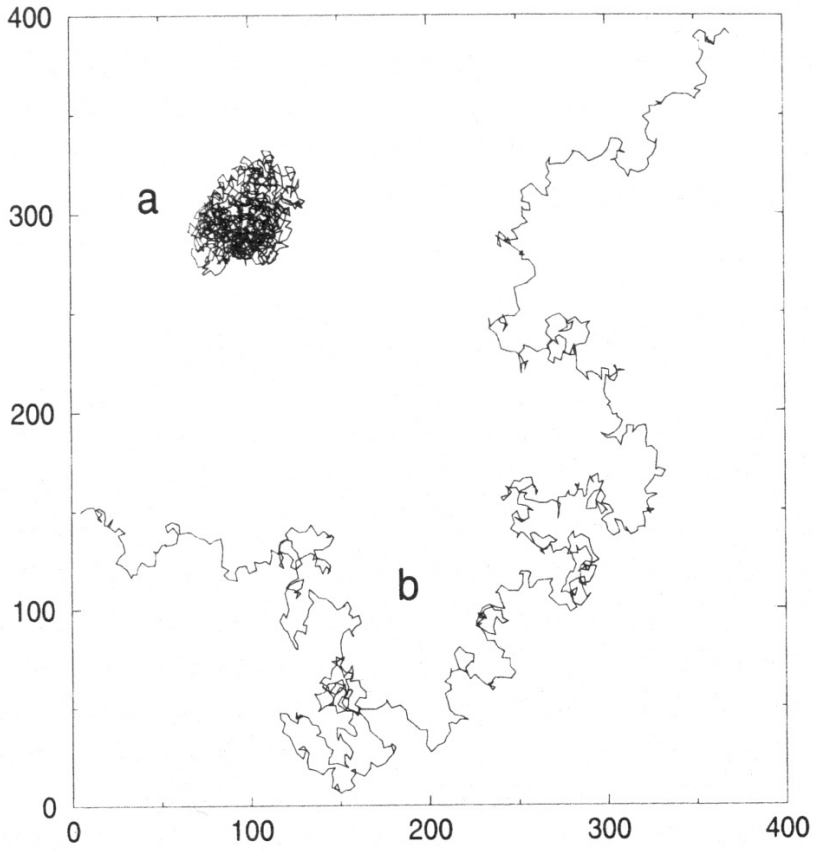

Figure 2.6: Computationally generated typical conformations of a polymer globule (a) and a polymer coil (b). Polymer has 1000 segments of the lenghth 1 each. The picture was taken from [24].

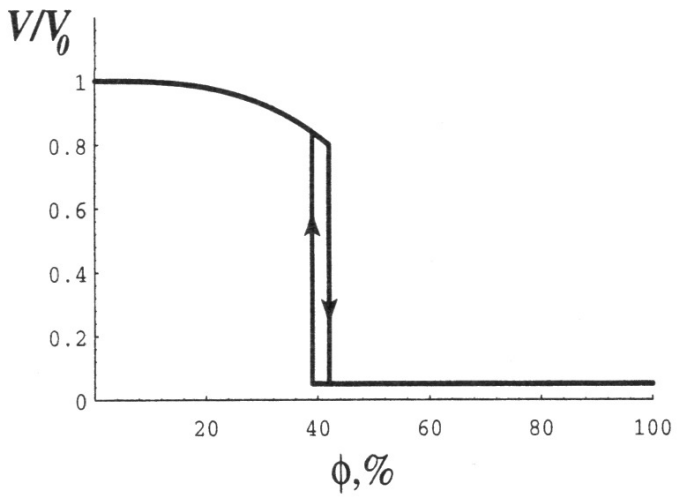

Figure 2.7: The volume of a polyacrylamide network in a mixture of acetone and water, as a function of the percentage of acetone (V_0 is the volume that the network had when first prepared). The picture was taken from [24].

solvent composition. The polymer–solvent interactions change after the addition of acetone into the solution: while water is a good solvent for PAAm, acetone is a bad solvent.

In a good solvent the pair interaction between monomers is repulsive and tends to swell the polymer coil; its radius R is determined by the balance between this repulsive energy and the elastic (entropic) energy prohibiting large deformations. For a single real flexible chain it can be then found [15, 21] that $R \sim N^{\frac{3}{5}}$, where N is the number of monomers in the chain. In a poor solvent the monomer–monomer interaction is attractive and the complete collapse of the chain is hindered only by a steric repulsion between the segments; the volume of the polymer globule is linear in N and in this collapsed regime $R \sim N^{\frac{1}{3}}$. In a Θ-solvent where attractive and repulsive forces compensate, the chains are quasi-ideal and $R \sim N^{\frac{1}{2}}$. Tanaka in [95] found the PAAm network collapse for a 42% acetone concentration at 25°C when its volume decreased by a factor of around 50. Later experiments showed that the presence of charges in the polymer chains seems to be necessary for the collapse to occur [93].

A hysteresis in temperature dependences of phase separation in polymer solutions was observed [50, 104]. It is probably due to the formation of the polymer-polymer hydrogen bonds within the globules.

In this thesis we deal with acrylamide-based polymers and polyvinylcaprolac-

tam. All these polymers posess hydrophillic C=O groups and hydrophobic alkyl groups. Presence of both types of groups in one polymer species ensures very complex behaviour in solvents that are capable of hydrogen bonding and thus enables phase separation to occur.

Cononsolvency Effect

Some polymers exhibit an interesting behaviour in mixtures of solvents. They are completely dissolvable in some solvents but a mixture of these good solvents becomes a bad solvent for these polymers. This formation of a "non-solvent" by mixing good solvents is called a cononsolvency effect. It is due to the preferable attractive interactions among solvent molecules of different types to polymer–solvent interactions.

2.2.3 Theoretical Description of the Coil–Globule Transition in Macromolecules

The phase transition in polymer solutions can be fundamentally described by two different approaches: the simplest Flory-type models [21, 24, 70] and the more rigorous Lifshitz-type model [48].

Flory-type models

The coil–globule transition is treated as a transition from a regime where attractive interactions between solvent molecules and monomers are dominant to a regime where attractive interactions between monomers prevail [21, 70]. The Gibbs energy of a swollen coil consisting of a single chain is expressed as a sum of two terms:

$$\mathrm{G} = \mathrm{G_{el}}(\alpha) + \mathrm{G_{int}}(\alpha) \tag{2.45}$$

where

α is the scalar order parameter of the chain (macromolecule) reflecting its size called the collapse ratio; $0 < \alpha \leq 1$,

$\mathrm{G_{el}}$ is the elastic entropy contribution to the free energy associated with stretching the coil by the factor α; $\mathrm{G_{el}}(\alpha) = -\mathrm{TS}(\alpha)$, where T is a thermodynamic temperature and S is an entropy,

$\mathrm{G_{int}}$ is the energy of the monomer interaction in the coil and involves both monomer-monomer and monomer-solvent interactions.

Ptitsyn et al. [70] estimated G_{el} using an assumption that Gaussian statistics is valid for both coil and globular states and obtained:

$$G_{el}(\alpha) = \frac{3}{2}RT(\alpha^2 - \ln(\alpha^2)) \tag{2.46}$$

where R is the gas constant.

For G_{int} expression the bonding of monomers in the chain was neglected and an approximate relation similar to the van der Waals equation for real gases was proposed:

$$G_{int}(\alpha) = -\frac{N^2 \upsilon z U}{2V} - NRTln(1 - \frac{N\upsilon}{2V}) \tag{2.47}$$

where

N is the number of statistical segments in the chain,

υ is the volume excluded by each statistical segment to other segments,

U is the energy gain that each statistical segment gives with respect to the contacts between statistical segments and solvent molecules,

z is the coordination number,

V= $\alpha^3 V_0$, where V_0 is the volume of the macromolecule at the Θ-temperature when segment–segment and segment–solvent interactions are equal and the chain has unperturbed dimensions.

In equilibrium the total Gibbs free energy $G(\alpha)$ is minimal. Minimization of $G(\alpha)$ with respect to α returns:

$$\alpha^5 - \alpha^3 - (\frac{\rho}{\alpha^3}) = q \tag{2.48}$$

where

q is a measure of the interaction between two statistical segments and

ρ is a measure of the interaction between three statistical segments.

Eq. (2.48) determines the size of a coil as a function of two characteristic parameters, q and ρ:

$$R = \alpha\sqrt{N}\ l \tag{2.49}$$

where l is the Kuhn length (any polymer segment shorter than l can be regarded as rigid which means that its end-to-end distance is approximately the same as its

contour length; different segments of length l then behave as independent [24]). The two parameters q and ρ correspond to particular system characteristics. While q can be related to the temperature, ρ parameter depends on the osmotic third virial coefficient and describes the rigidity of the polymer chain as followed from the study of this coefficient for different monomer types. Thus α, the collapse ratio, is a function of temperature, solvent quality and polymer chain rigidity. The fact that, in the thermodynamic limit, the coil–globule transition may be either of the first- or of the second-order, essentially depends on whether the rigidity of polymer is below or above some limiting value.

Lifshitz-type models

Lifshitz et al. [48] calculated the density distribution of monomers inside a spherically symmetric globule by solving a nonlinear Schrödinger-type equation. It turned out that the distribution depends on $\frac{T-\Theta}{\Theta}\sqrt{\mathrm{N}}$ only. For rigid and semi-rigid polymer chains the Gibbs energy has two minima located near the transition point Θ which corresponds to the first-order transition. They also found out that, at the transition point, the temperature derivative of the Gibbs energy has a step. The step is proportional to $\sqrt{\mathrm{N}}$ and corresponds to the latent heat associated with ordinary first-order phase transitions. On the other hand the transition for flexible polymer chains is smooth and looks like the second-order phase transition. Thus both the Flory-type and Lifshitz-type approaches lead to similar conclusions about the nature of the coil–globule transition in a macromolecular system.

2.3 Review of Studies on Phase Separation in Polymer Solutions

2.3.1 PIPMAm Solutions

There are not many studies on poly(N-isopropylmethacrylamide) (PIPMAm) phase transition behaviour. Much more research was done on poly(N-isopropylacrylamide) (PIPAAm) (see review by H. G. Schild [74]) which is structurally very similar – it differs only by the absence of an α-methyl group connected to the backbone chain in the monomer unit.

To our best knowledge the first work on phase transition in aqueous solutions of PIPMAm was published in 1989 by Fujishige et al. [23]. The authors studied solutions of both PIPMAm and PIPAAm by static and dynamic light scattering.

While the LCST of PIPAAm was reported to be 305 K, LCST of PIPMAm is significantly higher at 316 K. This increase in the LCST is due to the presence of an α-methyl group in the PIPMAm unit which makes a steric hindrance that prevents the hydrophobic groups to join together in the most favourable manner [16, 23, 100]. PIPMAm molecules in an aqueous solution adopt more expanded structures than PIPAAm even at the room temperature [40]. For PIPAAm Fujishige et al. [23] found out that the LCST does not depend on polymer molecular weight (in the range from 5×10^4 to 840×10^4 g.mol^{-1}) or concentration (from 0.01 to 1 wt%). During a heating/cooling cycle, PIPMAm exhibited a retardation during cooling which the authors attributed to effects of a restricted free rotation on the total polymer conformation caused by the presence of the α-methyl group. The thermal hysteresis was later confirmed in [50, 65], in comparison with PIPAAm, PIPMAm exhibits a greater hysteresis, which Maeda et al. [50], based on Fourier Transform Infrared (FTIR) Spectroscopy studies, attributed to higher degrees of the polymer–polymer hydrogen bonding in globules. From another FTIR spectroscopy study [16] it was found out that the hysteresis increases with polymer concentration, but for less concentrated solutions (0.05 – 1 wt%) it does not depend on the polymer concentration.

In 1997 Netopilík et al. [65] made an apparatus for turbidimetric measurements and studied time dependences of the transmitted light intensity at temperatures in the vicinity of the phase transition temperature. The time dependences consisted of an induction time with constant intensity and of a linear decrease. With incrasing concentration and temperature, the induction time was found to decrease, while the slope to increase. During a heating/cooling cycle, a thermohysteresis in the intensity was confirmed in accordance with [23]. It led the authors to the conclusion that cloud point temperature estimations can be reliable only if the induction time is negligibly short.

An extensive differential scanning calorimetry (DSC) study of PIPMAm thermal transitions was done by Sánchez et al. [73]. The authors explained thermal transitions in the temperature range from -100 to 60 °C based on the phase diagram of the system. From a certain polymer concentration in the solution the phase transition disappeared which the authors attributed to the vitrification that happens before the LCST is reached. This glass transition decreases the chain mobility which prevents the phase separation.

A comparative laser light scattering and ultra-sensitive DSC study of PIPMAm and PIPAAm solutions done recently by Tang et al. [99] focused on the role of the additional methyl group in the phase transition of PIPMAm. By studying of

the association and dissociation of PIPMAm chains in water, the auhors found out that above the LCST the chains form larger aggregates as their molar mass decreases. The PIPMAm aggregates formed during the phase transition are looser and undergo a smaller conformational change in comparison with PIPAAm. The additional methyl groups restrain the conformational changes, causing thus an LCST increase which is in agreement with [16, 23, 100].

Starovoytova et al. [88] used infrared spectroscopy to study the hydrogen bonding of polymer groups. Transition temperatures for PIPMAm C=O groups were found to be approximately 2 K higher than temperatures for CH_3 groups.

Charged PIPMAm

There are several reports on temperature-induced phase separation of charged PIPMAm in D_2O. A comonomer sodium methacrylate is used to charge the PIPMAm chains negatively. While for non-ionized PIPMAm the formation of globular structures does not depend on polymer concentration, negatively charged PIPMAm/D_2O solutions exhibit both concentration and comonomer mole fraction dependent phase transition behaviour [92]. An increase in polymer concentration and comonomer mole fraction was found to cause a decrease in the fraction of polymer segments involved in globular structures. In [88] besides ^{1}H NMR spectroscopy also infrared spectroscopy was used. It was revealed that with increasing content of sodium metacrylate units in the copolymer chains, the phase-separated fraction and the hysteresis during a gradual heating/cooling cycle decreases. This decreased hysteresis was interpreted as an indicator of a lower number of polymer-polymer hydrogen bonds. For sodium methacrylate contents $\geq$ 5 mol% the globular structures were found to be rather disordered and porous. For low sodium methacrylate contents (up to 5 mol%) part of water molecules stays bound in globular structures and these water molecules were not released even for 90 hours. Contrary, for uncharged PIPMAm in D_2O a release process of water molecules out of globular structures was observed after 35 hours [89]. The effect of time on hydration of uncharged PIPMAm mesoglobules is such that first the T_2 relaxation times are constant for 30 hours (so called induction period) and then the T_2 values increase manifesting thus the exclusion of the bound water molecules from the mesoglobules. Comparison of such time dependences of T_2 values for PIPMAm, PIPAAm and poly(vinyl methyl ether) (PVME) revealed that while PVME is in a rubbery state in mesoglobules, PIPMAm and PIPAAm are in a glassy state which is in agreement with [73]. PIPAAm is packed more

effectively which probably is the cause why its induction time is longer than that of PIPMAm.

Polymer mixtures with PIPMAm

Djokpe et al. [16] studied the phase separation behaviour in aqueous solutions of PIPMAm/PIPAAm mixtures and random copolymers by cloud point measurements. In the studied concentration range 0.05 – 1 wt% it was found out that the copolymer cloud point temperature depends linearly on the copolymer composition in the copolymer solutions. In the mixtures, two cloud points, which are approximately the same as those of the corresponding homopolymer/water systems, were observed. These two cloud points did not depend on the overall polymer concentration.

Phase separation in aqueous solutions of PIPMAm/PVME [91] and PIPMAm/-PIPAAm [90] polymer mixtures was studied extensively by NMR spectroscopy. In both cases two phase transitions were detected, their LCSTs had roughly the same value as those of the corresponding single-component-polymer solutions as in [16]. The phase transition at lower temperature was found not to be affected by the presence of the other polymer while the phase transition located at higher temperature was.

From ^{1}H spin–spin relaxation times T_2 of residual HDO molecules it was found out that part of solvent molecules is bound to globular structures and that a major part of bound water is present in those of the predominating polymer component in the mixture [91].

Kinetics of PIPMAm phase transition

Kinetics of the coil–globule transition was experimentally studied in [98] by fluorescence and Rayleigh scattering. The rapid temperature changes were achieved by fast laser pulse infrared heating which enables temperature changes of 8 K in 10 ns. The authors observed 2 stages: i) formation and growth of pearls and ii) their subsequent merging and coarsening (see Fig. 2.8) with their own characteristic times $\tau_{\text{fast}} = 10^{-4}$ s and $\tau_{\text{slow}} = 10^{-3}$ s. In theoretical works on the coil–globule kinetics, from 2 up to 4 stages were reported.

Detailed calorimetric measurements of the coil–globule transition in PIPMAm and/or PIPAAm sodium dodecyl sulfate solutions revealed that the transition has a "domain" nature, which means that these domains (cooperative units) are being quasi-independently disrupted during the transition [100]. Their number

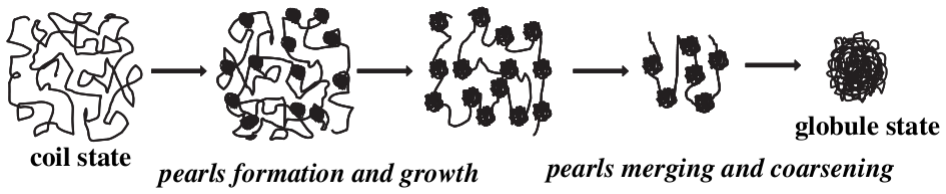

Figure 2.8: A schematic picture of two kinetic stages formed during a coil–globule transition. The picture was taken from [98].

is proportional to the polymer molecular weight. Such a conclusion suggests that in large proteins the domain nature of their denaturation does not need special amino acids sequences but it might be a typical behaviour of large macromolecules.

Results on (not only) PIPMAm obtained exclusively by NMR methods are covered in reviews by Spěváček [78, 80].

2.3.2 PAAM Solutions

Polyacrylamide (PAAm) does not belong to the temperature-sensitive polymers, it's phase separation is induced by the solvent composition. PAAm gels in a water/acetone mixture were the first which were experimentally found to exhibit the collapse [95]. The solubility of PAAm in several solvents was extensively studied via contact angles and surface tension measurements and calculations [107]. Water and ethylene glycol act as good solvents, while dimethylformamide, acetone and ethanol are bad solvents. In terms of mixtures of these solvents in water, PAAm is soluble in water/acetone mixtures up to 20 vol% of acetone, up to 40 vol% of ethanol in water/ethanol and up to 40 vol% of dimethylformamide in water/dimethylformamide mixtures. In [108] influence of various additives and cosolvents on conformation of PAAm in dilute aqueous solutions was examined by viscosimetry.

Dynamic light scattering was applied to study dynamic properties of PAAm gels and solutions as a function of temperature, PAAm concentration and crosslinking density [20]. The solutions exhibit two modes – a network mode formed through interchain entanglements and a slowly relaxing component of narrow distribution (disappears above 10 wt%). Existence of this slow-mode component was confirmed later in [52] where cohesive entanglements among PAAm chains in D_2O and their temperature-dependent behaviour for concentrations

from 2.5 to 10 wt% were studied by NMR. Such a system was found to have a high local viscosity and a soft-matter-like NMR relaxation nature. While in ordinary polymer solutions relaxation times increase with temperature, in this case methylene protons from the backbone chain exhibit an opposite behaviour – with rising temperature, the solvation weakens leading thus the chains to form curling coils, which reduces mobility (and T_1) of these methylene protons.

PAAm has a wide use. For instance in the form of gels, PAAm is used as a stationary phase for separation techniques such as electrophoresis, as an orienting medium to induce anisotropy of an environment. As a copolymer it is used as a water and nutrient reservoir for flowers in a vase. In the polymeric form, it is not harmful but in the form of monomers it is very toxic, mutagenic and carcinogenic.

2.3.3 PVCL Solutions

Aqueous Solutions of Linear PVCL

Poly(*N*-vinylcaprolactam) (PVCL) is a neutral water-soluble polymer that exhibits LCST behaviour triggered by temperature (see review by Aseyev et al. [4]). Its structure consists of a hydrophobic backbone chain with dangling cyclic amide (lactam) connected via the nitrogen atom on each monomer unit (see Fig. 3.5). This side ring has a chair conformation and it is syndiotactic when prepared by usual radical polymerization as was determined by quantum chemical calculations [33]. As one would expect, the polar nature of lactam determines the (partial) solubility in polar solvents such as water, alcohols or amides. But also some chlorinated and aromatic hydrocarbons such as tetrachlormethane, benzene, toluene or xylene can be good solvents due to the presence of hydrophobic parts in VCL units [34]. PVCL is amorphous with the glass transition temperature in the range between 147 °C [33] and 190 °C [102] (for dry linear PVCL) depending on its molecular weight. Such values determine PVCL to be a rather rigid-chain polymer. The authors reported that upon addition of 2 water molecules per monomer unit, hydrogen bonds between the carbonyl group C=O and H_2O establish which causes the chains' spacing increase and thus weakening of dipole–dipole (between polar amide groups) and dispersion forces (between caprolactam rings). Further increase of number of water molecules leads to the formation of associates that consist of molecules participating in hydrogen bonding with each other and with C=O. Upon addition of 2.6 to 8 water molecules per monomer unit the glass transition temperature decreases to a value between −17 and −43 °C. The carbonyl group dipoles act as "structure-breakers" (meaning breaking the water structure

made by a network of hydrogen bonds) – they disturb hydrogen bonding among water molecules weakening thus interactions between PVCL and water. The structure-breaking nature of PVCL is observable even in aqueous solutions with 200-300 water molecules per monomer unit as was revealed in an earlier study by Kirsh et al. from 1992 ([33] and references therein) using DSC measurements.

PVCL has come back into focus recently because of its potential applications in both chemical industry and biotechnology. It forms complexes and films easily and it is biocompatible – its LCST is near the temperature of human body and it exhibits a low cytotoxocity since, unlike *N*-alkylacrylamide-based polymers, upon hydrolysis, it does not produce low molecular weight amines because the amide group is a part of the ring. Vihola et al. [103] examined cytotoxicity of PVCL, PIPAAm and PVCL grafted with amphiphilic poly(ethylene oxide) (PEO) chains and of their monomers as well. These tests were performed on cells in vitro. PVCL and grafted PVCL were well tolerated (at concentrations 0.1 – 10.0 mg.ml^{-1}) after 3 hours of incubation at both room temperature and physiological temperature (37°C) (below and above the LCST). PIPAAm induced more clear cellular cytotoxicity at 37°C due to its more hydrophobic nature with respect to PVCL. The monomers exhibited much higher cytotoxicity in comparison with the corresponding polymers.

It is important to study PVCL/water systems also from the academic point of view since they have a high concentration of polar amide groups that surround water molecules and this can be found on the surface of protein molecules or inside their cavities, in reverse-osmotic membrane channels, active sites of enzymes, etc.

In the first work concerning the temperature-dependent solubility of PVCL in organic and aqueous solutions, which was published already in 1968 by Solomon et al. [77] the authors reported that the polymer precipitates from its aqueous solutions above 30°C and that the precipitation temperature does not depend on the concentration but on the molecular weight of the polymer. Later PVCL studies until 90's are reviewed in a book by Kirsh [34]. This book covers physico–chemical properties and synthesis of both the poly-*N*-vinylamides and their monomers. In particular solvation and conformational transformations of PVCL and poly-*N*-vinylpyrrolidone (PVP, it differs from PVCL only by the size of the ring on the monomer unit) in the solution are discussed. For PVP/water of polymer concentration around 8 mol% it is being proposed that there are 10 to 12 water molecules (altogether in 3 layers) per PVP monomer unit at room temperature (which is under the LCST of PVP). These results were obtained by NMR diffusion experiments, infrared spectroscopy and NMR ^{13}C chemical shifts.

In [19] properties of dilute aqueous PVCL solutions at 20°C (under the LCST) were examined by viscosimetry, static and dynamic light scattering and osmotic and refractometric measurements for a broad region of molecular weights.

A detailed study [94] of thermodynamic properties of PVCL aqueous solutions in the whole concentration range was published by Tager et al. State diagrams, thermodynamic functions of mixing and other parameters were obtained by cloud point method, by sorption of water vapour on polymer samples and by calorimetry. For molecular weight 12 000 g.mol^{-1} (similar to the systems we deal with in this thesis) the binodal in the state diagram exhibits the LCST at 307 K (34 °C). The authors concluded that both hydrophobic and hydrophilic hydration takes place. In the temperature and composition region close to the binodal the hydrophobic hydration predominates which leads to the decrease of the mutual miscibility of polymer and water and the phase separation is enabled.

From turbidimetric measurements [59] in the whole region of polymer concentrations in PVCL/water solutions it was reported that the LCST of PVCL is between 30 and 40 °C depending on both molar mass of the polymer and on its concentration in the solvent. With increasing length of the polymer chain the LCST shifts to lower polymer concentrations and temperature which is the classic Flory-Huggins miscibility behaviour. According to the general phenomenological analysis of this critical miscibility behaviour PVCL is a Type I polymer (as was confirmed later by DSC in [102]). From a calorimetric study of the melting behaviour of water Meeussen et al. obtained no evidence of the formation of a stable complex between polymer and water.

From a kinetic study of the phase separation in PVCL/water by modulated temperature DSC [102] it was found out that remixing is slower than demixing for PVCL of molecular weight between 30 000 and 68 000 g.mol^{-1}.

Aneufrieva et al. found out that both heating rate and heating profile affect the size and composition of mesoglobules – see [4] and references therein.

Maeda et al. [49] employed turbidimetry, DSC and FTIR to study phase separation in PVCL/water solutions with PVCL weight average molecular weight 13 000 and 150 000 g.mol^{-1} and concentration 50 g.l^{-1} (5 wt%). The critical value was found to be 32.5 °C for the LCST of the low-molecular-weight PVCL. FTIR revealed changes in hydrogen bonding of the amide group and the hydration states of the alkyl moieties.

Polymer dynamics in the PVCL/D_2O solution of a $c^* = 5$ g.l^{-1} threshold polymer concentration (the onset when the polymer molecules start to entangle) were studied by the neutron spin echo technique [46]. High-molecular weight

PVCL was used. The dynamical behaviour showed anomalies near the coil–globule transition. In globules the amplitude of the molecular motion was higher, being ascribed to a sequence of water hydrogen bonds breaking under the action of neighbouring amide groups. Under the LCST, the more apparent structure in water diminished the coil chain mobility.

In the later small angle neutron scattering study by Lebedev et al. [45] the globule association to form fractal structures (sponge-like) during the phase transition in PVCL/D_2O solutions was described. Again PVCL of high molecular weight in a c^* concentration was used. A broader range of phase separation 305 to 309 K was detected. Even at 305 K the initial decomposition was observed. With further increase of temperature the globule formation and later their aggregation was reported. The presence of surface fractals was confirmed. From changes in the surface fractal dimension the authors assumed that during the phase transition the interface geometry did not show significant changes. The interface area grew first due to the intense phase separation, then it became smaller because of the following aggregation.

There are many studies on dilute PVCL solutions although the coil–globule transition of single PVCL chains has not been experimentally observed since PVCL chains have a strong tendency to aggregate even in highly dilute solutions [5, 42, 44]. For such a polymer structure in the phase-separated solution the term mesoglobule is used. *"Mesoglobules are essentially equally sized globules obtained by association of more than one and less than all polymer chains in the system"* [101]. These compact structures are spherical with a rather monodisperse size distribution.

Properties of linear high molecular weight PVCL dilute aqueous solutions were extensively studied by dynamic light scattering (DLS) by Lau and Wu [42]. They obtained gyration radii, diffusion coefficients and hydrodynamic radii of the PVCL coils. The values were roughly the same as those reported by Makhaeva et al. [55]. Lau and Wu also obtained scalings between molecular weight and diffusion coefficient and between gyration ratio and molecular weight. The authors also introduced a novel method for the Flory Θ–temperature estimation which they found to be 29.5°C. They found out that at 25°C (under the LCST) water is a very good solvent for PVCL. Under these conditions of high dilution the LCST was found to be at 31.5°C and nearly independent of the PVCL concentration.

Colloidal stability as well as hydration changes during the phase transition were studied in PVCL/water dilute solutions (both H_2O and D_2O) by turbidimetry, DLS, high-sensitivity DSC and pressure perturbation calorimetry (PPC) for

polymers of molecular weight ranging from 21×10^3 to 1.5×10^6 g.mol^{-1} and keeping the solution concentrations in the dilute regime (0.1 g.l^{-1}) [44]. The authors reported that the LCST shifts to higher values with increasing molecular weight while the enthalpy is independent of the molecular weight. Above the LCST colloidally stable particles are formed – their hydrodynamic radius remains unchanged for several days if they were previously kept for an hour at 50°C. The hydrodynamic radius at 20°C (under the LCST) of polymer particles was reported to be from 4 to 24 nm depending on the molecular weight (the higher the molecular weight the bigger the hydrodynamic radius). At 50°C (above the LCST) the hydrodynamic radius was 180 nm for low molecular weight species and 80 nm for high molecular weight polymers. It implies that a globule (mesoglobule) consists of several polymer chains. A two-step phase transition was proposed – first a collapse of polymer chains occurs and then their aggregation comes. PPC was used to monitor the polymer hydration layer during the phase transition. It was found out that when the polymer chains collapse, the polymer-bound water molecules are released to the bulk solvent creating thus particles stabilized against further aggregation by hydrophilic surfaces. Also structure-making/structure-breaking properties of VCL and IPAAm monomers were studied by PPC and compared revealing thus that VCL has poorer water-structuring properties.

Aseyev et al. [5] were investigating properties of mesoglobules of PVCL, PIPAAm and PVME in dilute (0.025 wt%) aqueous solutions by static and dynamic light scattering. In the case of PVCL, the molecular weight was 30 000 and 330 000 g.mol^{-1}. The particles that formed above the LCST had a spherical shape and a very narrow size distribution. The size was dependent on the initial polymer concentration and the heating rate. It did not depend on the polymer molecular weight. The authors concluded that, generally, the observation of multimolecular aggregates does not rule out the possibility of high-molecular-weight polymers to adopt single-chain conformations. They expect long polymer chains to form single molecule globules whereas shorter chains to associate forming thus mesoglobules with the same fractal dimension 2.7 and a foam-like morphology of mesoglobules. Since the mesoglobules did not aggregate and since the osmotic second virial coefficient was zero, the authors concluded that the macromolecules self organize and build up particles with the polar groups turned towards the surrounding aqueous phase. The mesoglobules are very dense (even partial vitrification of PVCL in mesoglobules was observed [102]), thus the chain mobility is restricted which averts the chain reptation, the possibility of mesoglobules to merge during a collision is significantly reduced and this is what

makes mesoglobules colloidally stable.

Other PVCL Systems

Extensive studies were done on conformational changes of PVCL macromolecules and their complexes with ionic surfactants, salts, different organic compounds and copolymers with other polymer species in aqueous solutions. DLS results on systems PVCL/surfactant/water were reported in [55], PVCL/surfactant/salt/water and PVCL/surfactant/organic compound/water in [54], aqueous solutions of copolymers of PVCL and methacrylic acid in [53]. Temperature response of the LCST transition temperature depends on the molecular species (and its amount) added to the aqueous solutions and on the resulting hydrophobic/hydrophilic balance.

Also influence of the introduction of another polymer into PVCL/water solutions was investigated. LCST of PVCL shifts to lower values upon addition of poly(ethylene oxide) (PEO) into the PVCL/water solution as was revealed from DSC measurements [109]. PEO is a hydrophilic polymer, creates complexes with water molecules and is used to increase biocompatibility of a material when for example grafted on it. But despite its strong hydrophilic nature, in the studied PVCL/PEO/water ternary system the LCST decreased upon PEO addition, and since the LCST of PEO is 100°C, the authors assumed that there is a competition in interactions with water between PVCL and PEO in the ternary system. It results in weaking of PVCL–water interactions in the vicinity of PEO. In more concentrated solutions this phenomenon is more profound. The influence of the hydrophilic/hydrophobic balance on the LCST in thermosensitive water–polymer systems is governed by many factors that are interconnected and thus this effect is rather complicated.

Lowering of demixing temperatures caused by introduction of hydrophilic PEO grafts onto PVCL was confirmed by Van Durme et al. [102] for both aqueous PVCL solutions and hydrogels. Also the rate of phase separation became significantly higher.

PVCL gels are a subject of a great interest. As one would expect upon heating in water they undergo a sharp volume transition from a swollen state to a collapsed state as was revealed from turbidimetry and swelling curves measurements [56]. The same temperature dependence was studied in a water/alcohol mixture – with increasing temperature the PVCL gel shrunk first and then it expanded. In the presence of ionic surfactants the collapse temperature became

higher. Upon ionic surfactant introduction into the solution, additional swelling was observed. Later [61] two temperature-induced transitions were observed by high-sensitivity DSC: the first one at 31.5°C attributed to microsegregation resulting in hydrophobic domains formation (micromicelles), the second one at 37.6°C corresponding to the gel volume collapse itself.

Also PVCL physical gels can be created (at 50°C) using multifunctional phenols that make hydrogen bonds with VCL amide groups which are stable even at room temperature [43]. Such microgels have possible biomedical applications.

Interaction of water molecules with PVCL matrix in PVCL films was studied by dielectric spectroscopy [57], both water concentration and temperature were varied. It was found out that the mechanisms of temperature influence and water concentration are similar, they change the characteristics of hydrogen bonds. The main factor that determines the properties is temperature.

2.4 Review of Studies of Water/Ethanol Solutions

This chapter is devoted to results published on the peculiar solvent behaviour of water-ethanol mixtures. Such mixtures are, thanks to the ability of molecules to make hydrogen bonds, a rather complicated system. Even pure water has been studied for a very long time and still there is no unified conclusion on its structure in a liquid state.

One of the earliest works on water/ethanol solutions comes from 1960s by Bertrand et al. [8] who calculated partial molar entropies and other thermochemical parameters for ethanol in water and water in ethanol. From the entropy data the authors concluded that addition of small amounts of ethanol to water leads to an increase of the solution structuredness.

One of the concepts of the peculiar behaviour of water/ethanol mixtures is represented by works dealing with these mixtures in the whole range of compositions: [2, 11] use mainly NMR chemical shifts which can give information on the hydrogen bond strength while [66] determines cluster sizes using the mass spectrometric analysis.

First of the mentioned works was published in 1967 by Ageno and Indovina [2]. In the concentration dependence of water and ethanol OH chemical shifts, overlapping OH signals split into two (with increasing ethanol content). This signal splitting takes place at the concentration that corresponds exactly to the high-

est viscosity of the mixture and this conclusion is valid for both temperatures at which the authors carried out their experiments. At 32 °C this concentration is 56 vol% of ethanol in the mixture. The authors gave an explanation within the framework of the collective model of the hydrogen bond. When the ethanol concentration is smaller than that corresponding to the viscosity maximum, all ethanol molecules are hydrated and they join water clusters wherever a hydrogen bond is available. All the OH ^{1}H are then almost equivalent, owing to the rapid exchange of molecules between the different aggregates. When all hydrogen bonds available in water are saturated, the viscosity of the mixture reaches its maximum value. Further increase in the ethanol content results in a number of molecules and dimers of ethanol moving freely among the water aggregates decreasing thus the viscosity. When the excess of ethanol molecules becomes large, a growing number of alcohol molecules becomes hydrated (thanks to thermal collisions the mean water-chain length decreases and subseqent hydration of ethanol molecules takes place). As the excess of ethanol molecules increases, aggregates with a higher number of ethanol molecules become more probable.

Coccia et al. [11] in 1975 concluded from chemical shifts and lineshapes that the addition of small ethanol quantities ($\lesssim$ 22 vol% of ethanol at 20 °C) promotes hydrogen bonding among water molecules while in the concentration region 22 – 45 vol% of ethanol the water structures are being disrupted by the added ethanol and instead water–water hydrogen bonds, water–ethanol bonds are created and there are no purely water clusters. Between 45 and 93 vol% the ethanol prevents creation of water–water hydrogen bonds and ethanol–ethanol bonds start to occur. Above cca 93 vol% almost no water–water hydrogen bonds exist, there are water–ethanol bonds in the solution and water molecules either coordinate and/or are incorporated into linear ethanol aggregates.

In the work of Nishi et al. [66] mass spectrometry of clusters made by adiabatic expansion of liquid jets in vacuum revealed that up to 11.5 vol%, ethanol monomers and hydrated species $(C_2H_5OH)_m(H_20)_n$ are present – ethanol molecules tend to form chains (see Fig. 2.9) surrounded by water molecules which create hydration shells around ethyl groups. Above this concentration the hydrophobic hydration of ethanol is so strong that clusters consisting of pure water are non-detectable. Above 22 vol% the hydrogen bonding between water molecules becomes very week compared to ethanol-ethanol bonding. At 70 vol% the water–ethanol clusters are the most stable and fully saturated (at 30°C). In ethanol-rich solutions, larger ethanol polymers tend to dissociate with increasing ethanol content and temperature.

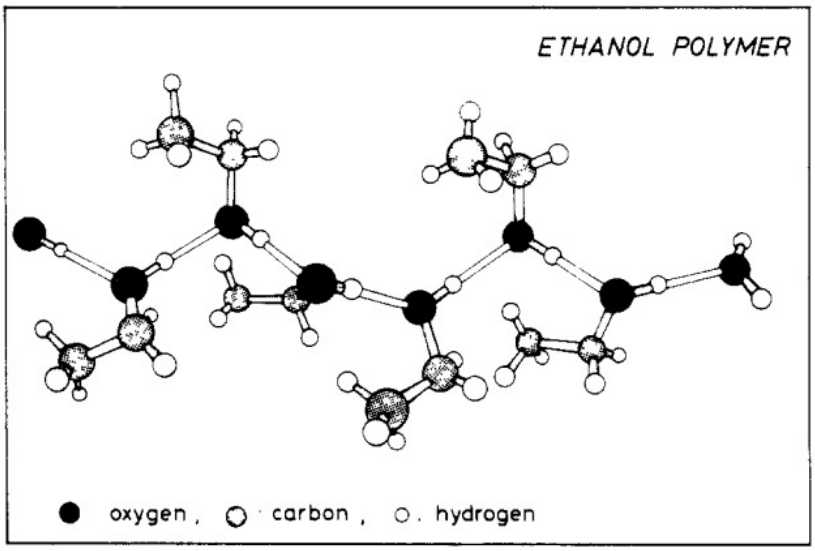

Figure 2.9: A proposed model of an ethanol polymer with water molecules at the ends. The picture was taken from [66].

Little bit different results were reported in [62] where the hydrogen bonding in water/ethanol mixtures was studied by means of NMR (using an external reference method) and FTIR. It was reported that the hydrogen bonds of water hydrogens become stronger with increasing content of ethanol in the mixture. The ethanol OH forms a hydrogen bond which bonding strength increases with increasing concentration of ethanol, both oxygen and hydrogen in OH of ethanol participate in the hydrogen bonding. They also concluded that the size of ethanol aggregates increases with ethanol concentration in the mixture and that this self-association of ethanol molecules may cause the cooperativity effect of the hydrogen bonds within the aggregate and the hydrophobic interaction of the alkyl groups.

Influence of various chemical compounds on hydrogen bonding in water/ethanol solutions was investigated too, e.g. for a NMR study of the influence of salts, acids and phenols see [68].

2.5 Review of Publications on Cononsolvency Effect

Cononsolvency is a phenomenon when two solvents that are good for a certain polymer become a bad solvent for it upon their mixing. A vast majority of conon-

solvency studies was done on PIPAAm solutions although several works on other polymer species were published recently (e.g. for a recent polyvinylpyrrolidone study see [25]).

To our best knowledge, the only cononsolvency study concerning PIPMAm is that by Alenichev et al. [3]. It deals with swelling and mechanical behaviour of neutral and charged PIPMAm and PIPAAm networks in mixed solvents of water and ethanol at room temperature by swelling and mechanical measurements. A strong cononsolvency effect was reported for uncharged and negatively charged gels of both polymer systems. For polymers in neat water and in neat ethanol high degree of swelling was observed while for polymers in solvent mixtures the swelling exhibited pronounced minima. These minima are connected with the coil–globule transition of network chains. For uncharged networks there is a minimum around 40 vol% of ethanol. In the case of negatively charged networks (by introducing a comonomer sodium methacrylate) it shifts with increasing content of the charge, becomes more shallow and from a certain ionic comonomer content two minima appear. For all systems it was reported that mechanical behavior is predominantly determined by the degree of swelling regardless of the charge concentration.

In further text we will focus on results on PIPAAm since it differs in its structure only by a methyl group from PIPMAm. Since 1968 when the LCST behaviour of PIPAAm was published for the first time [29], it attracted attention of many researchers. In all works mentioned below, unless specified otherwise, the solvents that were used were water and methanol.

Winnik et al. [106] performed cloud point measurements (by turbidimetry) of PIPAAm/water/methanol solutions and published the corresponding phase diagram (see Fig. 2.10). The authors stated that in PIPAAm/water solution water molecules can bond to the polymer's amide group leading thus to formation of a layer of highly organized water molecules surrounding the polymer. These polymer–water interactions contribute favourably to the free energy of mixing but unfavourably to the entropy of mixing. Upon a temperature increase, this bound water is released, the entropic term becomes dominant resulting in a positive free energy of mixing and a two-phase system is preferred. In water/methanol mixtures up to 5 mol% of methanol, the methanol molecules are few and in this solution they are hydrated and do not make hydrogen bonds neither with polymer nor with other methanol molecules. With increasing methanol concentration, methanol molecules interact with polymer segments. In solutions with high methanol content (above 45 mol%) the predominant interactions are those

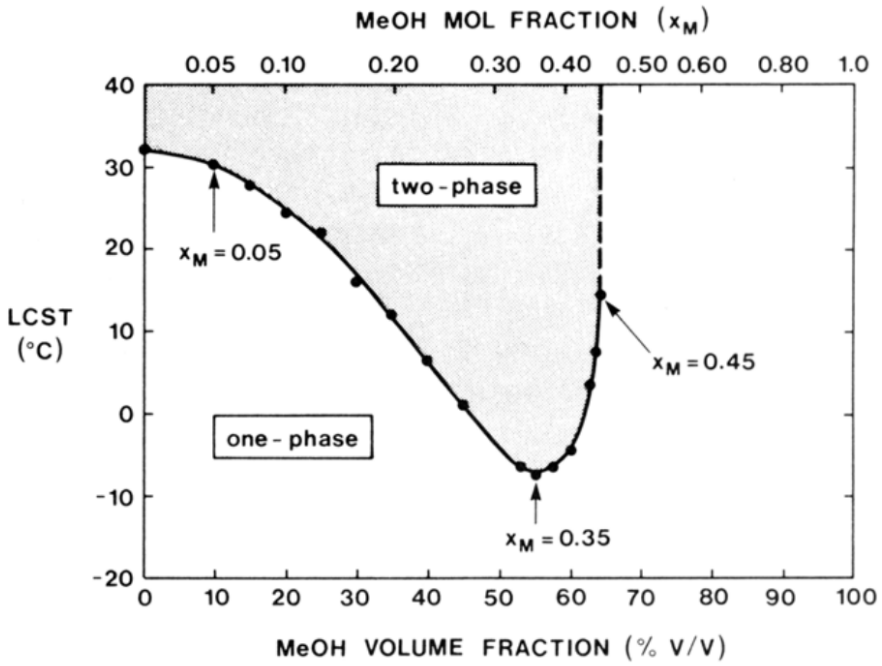

Figure 2.10: Phase diagram of 0.1 wt% PIPAAm in a water/methanol mixture. The picture was taken from [106].

between the polymer and methanol.

In an electron paramagnetic resonance (EPR) and ^{13}C NMR study of spin-labeled PIPAAm in water/methanol solutions published by Winnik et al. [105], the authors proposed a model that involved the preferential adsorption of methanol to the PIPAAm chains, as the main contributor to the cononsolvency effect. According to their results, there is a ternary complex between PIPAAm, water and methanol and the structural changes occur mainly at the outer solvent layers of the highly ordered structure that is present already in the dissolved phase. Their results are strongly against the mechanism that involves solely preferential adsorption around the nitroxide group.

These results are in agreement with those obtained by Schild et al. [75] by cloud point and microcalorimetric measurements. The authors found out that interactions that are relevant for cononsolvency effect arise from local contacts between polymer and solvent.

Costa et al. [12] studied PIPAAm phase-separation behaviour in several solvents. Methanol and acetone caused a single LCST behaviour while ethanol and other non-alcohols caused both LCST and UCST behaviour. The authors concluded that it depends on the hydrophobic nature (size and shape of hydrophobic

groups and the potential to hinder hydrophobic hydration) of the solvent. A correlation between the change from the LCST to the UCST and the competition between polymer–water and polymer–cosolvent interactions is mediated by compositional factors. The cononsolvency was qualitatively explained by weakening of the polymer-solvent interactions due to the preferential hydrophobic hydration among solvent molecules in the water-rich region. The disruption of hydration shells with increasing cosolvent concentration allows polymer–solvent interactions.

Similar results as in [106], obtained by viscosity and static light scattering measurements, were reported in [10]. From thermodynamic parameters it was concluded that water–methanol complexes were formed by direct bonding of one water molecule with one methanol molecule. These structures affect the phase transition remarkably. Up to 20 vol% of methanol there may be a preferential adsorption of purely water molecules on the polymer, the LCST decreases with the methanol content increase because of the small amount of water–methanol complexes. Above 70 vol% there is a preference for methanol adsorption. Between 40 and 55 vol% also complexes are adsorbed causing thus the clathrate-like structure around PIPAAm side chains to become more damaged which helps the phase separation to occur. The thermodynamic behaviour between the polymer and the mixed solvent was attributed to different preferential adsorption phenomena related to different degrees of the polymer–solvent and the solvent–solvent interactions.

F. Tanaka et al. [97] studied cononsolvency effect with PIPAAm in a mixed solvent of water and methanol. The authors extended their previously reported model of cooperative hydration [72] – see Fig. 2.11. They showed that the sharp reentrant coil–globule-coil transition is caused by the competition between formation of PIPAAm–water and PIPAAm–methanol hydrogen bonds and that this competition becomes stronger with the cooperativity. A new statistical-mechanical model based on this competitive hydrogen bonds was introduced. From the mean square end-to-end distance calculations it was found out that the chain collapses sharply at the 0.2 molar fraction of methanol, stays collapsed up to 0.4 and at 0.6 it regains the swollen state.

In their latest work [96] Tanaka et al. reported that the transition becomes sharper with the cooperativity parameter of hydration. From calculations and comparison of the results with experimental data the authors concluded that there is a decrease of the LCST with the methanol mole fraction due to the competition.

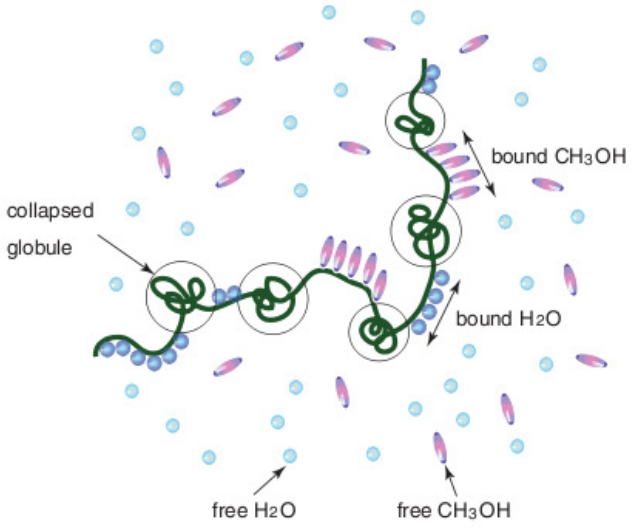

Figure 2.11: This picture describes a competition between PIPAAm-water and PIPAAm-methanol hydrogen bonds formation. When a strong cooperativity takes place, continuous one-species-sequences are formed along the chain causing thus the adoption of a pearl-necklace conformation of the chain. The picture was taken from [97].

Chapter 3

Experimental Part

3.1 Samples Preparation

3.1.1 PIPMAm in Binary Solvents

N-isopropylmethacrylamide (IPMAm, purchased from Fluka) (see Fig. 3.1 for the chemical structure) and sodium methacrylate (MNa) (Fig. 3.2) were used to prepare powdered PIPMAm homopolymer (uncharged) and powdered poly(*N*-isopropylmethacrylamide-*co*-sodium methacrylate) (P(IPMAm-*co*-MNa)) copolymers (negatively charged in aqueous solutions) with ionic comonomer mole fractions 0, 5 and 10 mol% (see Fig. 3.3 for the chemical structure of P(IPMAm-*co*-MNa)). 4,4'-azobis(4-cyanopentanoic acid) was used as an initiator and polymerization was carried out in a water/ethanol mixture (D_2O/EtOH) with D_2O/EtOH volume ratio 6/94; the volume fraction of the sum of the monomers in the mixture was 0.2 [92]. Since the nature of the initiator is free-radical we assume that the P(IPMAm-*co*-MNa) copolymers are statistical. After polymerization and subsequent drying of polymers to constant weight, PIPMAm/D_2O/EtOH and P(IPMAm-*co*-MNa)/D_2O/EtOH solutions (D_2O contained 99.9% of deuterium) with polymer concentration $c = 5$ wt% and EtOH volume fractions in D_2O/EtOH mixtures 0, 20, 30, 40, 50, 60, 80 and 95 vol% were prepared.

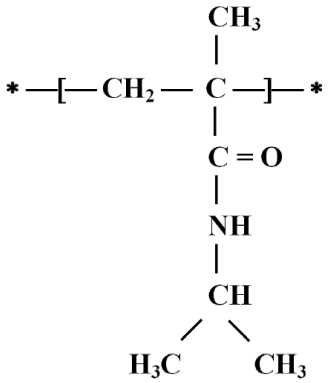

Figure 3.1: Chemical structure of PIPMAm

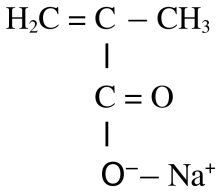

Figure 3.2: Chemical structure of sodium methacrylate

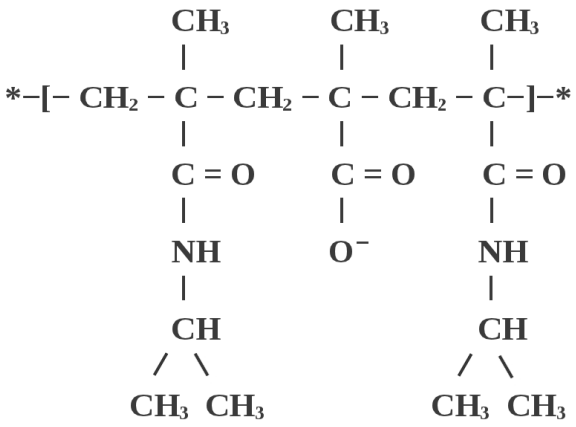

Figure 3.3: Chemical structure of P(IPMAm-*co*-MNa)

3.1.2 P(IPMAm-*co*-AAm) Copolymers in D_2O and in Binary Solvents

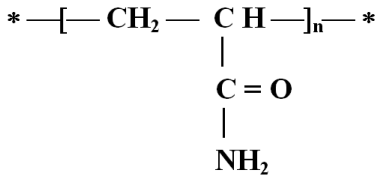

Figure 3.4: Chemical structure of PAAm

Linear PIPMAm homopolymer and poly(*N*-isopropylmethacrylamide-*co*-acrylamide) (P(IPMAm-*co*-AAm)) copolymers were prepared by radical copolymerization of powdered AAm (purchased from Fluka) (see Figure 3.4) and/or powdered IPMAm (purchased from Aldrich) in water/ethanol mixture (85/15 by volume) solutions at 60°C for 24 hours. The weight fraction of the sum of the monomers in the reaction mixture was 0.25 and the AAm molar fractions in the mixture were 0.05, 0.15, 0.25, 0.40, 0.50, 0.70 and 0.85. 4,4´-azobis(4-cyanovaleric) acid was used as an initiator. After polymerization diethylether, ethanol or hexane were used to precipitate copolymers and to wash out residual monomer units and short copolymer chains twice. Molecular weights M_w and M_n of PIPMAm and P(IPMAm-*co*-AAm) were determined by the gel permeation chromatography (GPC) with Superos 6 by Amersham Bio Sciences, M_w of copolymers ranged from 124 000 to 800 000 g.mol^{-1}, M_w/M_n were from 1.2 to 3.7 for copolymers and 3.7 for the PIPMAm homopolymer. M_w and polydispersity M_w/M_n for those copolymers that exhibit temperature-induced phase separation in solutions are shown in Tab. 5.4.

Several samples of the PIPMAm homopolymer and P(IPMAm-*co*-AAm) dissolved in D_2O and in mixed solvents of D_2O/EtOH or D_2O/acetone with polymer concentration 5 wt% and with various solvent compositions were prepared. Ethanol was purchased from Merck and acetone from Lach-Ner, s.r.o. D_2O (purchased from Sigma Chemical Co.) contained residual water – D_2O/H_2O volume ratio was 99.9/1. Results reported in this work were obtained on systems listed in Tab. 5.5 in Chapter 5.2.

3.1.3 PIPMAm/PVCL Mixtures

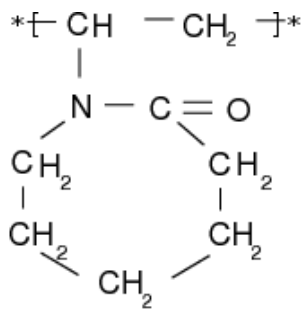

Figure 3.5: Chemical structure of PVCL

N-vinylcaprolactam (VCL, purchased from Aldrich) (see Fig. 3.5 for the chemical structure), distilled at low pressure (128°C at 2.8 kPa), was used for a radical polymerization with 2,2'-azobis(2-methylpropionitrile) (AIBN) as an initiator. The polymerizaton was carried out in toluene at 65 °C for 24 hours in a sealed glass ampule. Three rounds of precipitating the poly(*N*-vinylcaprolactam) (PVCL) in hexane and dissolving in THF were performed to dispose of oligomers. Then it was dried to constant weight. After the drying, samples of PIPMAm/-PVCL/D_2O solutions with several polymer concentrations (0.1 wt%, 1 wt%, 5 wt%, 10 wt%) and PIPMAm/PVCL molar ratios (0/1, 1/3, 1/1, 3/1, 1/0) were prepared. The weight average molecular weight of the prepared PVCL was 40 000 g.mol^{-1} and the polydispersity 3.33.

All samples (if not stated otherwise) were degassed and sealed under dry gaseous nitrogen in 5 mm NMR tubes, sodium 3-(trimethylsilyl)-1-propanesulfonic acid, sodium salt, 97% (DSS), purchased from Aldrich Chem. Co.) was used as an internal NMR standard.

3.1.4 Experiments Using an External Standard

Some experiments require a standard containing a constant number of resonating nuclei so that the number of resonating nuclei in our sample (and thus content of a given component) could be related. Integrated intensities correspond to the number of resonating nuclei [26]. To compare integrated intensities (and thus the content of a given component) between different experiments we used DSS an external standard to calibrate the number of resonating nuclei. A special

coaxial tube was used for such experiments. DSS was placed in a thin tube which was inserted into the 5 mm NMR tube containing the polymer solution. The inner tube containing DSS was sealed and it was possible to insert it into various samples of polymer solutions.

3.2 Methods of Measurement

All high-resolution NMR experiments were performed with a Bruker Avance 500 spectrometer with ^{1}H resonance frequency 500 MHz. Temperature was maintained constant within ± 0.5 K using a BVT 3000 temperature unit. After each change of temperature, experiments were started 15 minutes after the gas flow temperature stabilized to ensure the sample to get to equilibrium. From time dependences of NMR integrated intensities after a jump change of temperature (for both cooling and heating) through the phase transition, it was reported that the corresponding integrated intensity changes quickly, mostly in first 3 minutes, which is the time necessary to reach the desired temperature in the sample. After this time the integrated intensities are constant [28, 84, 85]. During the measurements of temperature dependences the temperature was increased (heating) in our experiments. This is important since there is a hysteresis between heating and cooling caused probably by formation of structures within one polymer chain (intrachain hydrogen bonding) in the globular state [104].

3.2.1 ^{1}H and ^{13}C Spectra

Typical experimental conditions used to obtain ^{1}H high-resolution NMR spectra were as follows: resonance frequency 500.1 MHz, 16 scans, spectral width 5 kHz, acquision time 1.64 s, relaxation delay 10 s, $\frac{\pi}{2}$-pulse duration 13.7 μs (for results in Section 5.1), 14 μs (for results in Section 5.2) and 13.25 μs (for results in Section 5.3).

^{13}C spectra were measured at a resonance frequency 125.7 MHz, usually with 128 scans separated by a relaxation delay 80 s, with a spectral width 30 kHz and under full proton decoupling. $\frac{\pi}{2}$-pulse width was 13.9 μs.

Integrated intensities were figured out using the spectrometer integration software (built in Topspin 1.3) with an accuracy of $\pm 1\%$ and $\pm 3\%$ for ^{1}H and ^{13}C spectra, respectively.

NMR Spectra Analysis

The stationary solution of Bloch equations gives the shape of the absorption signal ν at frequency ω in the dependence on the relaxation times as [1]

$$\nu = \omega_0 \chi_0 \mathrm{H_1 T_2} [1 + (\Delta\omega \mathrm{T_2})^2 + \gamma^2 \mathrm{H_1^2 T_1 T_2}]^{-1} \tag{3.1}$$

where

$\omega_0 = \gamma \mathrm{H_0}$ is the resonance frequency, where $\mathrm{H_0}$ is the external magnetic field intensity $\mathrm{H_0} = \dfrac{\mathrm{B_0}}{\mu_\mathrm{m}}$,

$\mathrm{H_1}$ is the intensity of the radiofrequency field,

$\Delta\omega = \omega_0 - \omega$,

γ is the gyromagnetic ratio and

χ_0 is the static nuclear susceptibility $\chi_0 = \dfrac{\mathrm{N}\mu^2}{3k_\mathrm{B}\mathrm{T}}$, where N is the number of nuclei per unit volume, μ is the magnetic moment of the nucleus, k_B is the Boltzmann constant and T is the absolute thermodynamic temperature.

Integration of the Eq. 3.1 gives the integrated intensity [87]:

$$I = \frac{\mathrm{KN}}{\mathrm{T}} (1 + \gamma^2 \mathrm{H_1^2 T_1 T_2})^{-\frac{1}{2}} \tag{3.2}$$

where $\mathrm{K} = \dfrac{(\pi \omega_0 \mu^2 \mathrm{H_1})}{3k_\mathrm{B}}$ and $(1 + \gamma^2 H_1^2 \mathrm{T_1 T_2})$ is the so called saturation factor σ. The saturation factor $\sigma \approx 1$ in the case of the Fourier transform (FT) pulse NMR methods. In addition, assuming that the relaxation delay (the delay between two following scans) is $\geq 5\mathrm{T_1}$ to enable the nuclei to get back to the equilibrium state, the temperature dependence of the integrated intensity is given by:

$$I_0(\mathrm{T}) = \mathrm{KN} \frac{1}{\mathrm{T}} \tag{3.3}$$

When the phase separation occurs in a polymer solution, two components appear – a component consisting of the phase-separated polymer units ($\mathrm{N_{phase\text{-}separated}}$) and a solution with non-phase-separated polymer units ($\mathrm{N_{non\text{-}phase\text{-}separated}}$). As was said earlier, integrated intensities of polymer peaks are directly related to the phase-separated fraction of polymer units. For segments forming globular-like structures in $\mathrm{D_2O}$ solutions of PIPAAm or poly(*N*,*N*-diethylacrylamide)

(PDEAAm) linewidths 3 – 4 kHz were detected [85, 86] which are comparable to the spectral width 5 kHz used in our measurements, so the signals of units involved in globular-like structures are thus not detectable in high-resolution spectra.

The phase-separated fraction of polymer units (p–fraction) can be determined directly from the spectra using integrated intensities [28, 83, 84, 85]:

$$p = \frac{\mathrm{N_{phase\text{-}separated}}}{\mathrm{N_{non\text{-}phase\text{-}separated}}} = 1 - \frac{I(\mathrm{T})}{I_0(\mathrm{T})} \tag{3.4}$$

where I is the integrated intensity of a given polymer signal while I_0 is the integrated intensity of the same signal in the homogeneous (non-phase-separated) state.

Since the integrated intensity depends on temperature (Eq. 3.3), when analyzing temperature dependences of p–fraction, one has to use this relation for determination of the p–fraction:

$$p = 1 - \frac{I(\mathrm{T})}{\frac{\mathrm{T_0}}{\mathrm{T}} * I_0(\mathrm{T_0})} \tag{3.5}$$

where $I_0(\mathrm{T_0})$ is the integrated intensity of a given polymer signal in a non-separated solution at temperature $\mathrm{T_0} <$ LCST and $I(\mathrm{T})$ is the integrated intensity of the same polymer signal in a partly/completely phase-separated solution at temperature $\mathrm{T} > \mathrm{T_0}$.

When determining the LCST temperature from NMR tempertaure dependences of the p–fraction, we take the temperature value at the beginning of the phase transition region.

3.2.2 Relaxation Experiments

For the **^{1}H spin-spin relaxation times $\mathbf{T_2}$** of HDO protons the CPMG [60] pulse sequence

$$90^\circ_x \text{ — } (\ \mathrm{t_d} \text{ — } 180^\circ_y \text{ — } \mathrm{t_d}\ )_\mathrm{n} \text{ — acquision}$$

was used. The experimental conditions were as follows: for results in Section 5.1 the delay $\mathrm{t_d}$ (echo time) was 5 ms and 0.5 ms for homogeneous and phase-separated solutions, respectively, number of scans (NS) was 8 or 16, relaxation delay between scans (D1) was 80 s; for results in Section 5.2 $\mathrm{t_d}$ =5 ms, NS = 4 and D1 = 180 s; for results in Section 5.3 $\mathrm{t_d}$ =5 ms, NS = 1 and D1 = 100 s.

Spectral width was 3.5 kHz in all cases.

In the case of **^{13}C spin–spin relaxation times T_2** the relaxation delay was 80 s and t_d was set to 5 or 0.5 ms.

For **^{1}H spin–lattice relaxation times T_1** determination the inversion recovery pulse sequence was used:

$180° — \tau — 90°$ — acquisition

The number of scans was 4, relaxation delay 180 s, spectral width 3.5 k Hz, 10 – 18 τ values ($\tau \in < 0.1; 250 >$ s) were used.

In all cases the relaxation delay was long enough to allow the complete recovery of magnetization. All obtained ^{1}H and ^{13}C relaxation curves were monoexponential and the fitting process enabled us to determine a single value of the relaxation time.

3.2.3 Experiments for Signal Assignment

HMQC

The experimental settings for the Heteronuclear Correlation through Multiple Quantum Coherence (HMQC) experiment (2D ^{1}H–^{13}C correlation via heteronuclear zero and double quantum coherence with decoupling during acquisition using gradient pulses for selection) were following: 4 scans, relaxation delay 2 s, ^{1}H $\frac{\pi}{2}$-pulse length 8.7 μs at 6 dB and for ^{13}C pulses the length was adjusted to 17.5 μs at 5 dB and for the decoupling sequence it was 80 μs at 18 dB.

INEPT

Insensitive Nuclei Enhanced by Polarization Transfer (INEPT) experiment for non-selective polarization transfer with decoupling during acquisition was performed with the following adjustment: 1024 scans, relaxation delay 5 s, ^{13}C $\frac{\pi}{2}$ -pulse length 9.5 μs at 7 dB, ^{1}H $\frac{\pi}{2}$-pulse length 14.3 μs at 5 dB and cnst11 adjusted to view either CH, CH_2 and CH_3 groups with positive intensity or CH groups only or CH and CH_3 positive while CH_2 negative.

Chapter 4

The Aims of the Thesis

In this work we will focus on the following problems:

1. Cononsolvency effect – we will study PIPMAm in binary D_2O/EtOH solvents. Our focus will be on the shift of the LCST temperature and extent of the phase transition in dependence of D_2O/EtOH composition.

2. Effect of charge in PIPMAm/D_2O/EtOH solutions – we will introduce negative charge into the polymer chains and we will study its influence on the phase separation properties. To our best knowledge, the effect of charge introduced into polymer chains on cononsolvency effect has not been studied yet.

3. Random copolymers of IPMAm and AAm in D_2O and in binary D_2O/EtOH or D_2O/acetone solvents. PIPMAm/D_2O was already studied and we are interested in the importance of the presence of AAm units in the polymer chains. PAAm does not undergo the temperature-induced phase separation while PIPMAm does, PAAm undergoes phase separation upon change of solvent composition. Moreover, PIPMAm exhibits cononsolvency effect in water/alcohol solutions while PAAm does not. So AAm units should influence the phase separation strongly.

4. Mixtures of PIPMAm and PVCL in D_2O – in the polymer solution, two linear polymers are present so both phase transitions should be observable. We will study the mutual influence on each other's phase separation behaviour.

In all cases we will also study relaxation behaviour of the solvent to get insight into dynamical properties of polymer structures in the phase-separation region.

Chapter 5

Results and Discussion

Phase separation in polymer solutions can be influenced by changes of various parameters. This thesis deals with influences of temperature, solvent composition, charge introduced in polymer chains, composition of monomer species in the polymer chain and composition of mixtures of different one-monomer-type-polymers. NMR is a powerful tool for the study of various properties of the phase separation which enables us to examine individual polymer groups separately. In the case of the copolymer systems the biggest advantage of NMR is that it can provide quantitative information on the phase-separation behaviour of both copolymer components separately. Also relaxation behaviour of solvent molecules is treated in this thesis. Upon phase separation, part of solvent molecules stays bound inside globular structures or bound to their surface. The mobility of these bound solvent molecules is restricted. The remaining bulk water molecules are relatively free. NMR relaxation times reflect the mobility of molecules and thus are used as a useful tool to study changes in the molecular mobility induced by the phase separation.

As was said earlier, the solution where a polymer is dissolved is transparent. Upon phase separation globular structures occur, which diffract light and the solution becomes turbid (see Fig. 5.1).

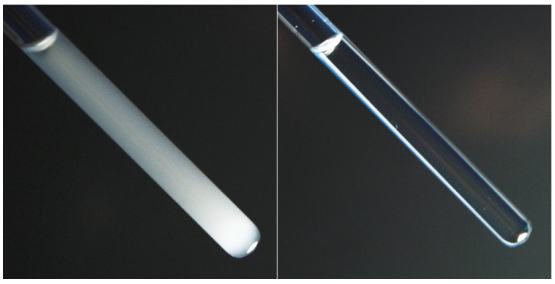

Figure 5.1: Phase separated (on the left-hand side) and homogeneous (on the right-hand side) PIPMAm/D_2O/EtOH solution [39].

5.1 PIPMAm in D_2O/EtOH Solutions

5.1.1 PIPMAm/D_2O/EtOH Solutions. Cononsolvency Effect

In the case of PIPMAm/D_2O, the factors that induce phase separation in solutions are both temperature and solvent composition. The temperature-induced behaviour of this polymer in neat D_2O is well described already (see Chapter 2.3). We focused on the phase separation behaviour in mixed D_2O/ethanol solvents in our work.

Fig 5.2 shows ^1H NMR spectra of PIPMAm in D_2O/EtOH mixtures with various EtOH content (20 vol%, 30 vol% and 40 vol%) measured at 298 K under the same instrumental conditions. The spectral lines assignment is shown directly in the spectra. The strong signal on the left-hand side is a merged signal of D_2O and EtOH OH ^1H (with predominant contribution of EtOH). PIPMAm isopropyl CH_3 ^1H signal overlaps with the strong CH_3 signal of EtOH. A comparison of these three spectra exhibits partial and total suppresion of PIPMAm signals for samples containing 30 and 40 vol% of EtOH, respectively. It is caused by the fact that a part (Fig. 5.2b) or all (Fig. 5.2c) PIPMAm units are involved in globular-like structures formed by aggregated polymer chains with resticted mobility. This interpretation is in agreement with the fact that PIPMAm/D_2O/EtOH solutions containing 30 and 40 vol% of EtOH are turbid at 298 K. It is evident that the mobility of PIPMAm segments in mesoglobules is reduced to such an extent that the corresponding NMR lines become too broad to be detected in high-resolution NMR spectra. (The lines are actually broader than the whole measured spectrum and contribute to the baseline which results in a significant decrease of polymer signals' integrated intensities - see Chapter 3.2.1). Such changes have been previ-

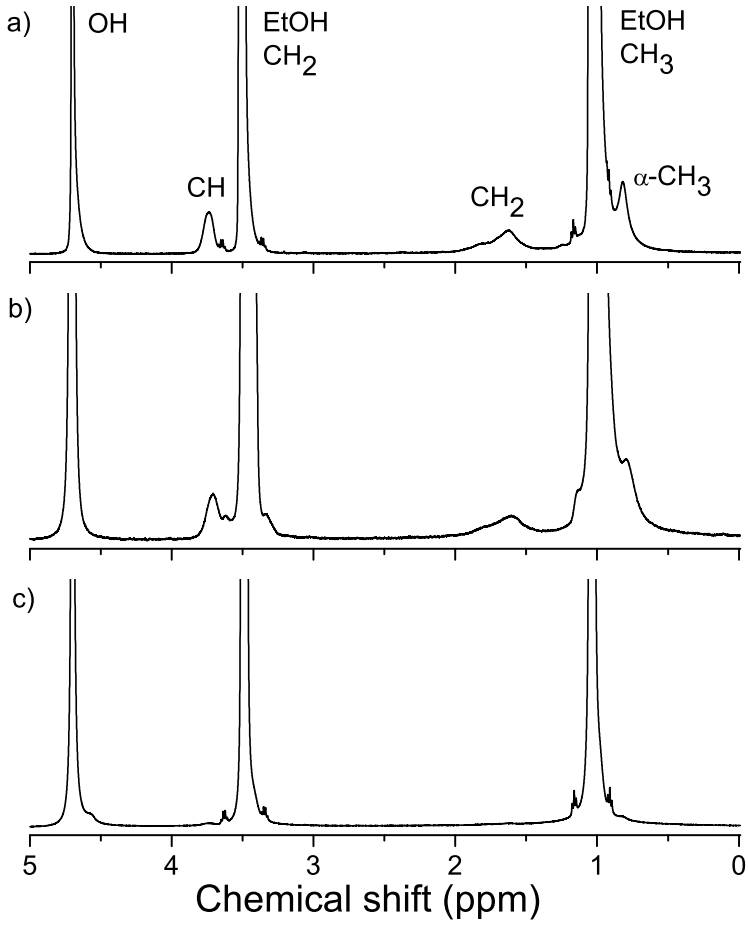

Figure 5.2: ^{1}H NMR spectra of PIPMAm in D_2O/EtOH mixtures with EtOH content 20 vol% (a), 30 vol% (b) and 40 vol% (c) measured at 298 K [38].

ously observed for the temperature-induced phase separation in PIPMAm/D_2O solutions [92]. The integrated intensities of EtOH signals in (Fig. 5.2a–c) follow the ratio of molar EtOH fractions in the corresponding solutions, thus confirming that all EtOH molecules are directly detected in ^{1}H NMR spectra in all cases. In these PIPMAm/D_2O/EtOH systems no precipitation (sedimentation) was observed even after a long time in the order of days.

It turned out that it is useful to observe the phase-separated fraction of the polymer (p–fraction – see Chapter 3.2.1 for its definition). Dependences of the p–fraction in PIPMAm/D_2O/EtOH solutions on the EtOH content in the D_2O/EtOH mixtures were obtained from integrated intensities of polymer CH and CH_2 ^{1}H at various temperatures (see Fig. 5.3). At 298 K (Fig. 5.3a) the dependence of p–fraction on EtOH content exhibits a maximum for the solution containing 40 vol% of EtOH (i.e. 17.6 mol% of EtOH in the D_2O/EtOH mixture). At this critical value of EtOH content, the p–fraction for CH_2 protons $p \approx 1$. It means that the mobility of all these protons is restricted and one can say that all PIPMAm units are involved in the phase-separated mesoglobules for this solvent composition. With the increase of EtOH content above 40 vol% the fraction of PIPMAm units with restricted mobility decreases and for the solution with the highest EtOH content (95 vol%) the p–fraction $p \approx 0$ (as in the PIPMAm/D_2O solution). Similar cononsolvency effect was previously found for PIPMAm networks in water/EtOH mixtures at room temperature; in solutions containing 40 vol% of EtOH a significant swelling minimum was observed [3].

Dependences of p–fraction vs. EtOH content at temperatures above ambient are plotted in Fig. 5.3b and c for 313 K and 328 K, respectively. Values of p–fraction of PIPMAm in neat D_2O ($p \approx 0$ at 313 K, $p \approx 1$ at 328 K) agree with the fact that LCST of aqueous PIPMAm solutions is around 315 K [23, 65, 88, 91, 92]. With increasing temperature the region of the phase separation in PIPMAm/D_2O/EtOH solutions extends towards lower EtOH content. At the highest temperature (328 K) the maximum value of p–fraction $p \approx 1$ was observed in the solutions with 0 – 40 vol% EtOH content. This probably is due to the disruption of hydrogen bonds between solvent molecules and polymer groups and higher preferences of polymer–polymer hydrophobic interactions during the increase of temperature above the LCST [22]. The fact that the solutions with rather high EtOH content (above 60 vol%) remain homogeneous regardless of the temperature indicates the positive role of EtOH in stabilization of the polymer–solvent interactions.

Another interesting result can be extracted from these dependences. At 298 K,

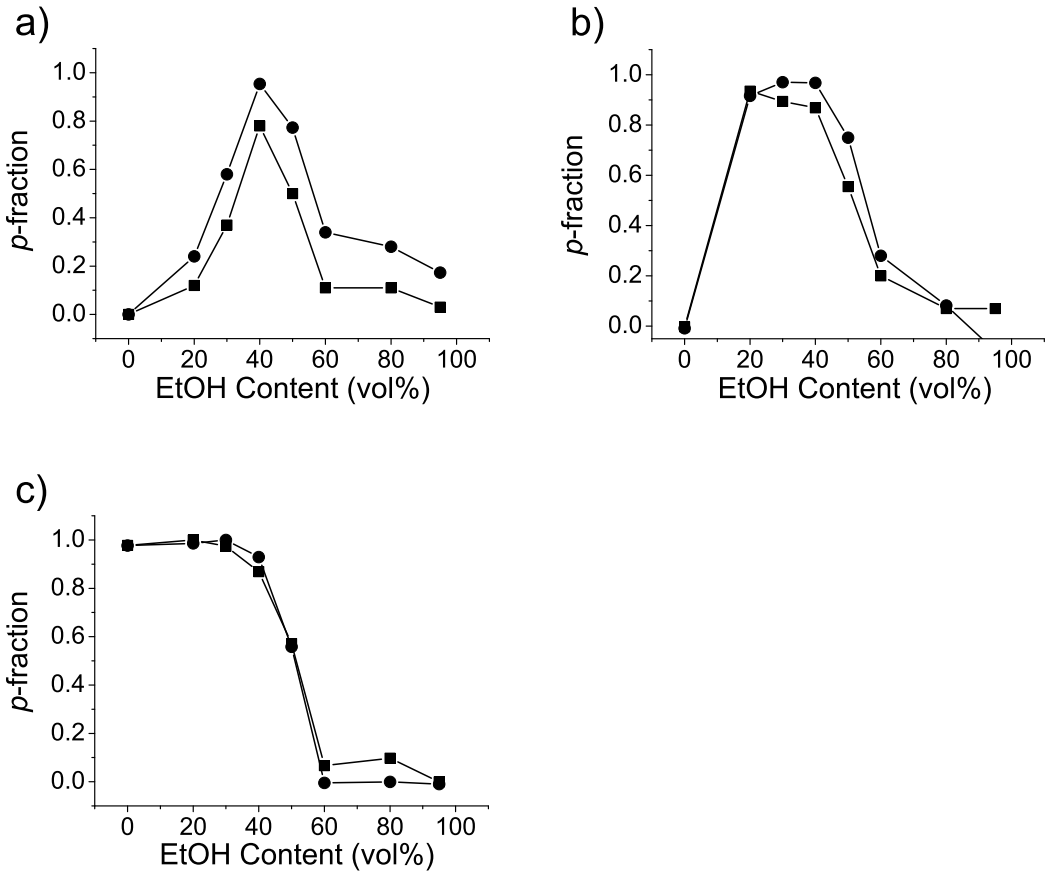

Figure 5.3: Phase-separated fraction p for PIPMAm solutions in D_2O/EtOH mixtures ($c = 5$ wt%) as a function of EtOH content as determined for CH (■) and CH_2 (●) protons of PIPMAm at 298 K (a), 313 K (b) and 328 K (c) [38]. Estimated experimental error ±2%.

when the phase separation is induced by the cononsolvency effect, a noticeable difference in the dependences of p on EtOH content for polymer CH and CH_2 groups is observed (signals corresponding to PIPMAm CH_3 groups were not processed because of the overlap with the CH_3 band of EtOH as was shown in Fig 5.2). p–fraction values which were determined from integrated intensities of the main chain CH_2 protons are systematically higher than those of the side chain CH group. This could give rise to a presumption that some side chains of the phase-separated PIPMAm units probably still are in the interaction with the solvent molecules (and thus are more mobile) while the backbone chains are not. Such a behaviour is in contrast to the phase separation induced by temperature (328 K, see Fig. 5.3c) where the p–fraction dependences on the EtOH content are essentially the same for main chain CH_2 and side chain CH polymer protons. Behaviour of the polymer protons during the temperature-induced phase separation was reported to be identical (the main chain protons behaved similarly to the side chain protons) in PIPMAm/D_2O and poly(vinyl methyl ether)/D_2O solutions [28, 92].

To characterize the influence of the phase separation on various polymer groups, ^{13}C NMR spectra of PIPMAm solutions were measured as well. ^{13}C spectra for PIPMAm/D_2O/EtOH solutions containing 0, 95 and 40 vol% of EtOH are shown in Fig 5.4a, b and c, respectively. The NMR pulse sequences HMQC and INEPT (see Fig. 5.5) were used for the ^{13}C resonances assignment. This assignment is denoted in the Fig. 5.4a. Spectral lines of various PIPMAm carbons are well resolved except for the α–CH_3 carbons line which is overlapped with the CH_3 line of EtOH. Essentially total supression of polymer bands can be observed in Fig. 5.4 due to the formation of rather compact globular structures which corresponds to the results obtained from the ^1H NMR spectra. The same procedure for p–fraction calculation was performed as in the case of ^1H p–fractions. An example of one of the obtained dependences of ^{13}C p–fraction on EtOH content which was measured at 313 K is shown in Fig. 5.6. It can be seen that behaviour of various types of carbons depends on their position in the PIPMAm structural unit which is in agreement with the conclusions obtained from ^1H p–fraction results. $p \approx 1$ for all PIPMAm carbon types in the solutions containing 20 – 30 vol% of EtOH. However, with further increase of EtOH content, p values are smaller for the isopropyl CH_3 carbons showing that their mobility increases prior to other carbon types. This statement is supported by the fact that in the ^{13}C spectrum of the solution containing 40 vol% of EtOH, all polymer signals except for that of the isopropyl CH_3 carbons are supressed. On the other hand, CH_2

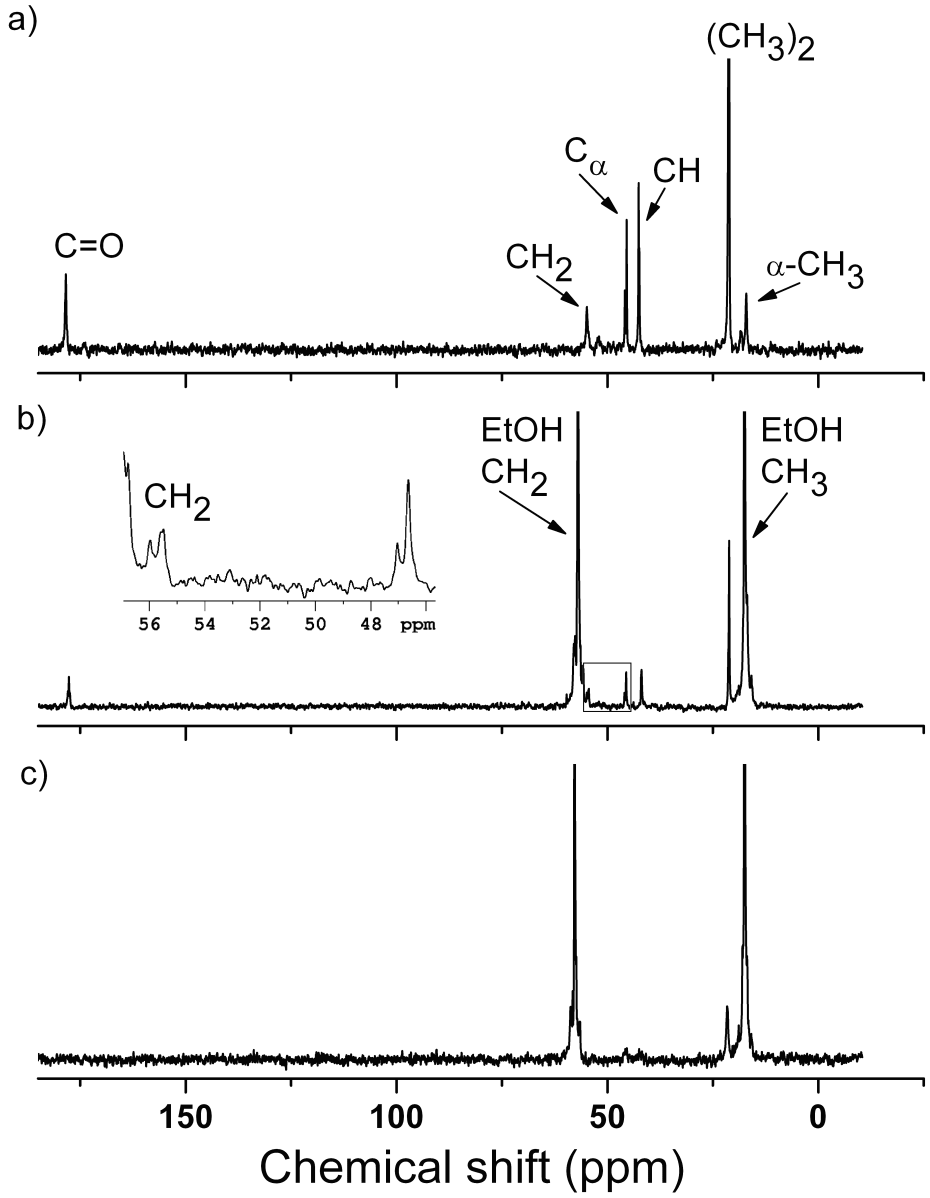

Figure 5.4: ^{13}C NMR spectra of PIPMAm in D_2O/EtOH mixtures with EtOH content 0 vol% (a), 95 vol% (b) and 40 vol% (c) measured at 313 K [38]. The inset in (b) shows the signal of PIPMAm CH_2 carbons which is located near the intensive signal of EtOH CH_2 carbons.

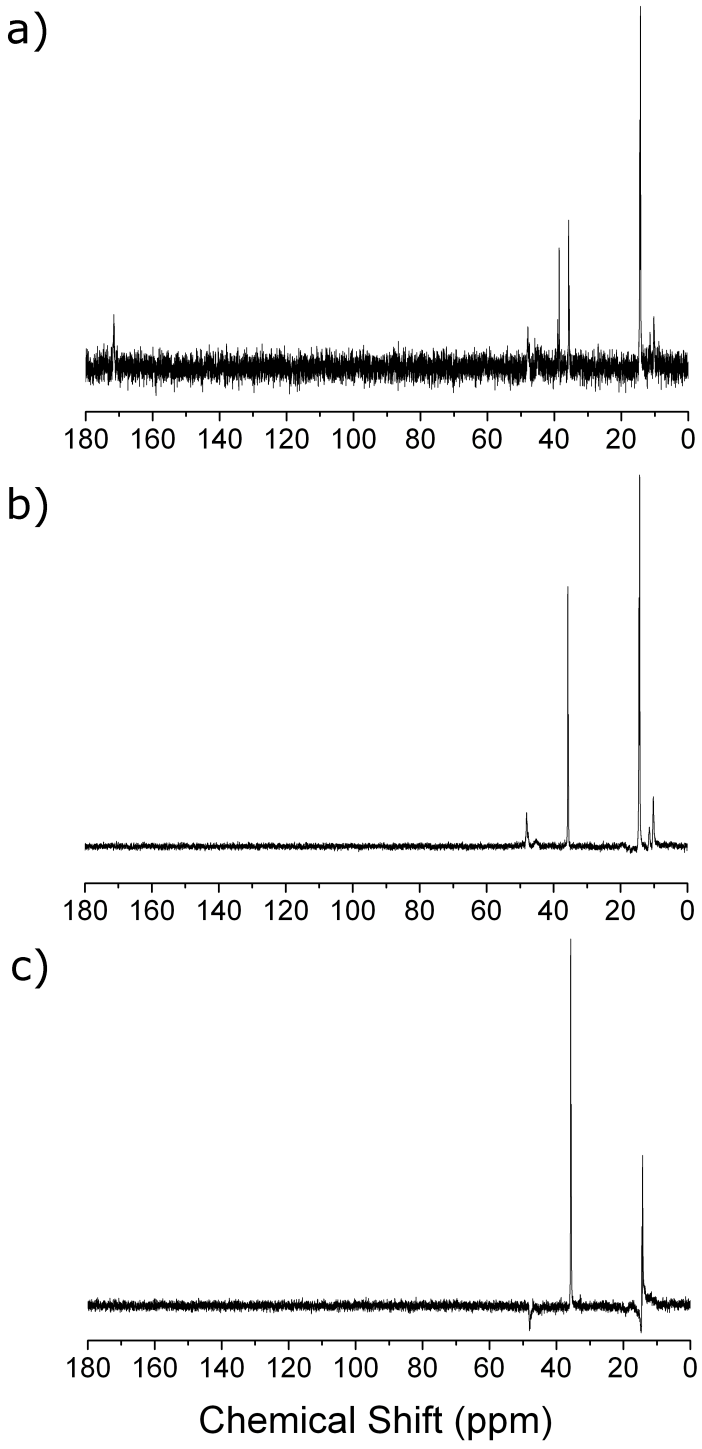

Figure 5.5: ^{13}C spectrum (a) and INEPT spectra (b, c) of PIPMAm in D_2O ($c = 5$ wt%) measured at 298 K. The adjustment of the INEPT experiment in (b) was set to reveal CH, CH_2 and CH_3 carbons with a positive intensity while in (c) CH, CH_3 carbons with a positive and CH_2 carbons with a negative intensity. For the peak assignment see Fig. 5.4.

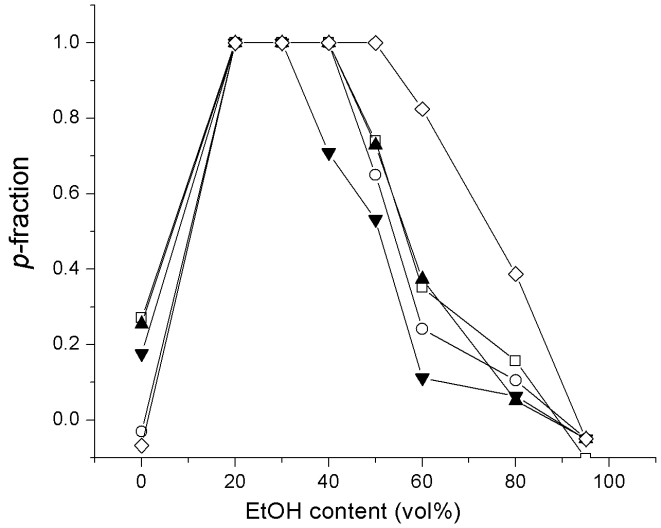

Figure 5.6: Phase-separated fraction p for PIPMAm solutions in D_2O/EtOH mixtures ($c = 5$ wt%) as a function of EtOH content as determined for various types of PIPMAm carbons at 313 K [38]; CH_2 (◊), quaternary (□), C = O (◯), CH (▲), isopropyl CH_3 (▼). Estimated experimental error ±6%.

and quarternary main chain carbons show the highest p value (Fig. 5.6). This means that, in comparison with the side chains carbons, it is necessary to add more EtOH into the solution to make these backbone carbons highly mobile.

5.1.2 Effect of Charge in PIPMAm Chains

Influence of the ionization on the phase separation in D_2O/EtOH solutions of negatively charged P(IPMAm-*co*-MNa) copolymers was investigated too. The MNa units dissociate in the solutions and charge the chains negatively. (For the details on the structure of the charged polymer see Chapter 3.) From ^{1}H spectra polymer integrated intesities and subsequently values of p–fraction for samples with ionic comonomer mole fractions $i = 5$ and 10 mol% were obtained. Comparison of these results with those of the uncharged PIPMAm homopolymer is shown in Fig. 5.7 where the dependences of p–fraction on EtOH content are plotted. While the D_2O/EtOH solution of the uncharged PIPMAm shows a distinct transition between homogeneous and phase-separated states, for the negatively charged P(IPMAm-*co*-MNa) copolymers the phase-separated fraction $p \approx 0$ in the whole range of EtOH contents. Evidently, charges and hydrophillic charac-

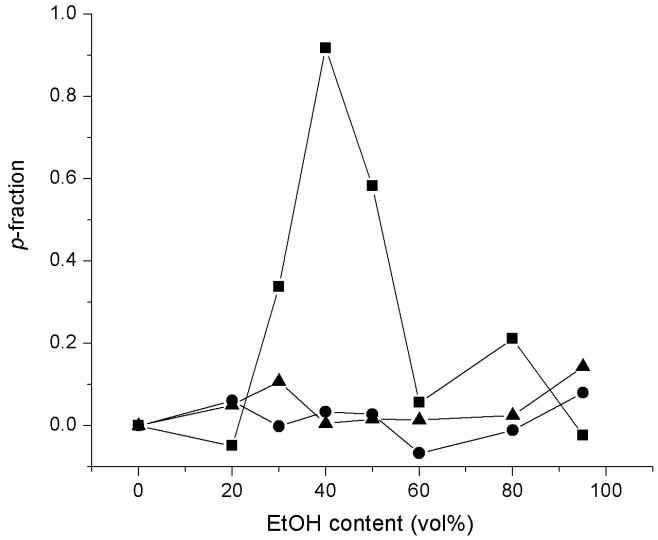

Figure 5.7: Phase-separated fraction p for P(IPMAm-*co*-MNa) copolymers with various content of MNa units in D_2O/EtOH mixtures ($c = 5$ wt%) as a function of EtOH content as determined for CH protons at 298 K [38]; 0 mol% MNa (■), 5 mol% MNa (●), 10 mol% MNa (▲).

ter of MNa units in copolymer chains prevent the cononsolvency-induced phase separation to occur.

On the other hand, at a higher temperature (328 K) the presence of MNa units in polymer chains has a strong influence but phase separation occurs although the values of phase-separated fraction of polymer units reaches 0.2 as the maximum value only (see Fig. 5.8). This is in agreement with results in [92] where the maximum value of p–fraction of charged PIPMAm was reported to decrease with increasing MNa content. For uncharged PIPMAm our results reveal that p–fraction reaches maximum values 1 in the ethanol concentration range of phase separation from 0 to 50 vol%. The fact that even charged P(IPMAm-*co*-MNa) exhibits the phase separation at this higher temperature is in agreement with our conclusion that there is a difference between mesoglobules induced by the cononsolvency and mesoglobules induced by the temperature effect. In this case we consider the phase separation to be temperature-induced and the mesoglobules might be more compact than when they are induced by the cononsolvency effect. In the case of cononsolvency-induced phase separation the formed mesoglobules might be more loose so the amount of MNa introduced into the chains is enough for their electrostatic stabilization in the solution and thus it prevents them from

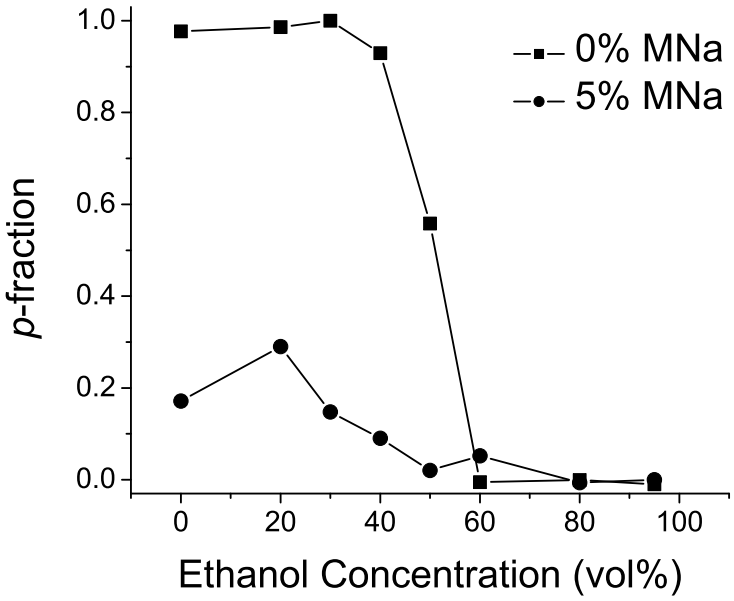

Figure 5.8: Phase-separated fraction p for PIPMAm and P(IPMAm-*co*-MNa) copolymers in D_2O/EtOH mixtures ($c = 5$ wt%) at 328 K as a function of EtOH content as determined for CH_2 protons; PIPMAm (0 mol% MNa) (■), P(IPMAm-*co*-MNa) (5 mol% MNa) (●).

the phase separation – this conclusion will be discussed in more detail in Section 5.1.4.

5.1.3 Chemical Shifts of OH Protons and Chemical Exchange

The chemical shift and the shape of ^{1}H NMR signals of OH protons in binary water/EtOH mixtures are known to be sensitive to the mixture composition [11]. Fast chemical exchange of OH protons in EtOH and water induces broadening of the corresponding signals. For water/EtOH mixtures containing small amount of salts, acids and phenols merging of OH peaks into a single peak was observed [67, 68]. These additives are supposed to tighten EtOH molecules into the water structures by strenghtening the hydrogen-bonding and thereby they promote the chemical exchange.

Fig. 5.9 shows dependences of the OH ^{1}H chemical shifts on EtOH content in the D_2O/EtOH mixture at 298 K for three systems: PIPMAm/D_2O/EtOH solution, P(IPMAm-*co*-MNa)/D_2O/EtOH solution (negatively charged copoly-

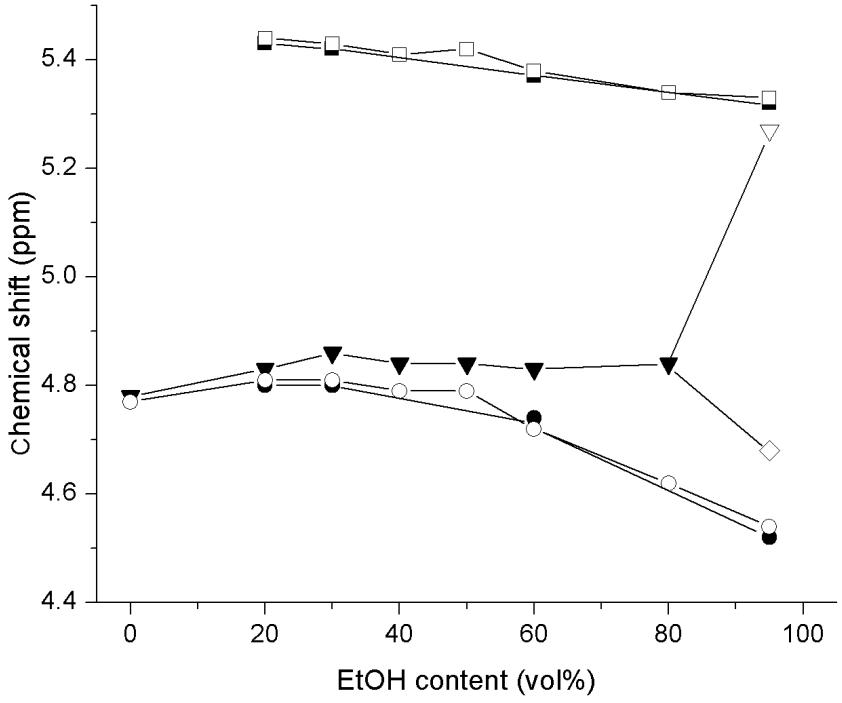

Figure 5.9: ^{1}H NMR chemical shifts of OH protons for PIPMAm and P(IPMAm-*co*-MNa) solutions in D_2O/EtOH mixtures ($c = 5$ wt%) and for neat D_2O/EtOH mixtures as a function of EtOH content measured at 298 K [38]; EtOH in D_2O/EtOH mixtures (■), HDO in D_2O/EtOH mixtures (•), merged EtOH/HDO in PIPMAm/D_2O/EtOH solutions (▼), EtOH in PIPMAm/D_2O/EtOH solution (95 vol% of EtOH) (▽), HDO in PIPMAm/D_2O/EtOH solution (95 vol% of EtOH) (◇), EtOH in D_2O/EtOH solutions of P(IPMAm-*co*-MNa) (5 mol% MNa) (□), HDO in D_2O/EtOH solutions of P(IPMAm-*co*-MNa) (5 mol% MNa) (◯).

mer) and neat D_2O/EtOH mixtures (without the polymer). In the spectra of negatively charged P(IPMAm-*co*-MNa) and neat D_2O/EtOH solutions two separate OH peaks were detected in the whole range of EtOH contents. The weaker signal with smaller chemical shift corresponds to HDO while the stronger signal with larger chemical shift corresponds to EtOH hydroxyl which follows from the integrated intensities. These chemical shift dependences are approximately identical for both systems. All uncharged PIPMAm/D_2O/EtOH solutions show one merged HDO/EtOH OH peak only except for the highest EtOH content (95 vol% of EtOH in the D_2O/EtOH mixture). This shows that the presence of PIPMAm in the D_2O/EtOH mixtures accelerates the chemical exchange between HDO and EtOH hydroxyl protons. It is analogous to the effect of salts, acids and phenols in [67, 68]. On the contrary, negatively charged P(IPMAm-*co*-MNa) copolymer does not affect the chemical exchange in comparison with the neat D_2O/EtOH mixtures.

5.1.4 Relaxation Behaviour of the Solvent in PIPMAm/-D_2O/EtOH Solutions

The effect of the fast chemical exchange is not manifested only in the marked broadening of the OH signal but also in the reduction of ^{1}H spin–spin relaxation times T_2. For solutions of PIPMAm in D_2O/EtOH mixtures the OH T_2 values are 2 orders of magnitude shorter in comparison with those in neat D_2O (see Tab. 5.1). In all systems represented in Tab. 5.1 the cononsolvency-induced phase separation does not exist or is negligible (see Fig. 5.3a).

EtOH content in D_2O/EtOH mixture (vol%)	^{1}H T_2 (s) [a]	Halfwidth (Hz)
0	5.3	2.8
60	0.03	13.7
95	0.02	103.0

[a] Estimated experimental error ±5%.

Table 5.1: ^{1}H spin–spin relaxation times T_2 of OH protons and halfwidths of OH bands in PIPMAm/D_2O/EtOH solutions at 298 K [38].

In general, NMR relaxation times of solvent nuclei should provide information on mobility of solvent molecules, and consequently on polymer–solvent interac-

tions. In earlier studies of the temperature-induced phase separation in D_2O solutions of PIPMAm, PIPAAm and PVME it was shown that when phase-separated mesoglobules are formed, spin–spin relaxation times T_2 of HDO are 1 order of magnitude shorter than those corresponding to the homogeneous solution [27, 81, 82, 89, 91]. The explanation of the T_2 shortening is as follows: After the phase separation part of solvent molecules stays bound inside mesoglobules or to their surface. Since there is a single peak corresponding to these bound types of water and to the free water in the spectrum, we measure a weighted-average value of T_2 [80, 82, 88, 89, 91]. Mobility of the bound water is restricted and thus the average value of T_2 shortens. However, for PIPMAm/D_2O/EtOH solutions, the T_2 shortening might originate from both the chemical exchange (see Tab. 5.1) and the existence of water bound in globular-like structures. Thereby we used the ^{13}C spin–spin relaxation times for the solvent mobility and polymer–solvent interactions characterization.

Tab. 5.2 summarizes ^{13}C spin–spin relaxation times T_2 of EtOH CH_2 and CH_3 carbons in PIPMAm/D_2O/EtOH solutions and D_2O/EtOH mixtures with various EtOH content at 298 K. T_2 values of both carbon types in PIPMAm solutions are systematically shorter than those in D_2O/EtOH mixtures without the polymer. In the polymer solution the T_2 values of EtOH carbons in the system where the major part of polymer segments is included in the phase-separated mesoglobules (50 vol% of EtOH in the mixed solvent) are within the estimated experimental error ($\pm$10%) the same as in systems where the cononsolvency-induced phase separation is negligible (20 and 95 vol% of EtOH). In an earlier study of PVME/D_2O/EtOH solutions [27] ^{13}C T_2 values in the range 4 – 9 s were determined for EtOH molecules with non-restricted mobility (i.e. molecules that either interact with flexible polymer segments (in the non-phase-separated system) or are expelled from globular-like structures (in the phase-separated system)). Therefore nothing indicates existence of the bound water in PIPMAm/D_2O/EtOH solutions at 298 K due to the cononsolvency effect.

EtOH content in D_2O/EtOH mixture (vol%)	PIPMAm/D_2O/EtOH ^{13}C T_2 (s) [a]		D_2O/EtOH ^{13}C T_2 (s) [a]	
	CH_2	CH_3	CH_2	CH_3
20	4.5	5.2	7.4	5.7
50	4.8	4.4	6.7	5.4
95	5.0	5.0	7.1	5.9

[a] Estimated experimental error ±10%.

Table 5.2: ^{13}C spin–spin relaxation times T_2 of CH_2 and CH_3 carbons of EtOH in PIPMAm/D_2O/EtOH solutions ($c = 5$ wt%) and in D_2O/EtOH binary mixtures with various EtOH content at 298 K [38].

EtOH content in D_2O/EtOH mixture (vol%)	PIPMAm/D_2O/EtOH ^{13}C T_2 (s) [a]		D_2O/EtOH ^{13}C T_2 (s) [a]	
	CH_2	CH_3	CH_2	CH_3
20	2.5	0.45	6.2	9.2
50	8.6	7.3	9.4	9.6
95	4.0	5.5	6.0	7.8

[a] Estimated experimental error ±10%.

Table 5.3: ^{13}C spin–spin relaxation times T_2 of CH_2 and CH_3 carbons of EtOH in PIPMAm/D_2O/EtOH solutions ($c = 5$ wt%) and in D_2O/EtOH binary mixtures with various EtOH content at 328 K [38].

A different NMR relaxation behaviour of EtOH molecules was found upon heating the samples to 328 K (Tab. 5.3). The PIPMAm solution containing 20 vol% of EtOH in the mixed solvent shows significantly reduced T_2 values when the phase separation is induced by the temperature increase ($p \approx 1$, see Fig. 5.3c). T_2 value of CH_3 carbons shortens the most markedly – it is 20 times shorter in the PIPMAm/D_2O/EtOH solution than in the neat D_2O/EtOH mixture. It suggests that a certain portion of EtOH molecules is bound in PIPMAm globular-like structures induced by temperature (probably due to hydrogen bonding with polymer C=O and/or NH groups [81, 88]) which is in agreement with previously observed results on temperature-induced phase separation in PVME/D_2O/EtOH

solutions [27]. Such solvent molecules might occupy pores in the sponge-like mesoglobules [27, 82, 89] and exhibit a lower spatially restricted mobility with a fast exchange between bound and free sites.

5.2 Solutions of Random Copolymers poly(*N*-isopropylmethacrylamide-*co*-acrylamide)

5.2.1 P(IPMAm-*co*-AAm) in D_2O

^{1}H NMR spectra of a solution of poly(*N*-isopropylmethacrylamide-*co*-acrylamide) (P(IPMAm-*co*-AAm)) random copolymers in D_2O at 298 and 340 K are shown in Fig. 5.10. The IPMAm/AAm molar ratio of the copolymers in the reaction mixture is 75/25. The assignment of the peaks to polymer groups can be found in the spectra. Peak A comes from HDO protons. B, D and E signals correspond to CH, $(CH_3)_2$ and α-CH_3 IPMAm groups, respectively. The H band is formed by an overlap of CH AAm protons and of CH_2 groups of both IPMAm and AAm monomer units. The weak signals at 1.29 and 3.63 ppm come from the residual ethanol from the polymerization process. At 340 K one can observe a significant decrease in polymer lines intensities. The signals of all polymer groups, except for the IPMAm isopropyl CH_3 groups, have approximately a zero intensity. At this temperature (above the LCST) the solution is phase-separated and polymer chains form compact globular-like structures. This statement is confirmed by the fact that while at 298 K the solution is transparent, at 340 K it is milk-white turbid.

For the copolymers the real composition (IPMAm/AAm molar ratio) was slightly different from the composition of the reaction mixture. The real copolymer composition was determined from ^{1}H NMR spectra (see Fig. 5.10) at temperatures below the phase transition: peak B (belonging to CH protons of IPMAm units) and H peak (overlapped signal of IPMAm CH_2 protons and CH and CH_2 protons of AAm units) were used for this purpose. The molar ratio of IPMAm and AAm units was determined from this equation:

$$\frac{[\mathrm{IPMAm}]}{[\mathrm{AAm}]} = \frac{3I_\mathrm{B}}{I_\mathrm{H} - 2I_\mathrm{B}} \tag{5.1}$$

where I_B is the integrated intensity of the peak B and I_H is the integrated intensity of the peak H. The real composition of the copolymers obtained this way is shown

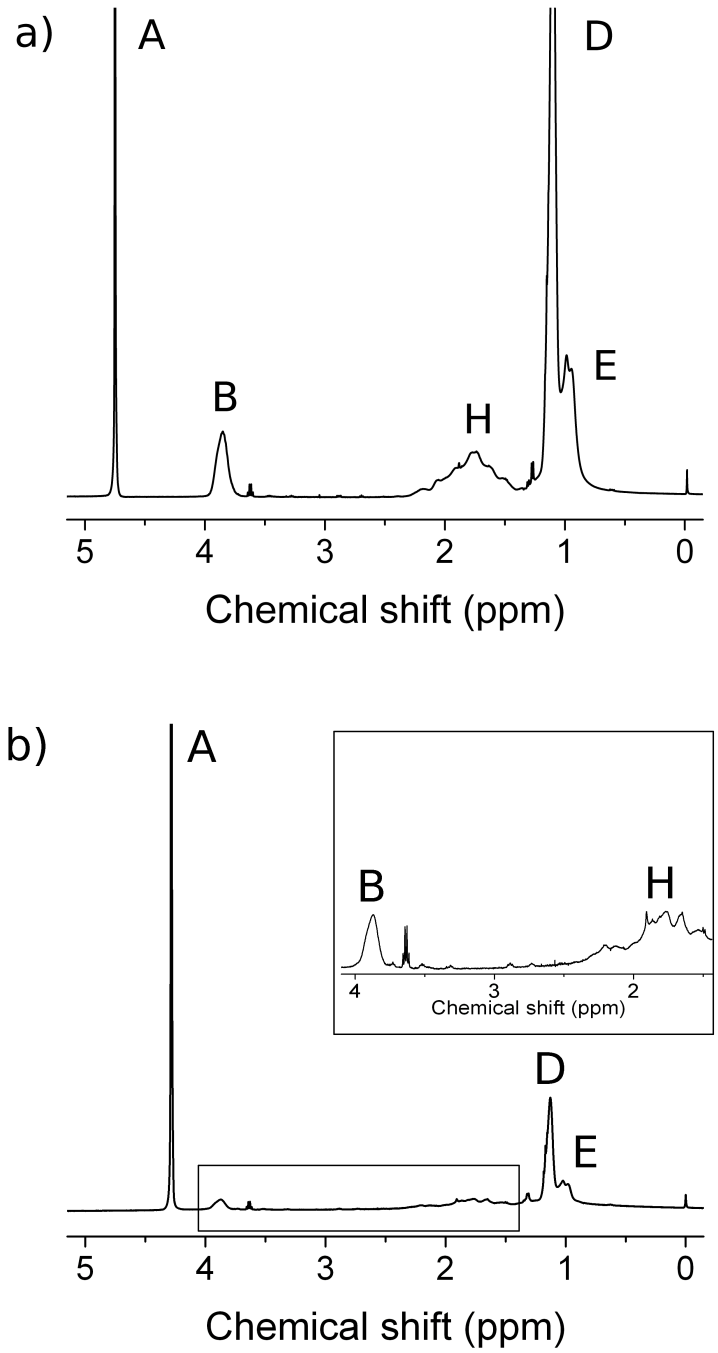

Figure 5.10: ^{1}H NMR spectra of 75/25 (IPMAm/AAm molar ratio in the reaction mixture) P(IPMAm-*co*-AAm) copolymer in D_2O solution ($c = 5$ wt%) measured at 298 K (a) and 340 K (b) under the same instrumental conditions [37]. The inset in part (b) shows the spectrum with higher amplification. Peak assignment is explained in the text.

in Tab. 5.4. In all cases the content of AAm units in the final copolymer is little bit lower than that in the reaction mixture. Such result indicates that AAm is less reactive than IPMAm. In this work the composition of the reaction mixture is used for samples labelling since this analysis has the inherent error (especially in the case of the 95/5 copolymer where the AAm units content is very small).

Composition of reaction mixture (IPMAm/AAm molar ratio)	Molecular weight M_w (g.mol^{-1})	Polydispersity M_w/M_n	Real composition of the copolymer determined from ^{1}H NMR spectra (IPMAm/AAm molar ratio)
100/0	136 300	3.67	-
95/5	799 900	1.17	99/1
85/15	730 300	1.27	94/6
75/25	132 400	2.09	84/16
60/40	502 100	1.51	71/29
0/100	147 300	2.57	-

Table 5.4: Molecular characteristics of investigated samples of PIPMAm, PAAm and P(IPMAm-*co*-AAm) copolymers. The real composition of the copolymer was determined from ^{1}H spectra using Eq. 5.1.

Copolymer solutions were studied in a broad range of IPMAm/AAm molar ratios and in three types of solutions: D_2O, D_2O/EtOH and D_2O/acetone. Overview of the studied samples is summarized in Tab. 5.5.

	IPMAm/AAm molar ratio in the copolymer					
	100/0	95/5	85/15	75/25	60/40	0/100
Ethanol content (vol%)	0	10	20			
	20	20	40			
Acetone content (vol%)	0	20	20	20	20	0
		40	40			
		50				

Table 5.5: List of studied P(IPMAm-*co*-AAm) solutions.

Although there is no separate AAm peak in the ^{1}H NMR spectrum of P(IPMAm-*co*-AAm)/D_2O (signals of both CH and CH_2 AAm groups overlap with that of IPMAm CH_2 as can be seen in Fig. 5.10a), the *p*–fraction values of the AAm component can be extracted through the values of the composition of the part that is detected in ^{1}H spectra at temperatures above the phase transition. We made this analysis for copolymer solutions with IPMAm/AAm molar ratio in the reaction mixture 75/25 and 85/15. These systems are suitable since the AAm units content is not too small (see Tab. 5.4) and at the same time the *p*–fraction values are still quite high (see Fig. 5.11).

Application of Eq. 5.1 to the overlapped signal H gave us these results: In the case of the 75/25 copolymer, the IPMAm/AAm molar ratio in the mobile part at 345 K (above the LCST) is $(\text{IPMAm/AAm})_{\text{above}} = 63/37$, while the real composition of this sample is $(\text{IPMAm/AAm})_{\text{real}} = 84/16$ (determined below the LCST at 310 K; see Tab. 5.4). In the case of the 85/15 copolymer the IPMAm/AAm molar ratio of the part that remains mobile above the LCST is $(\text{IPMAm/AAm})_{\text{above}} = 75/25$ at 334 K while the real composition of this sample determined at 310 K is $(\text{IPMAm/AAm})_{\text{real}} = 94/6$. The AAm fraction values in the mobile part detected in the spectra above the LCST are higher compared to their real composition. It means that the phase-separated fraction of AAm units is significantly smaller than the phase-separated fraction of IPMAm units which is in agreement with the conclusion we derived from Fig. 5.11 (see further in the text). This is valid for both systems. The molar fraction of AAm units in the part directly detected in NMR spectra above the LCST can be calculated using this relation:

$$(\text{AAm})_{\text{above}} = (1 - p_{\text{IPMAm}})(\text{IPMAm})_{\text{real}}(\text{AAm/IPMAm})_{\text{above}} \qquad (5.2)$$

where

p_{IPMAm} is the *p*–fraction of IPMAm units at the temperature above the phase transition,

$(\text{IPMAm})_{\text{real}}$ is the real molar fraction of IPMAm units in the copolymer determined at the temperature below the phase transition,

$(\text{AAm/IPMAm})_{\text{above}}$ is the AAm/IPMAm ratio at the temperature above the phase transition.

For the 75/25 copolymer $(\text{AAm})_{\text{above}} = (1\text{–}0.68) \times 0.84 \times \dfrac{37}{63} = 0.16$ which is

the same as the real AAm units molar fraction $(\mathrm{AAm})_{\mathrm{real}}$. It means that at temperatures above the phase transition all AAm units are visible in the ^{1}H NMR spectrum and thus the phase-separated fraction of AAm units $p_{\mathrm{AAm}} = 0$. This statement is valid for the 85/15 copolymer too: $(\mathrm{AAm})_{\mathrm{above}} = (1 - 0.77) \times 0.94 \times \frac{25}{75} = 0.07$ which is approximately the same as the real molar fraction of AAm units in the copolymer $(\mathrm{AAm})_{\mathrm{real}} = 0.06$. These results reveal that roughly all hydrophilic AAm units are quite mobile even at temperatures above the phase transition. This rather high mobility of AAm units in globular-like structures claims that they are hydrated. The conclusion that AAm units in the copolymer retain a high mobility even at temperatures above the phase transition makes clear the fact that there is a portion of IPMAm units which retain high mobility even above the transition (fraction $(1 - p_{\mathrm{IPMAm}})$) and which increases with increasing content of AAm units in the copolymer (see Fig. 5.11). We assume that these units are in short hydrated IPMAm sequences in the neighbourhood of AAm sequences while only sufficiently long IPMAm sequences undergo a cooperative coil–globule transition. These long IPMAm sequences are dehydrated and their mobility is strongly reduced. This overall picture is consistent with the existence of mesoglobules which are rather porous and disordered.

We investigated temperature dependences of ^{1}H NMR spectra of copolymer solutions with various molar ratios of the IPMAm/AAm units and determined the *p*–fractions of the resolved polymer bands. Both of them exhibited the same behaviour. These dependences for the CH proton bands of IPMAm units are shown in Fig. 5.11. Copolymer solutions with the IPMAm/AAm molar ratio from 100/0 (neat PIPMAm in D_2O) to 75/25 exhibit a rapid increase of the *p*–fraction with an increase of temperature. On the contrary, 60/40 and 0/100 (neat PAAm in D_2O) do not show phase separation which is in agreement with the fact that these samples do not become turbid upon heating. In solutions that exhibit phase separation the dependences revealed that the range of phase separation shifts to higher temperatures with increasing fraction of AAm units. For the PIPMAm homopolymer the temperature interval of the phase separation is 316 – 319 K, it is quite sharp and *p*–fraction above LCST reaches value 0.96. The copolymer solutions show broader transitions: P(IPMAm-*co*-AAm) copolymer with the IPMAm/AAm 75/25 molar ratio in the reaction mixture undergoes the phase separation at 323 K, the transition is approx. 14 K broad and $p = 0.68$. PAAm does not undergo temperature-induced phase separation and AAm units are hydrophilic [107]. Since the character of the copolymer is statistical, there are some

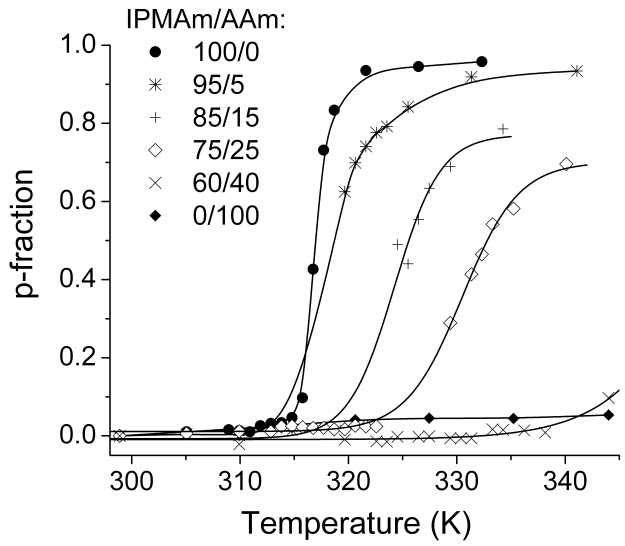

Figure 5.11: Temperature dependences of the phase-separated p–fraction of IPMAm determined from the line of CH protons of IPMAm units in D_2O solutions (c = 5 wt%) of PIPMAm and of P(IPMAm-*co*-AAm) copolymers with various IPMAm/AAm molar ratio in the reaction mixture [9, 37]. The plot obtained from the CH protons signal of PAAm in D_2O solution is shown for comparison. The lines are eye-guides only.

parts of the chain which contain more AAm units. Above the LCST, mesoglobules created from chains with higher AAm content are less compact. So with increasing content of AAm units in P(IPMAm-*co*-AAm) copolymers the mesoglobules are more porous and disordered, and therefore relatively large portion of IPMAm segments is highly mobile even above the LCST. Similar behaviour was reported on aqueous solutions of negatively charged P(IPMAm-*co*-MNa) copolymers and poly(*N*,*N*-diethylacrylamide-*co*-MNa) copolymer gels [86, 88, 92].

5.2.2 P(IPMAm-*co*-AAm) in Mixed Solvents D_2O/EtOH and D_2O/acetone

Fig. 5.12 and 5.13 show temperature dependences of p–fraction of P(IPMAm/AAm) copolymers in mixed solvents D_2O/EtOH and D_2O/acetone for various IPMAm/-AAm molar ratios and various solvent compositions. The p values were obtained from protons in CH group of IPMAm units. Dependences for protons from other polymer groups exhibit a similar behaviour.

Let us concentrate on solutions containing EtOH (see Fig. 5.12). A compar-

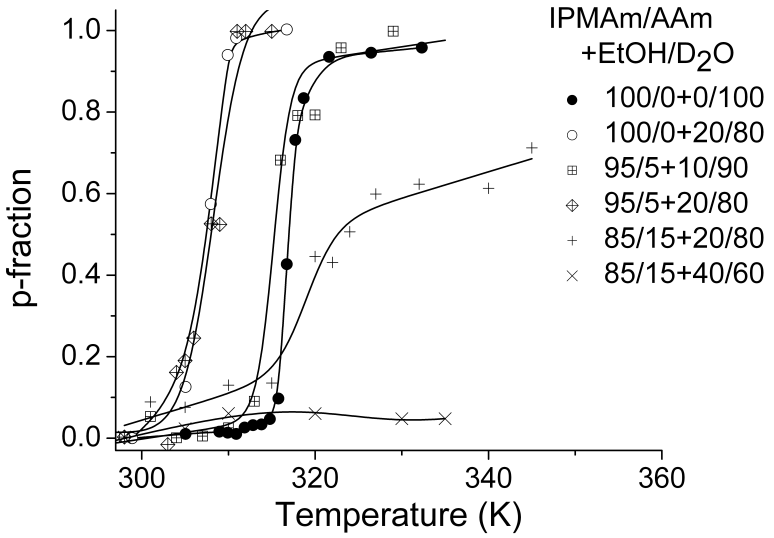

Figure 5.12: Temperature dependences of the phase-separated p–fraction of IPMAm determined from the signal of CH protons of IPMAm units in PIPMAm and P(IPMAm/AAm) copolymers with various IPMAm/AAm molar ratio in the reaction mixture in D_2O/EtOH solutions ($c = 5$ wt%) with various EtOH/D_2O volume composition [9, 37]. The lines are eye-guides only.

ison of the p dependences of the homopolymer PIPMAm reveals that the phase transition of PIPMAm D_2O/EtOH is 9 K lower than that of PIPMAm in neat D_2O; in both cases p reaches max. values $p_{\max} \cong 1$. In the case of the 95/5 copolymer (IPMAm/AAm molar ration in the reaction mixture) the situation is similar – transition temperature in D_2O/EtOH with 20 vol% of EtOH is approximately 7 K lower than in D_2O/EtOH containing 10 vol% and p reaches $p_{\max} \cong 1$. The dependence for the 85/15 copolymer with 20 vol% of the EtOH in the solvent is shifted towards higher temperatures, the transition region is broader and $p_{\max} < 1$. This copolymer in the mixed solvent containing 40 vol% of EtOH does not undergo phase separation at all; this is the same for 75/25 copolymer in the mixture with 20 vol% of EtOH and for copolymers with higher AAm content and/or higher EtOH content in the solvent. The LCST shift to lower temperatures has been observed already in PIPAAm/water/methanol solutions containing < 50 vol% of methanol in the mixed solvent. A conclusion was made that is is caused by the cononsolvency effect [106]. In PVME/D_2O/EtOH solutions the situation is completely different: with increasing EtOH content the transition region shifts towards higher temperatures continuously and $p_{\max}$ decreases [27].

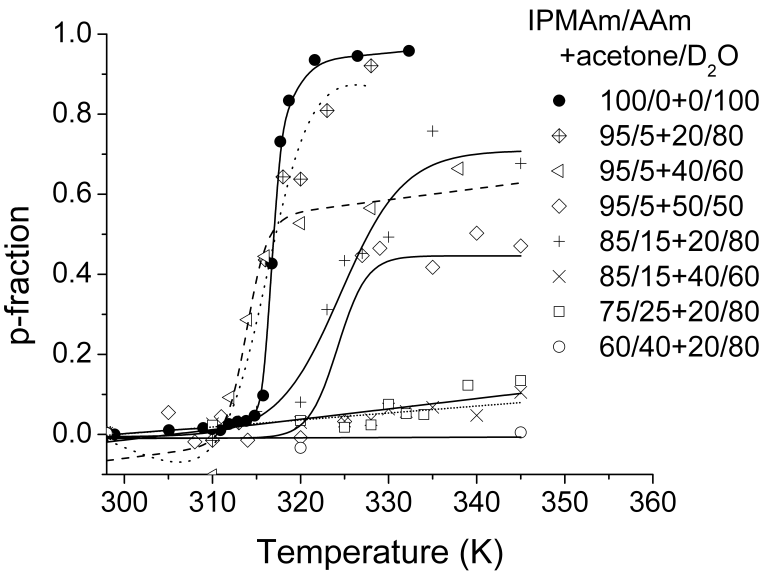

Figure 5.13: Temperature dependences of the phase-separated fraction p as determined from the signal of CH protons of IPMAm units in PIPMAm and P(IPMAm/AAm) copolymers with various IPMAm/AAm molar ratio in the reaction mixture in D_2O/acetone solutions ($c = 5$ wt%) with various acetone/D_2O volume composition [9, 37]. The lines are eye-guides only.

The behaviour of the homopolymer and copolymers in the mixed solvent D_2O/EtOH described above is connected with both the cononsolvency effect (water-ethanol interactions are preferred to polymer-water hydrogen bonds) and the fact that AAm units in the chains are hydrophillic and counter-operate (they strenghten polymer-solvent interactions) against the cononsolvency effect. This is in agreement with the fact that while for the PIPMAm homopolymer the cononsolvency effect was strongest at 298 K in the D_2O/EtOH mixture containing 40 vol% of EtOH ($p \approx 1$) [38, 79] while in the case of the 85/15 copolymer in the same mixed solvent $p \approx 0$ in the whole temperature range. Such behaviour is completely different from that of PVME. The explanation can be as follows: while polymer-polymer hydrogen bonds can be formed between IPMAm sequences in the globular state (which was confirmed by infrared spectroscopy in aqueous solutions of PIPMAm and P(IPMAm-*co*-MNa) copolymers [50, 51, 88]), in PVME solutions similar polymer-polymer hydrogen bonding cannot take place.

The 95/5 P(IPMAm-*co*-AAm) copolymer in D_2O/acetone (see Fig. 5.13) has approximately the same LCST in mixed solvents containing 20 and 40 vol% of acetone. But the maximum values of p differ significantly. While in the first

case (20 vol% of acetone) the transition $p_{\max}$ reaches almost 1, in the latter case $p_{\max} \cong 0.6$. The increasing acetone content in the mixed solvent shifts the copolymer transition to higher temperatures and $p_{\max}$ exhibits a further decrease. Phase separation was not observed for copolymers 85/15 containing 40 vol% of acetone and more and for 75/25 and 60/40 copolymers with at least 20 vol% of acetone.

The last thing we obtained from the ^{1}H NMR spectra was the information on the phase separation behaviour of AAm units in the P(IPMAm-*co*-AAm) copolymers in mixed solvents. We analyzed the 85/15 copolymer: at 345 K the phase-separated fraction of the IPMAm component $p_{\mathrm{IPMAm}} = 0.69$ in D_2O/EtOH and $p_{\mathrm{IPMAm}} = 0.67$ in D_2O/acetone. We used Eq. 5.1 and found out that the IPMAm/AAm molar ratio in the mobile fraction (which is the part that can be directly detected in the ^{1}H NMR spectrum at 345 K) is $(\mathrm{IPMAm/AAm})_{\mathrm{above}} =$ 83/17 for D_2O/EtOH and 86/14 for D_2O/acetone while the real composition of this copolymer is $(\mathrm{IPMAm/AAm})_{\mathrm{real}} = 94/6$ (see Tab. 5.4). An application of Eq. 5.2 gave us these results for the copolymer in mixed solvents: the molar ratio of AAm units in the part directly detected in spectra at 345 K the $(\mathrm{AAm})_{\mathrm{above}} =$ 0.06 for D_2O/EtOH, for D_2O/acetone it is the $(\mathrm{AAm})_{\mathrm{above}} = 0.05$. Both values correspond to $(\mathrm{AAm})_{\mathrm{real}}$ value in neat water which is 0.06 (see Tab. 5.4). These results suggest that in both mixed solvents essentially all hydrophilic AAm units are rather mobile and, therefore, directly detected in high-resolution NMR spectra even at temperatures above the phase transition. AAm sequences as well as short surrounding sequences in polymer chains forming mesoglobules extensively interact with solvent molecules which is similar to the situation in neat D_2O solutions.

5.2.3 Relaxation Behaviour of the Solvent

We examined relaxation behaviour of HDO solvent molecules in D_2O solvent molecules via ^{1}H spin-lattice and spin-spin relaxation times. Their temperature dependences in PIPMAm/D_2O and P(IPMAm/AAm)/D_2O with IPMAm/AAm molar ratio 95/5 are shown in Fig. 5.14 and 5.15. There is a significant decrease in the region of phase separation in both cases. This region is in agreement with that determined from the temperature dependences of p (see Fig. 5.11). The shortening of relaxation times upon phase separation confirms that there is a part of HDO molecules with a lower, spatially restricted mobility. These molecules correspond to HDO molecules bound in mesoglobules [78]. There is

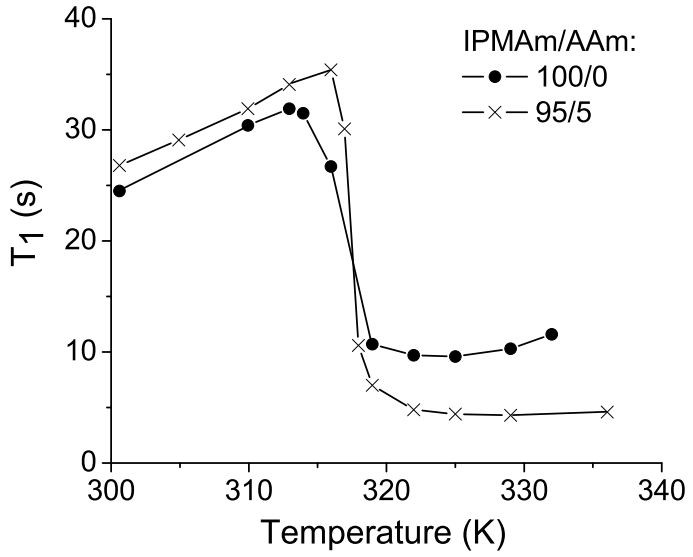

Figure 5.14: Temperature dependences of ^{1}H spin-lattice relaxation time T_1 of HDO in D_2O solutions (c = 5 wt%) of PIPMAm (•) and 95/5 (molar IPMAm/AAm ratio in the reaction mixture) P(IPMAm/AAm) copolymer (×) [37]. The lines are eye-guides only.

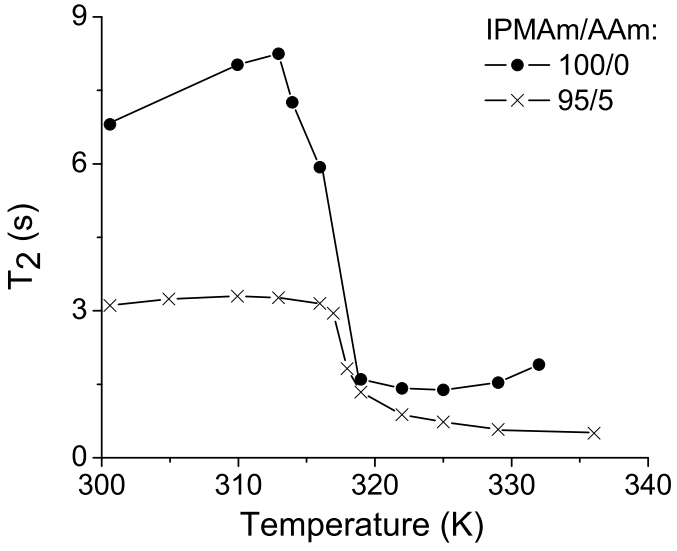

Figure 5.15: Temperature dependences of ^{1}H spin-spin relaxation time T_2 of HDO in D_2O solutions (c = 5 wt%) of PIPMAm (•) and 95/5 (molar IPMAm/AAm ratio in the reaction mixture) P(IPMAm/AAm) copolymer (×) [37]. The lines are eye-guides only.

a fast chemical exchange between bound and free water which is supported by these two facts: (i) there is a single peak HDO in the spectrum, (ii) the relaxation curves are single-exponential. So the determined relaxation times are weighted-average values of bound and free water which is the same situation as in Section 5.1.4. Similar temperature dependences of ^{1}H T_1 and T_2 were observed for PIPMAm aqueous solutions, P(IPMAm-*co*-ethylene glycol) and P(IPMAm-*co*-MNa) copolymers already [71, 88, 91, 110]. For the 85/15 P(IPMAm/AAm) copolymer in D_2O the relaxation times are $T_1 = 26.7$ s and $T_2 = 3.8$ s at 301 K, at 332 K $T_1 = 6.0$ s and $T_2 = 0.8$ s. These values are similar to those in Fig. 5.14 and 5.15. The temperature dependences of ^{1}H T_1 of HDO are very similar for both the PIPMAm/D_2O and 95/5 P(IPMAm/AAm)/D_2O (Fig. 5.14). In terms of the ^{1}H T_1 dependences, the behaviour is slightly different at temperatures below the LCST (Fig. 5.15). Below the phase transition, the T_2 values of HDO in the 95/5 P(IPMAm/AAm)/D_2O are significantly shorter than those in the PIPMAm/D_2O solution. This is true above the LCST too (in both cases) but the difference is not so big. The probable explanation of such a behaviour is as follows: in solutions where the polymer chains contain the hydrophilic AAm units the polymer-water interactions are stronger so the globular-like structures are not as compact as in the case of the PIPMAm homopolymer (see Section 5.2.1) and thus, the number of HDO molecules that can bound to polymer is higher. This higher number of bound HDO molecules causes the shortening of T_1 and T_2 in the 95/5 and 85/5 P(IPMAm/AAm) copolymer solutions.

Since there is a simple relation (Eq. 2.38) between the HDO linewidth and the T_2 (under the assumption that the shape of the peak is Lorentzian), we plotted temperature dependences of these HDO linewidths $\Delta\nu$ for D_2O solutions of PIPMAm and P(IPMAm/AAm) copolymers (see Fig. 5.16). In the case of PIPMAm and 95/5 and 85/5 P(IPMAm/AAm) copolymers the $\Delta\nu$ temperature dependences exhibit a significant increase with increasing temperature in the LCST region. With increasing AAm content this $\Delta\nu$-phase-transition-region shifts to higher temperatures which is in agreement with the temperature dependences of p in Fig. 5.11. Fig. 5.16 shows also that in the case of the copolymer solutions the phase transition is not as significant as in the PIPMAm solution. For 75/25 and 60/40 copolymers there is no increase in $\Delta\nu$ of HDO.

The linewidths $\Delta\nu$ contain qualitative information on T_2 only since the $\Delta\nu$ values are dominated by inhomogeneous line broadening, which can be seen from a comparison with linewidths $\Delta\nu_{\mathrm{exp}}$ calculated from experimental T_2 values – $\Delta\nu$ are at least one order of magnitude larger than $\Delta\nu_{\mathrm{exp}}$.

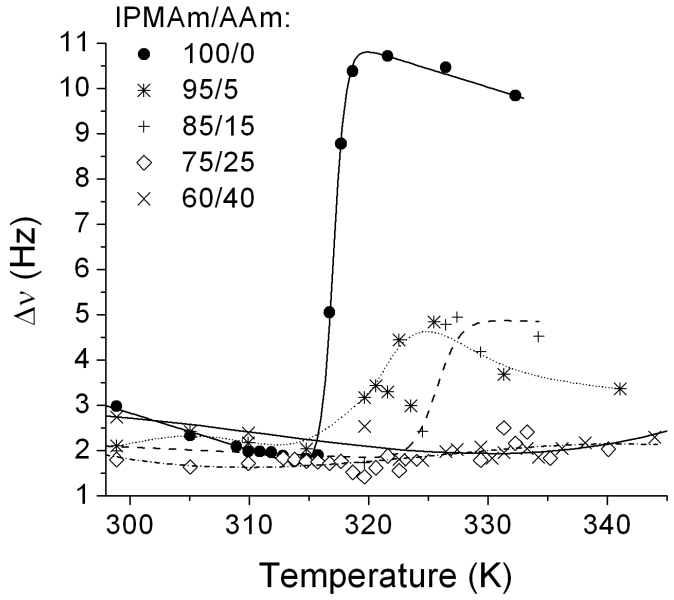

Figure 5.16: Temperature dependences of HDO NMR linewidth $\Delta\nu$ for D_2O solutions ($c = 5$ wt%) of PIPMAm and P(IPMAm/AAm) copolymers with various IPMAm/AAm molar ratios in the reaction mixture [37]. The lines are eye-guides only.

5.3 Results on PIPMAm/PVCL/D_2O Mixtures

5.3.1 Information Obtained from Spectra

Mixtures of various polymer species were reported earlier. Results obtained for mixtures with PIPMAm as one of the polymers were studied by Starovoytova et al. [90] (mixtures of PIPMAm and PIPAAm), PVCL/PEO mixtures were published by Yanul et al. [109].

^{1}H NMR spectra of PIPMAm/PVCL/D_2O sample with PIPMAm/PVCL molar ratio 3/1 and polymer concentration 5 wt% together with the peak assignment is shown in Fig. 5.17 for three temperatures: 298 K (under the LCSTs of both PVCL and PIPMAm, both polymers are dissolved), 308 K (above the LCST of PVCL and under the LCST od PIPMAm, PVCL separates while PIPMAm is dissolved) and 323 K (above the LCSTs of both PVCL and PIPMAm, both polymers are phase separated). For the chemical structures of PIPMAm and PVCL see Fig. 3.1 and 3.5.

PIPMAm/PVCL/D_2O mixtures concerned in this work were studied in a broad range of polymer molar ratios and concentrations. These parameters as

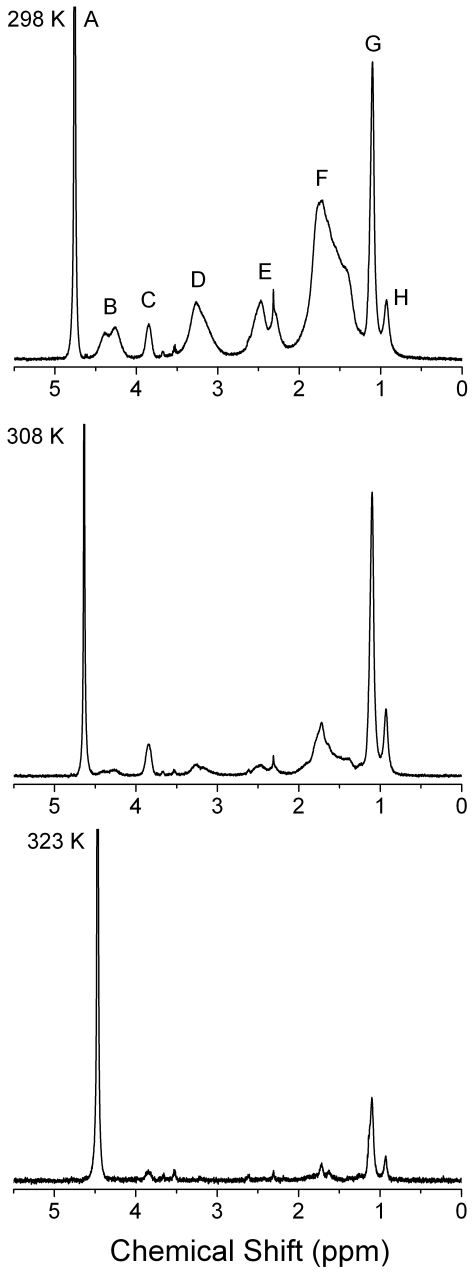

Figure 5.17: ^{1}H NMR spectra of PIPMAm/PVCL/D_2O mixture with 1/3 PIPMAm/PVCL molar ratio and 5 wt% polymer concentration in the solution at (from top to bottom) 298, 308 and 323 K [36]. The peak assignment is as follows: B and C peaks belong to CH groups of PVCL and PIPMAm, respectively; D and E signals come from the CH_2 groups of PVCL caprolactam ring, D connected to N while E connected to C=O; F is an overlap signal of the remaining CH_2 groups in the PVCL ring and CH_2 groups in the backbone chains of both polymers; G peak comes from $(CH_3)_2$ at the end of PIPMAm dangling chains and H belongs to α-methyl CH_3. The peak at the highest ppm value is the OH peak of the residual water.

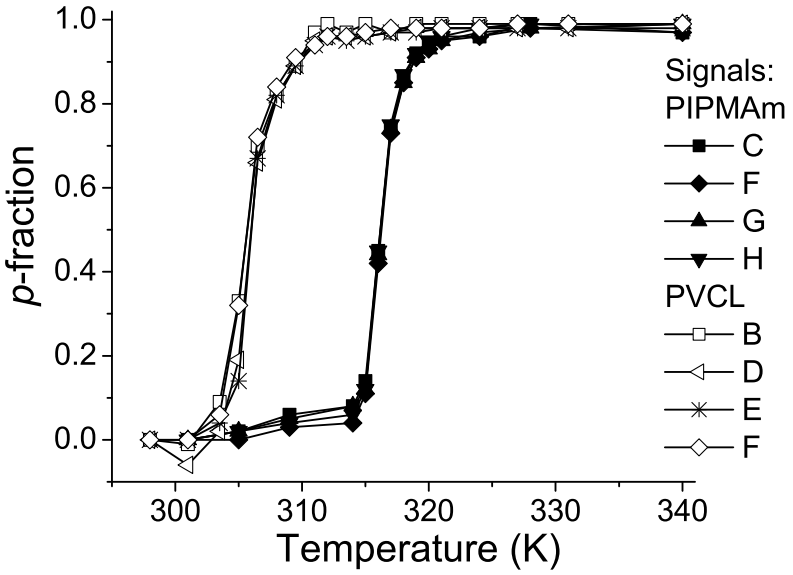

Figure 5.18: Temperature dependences of p–fraction obtained from ^{1}H NMR spectra of pure PIPMAm in D_2O and of pure PVCL in D_2O with 5 wt% polymer concentration in the solution in both cases [36]. For the peak assignment see Fig. 5.17. The lines are eye-guides only.

well as their LCSTs are summarized in Tab. 5.6 further in the text.

The temperature (LCST) and extent of the phase separation were determined from temperature dependences of the p–fraction. Separate phase transitions of both polymers were clearly detected for all polymer samples we studied. In the case of pure PVCL in D_2O the LCST was found to be 306 K which is in agreement with results obtained earlier by other methods on PVCL solutions of similar concentration and PVCL molecular weight [49, 94]. The temperature dependences of p–fraction for pure PIPMAm in D_2O and for pure PVCL in D_2O are shown in Fig. 5.18. Polymer peaks belonging to one polymer species exhibit approximately the same behaviour. The temperature dependences of p–fraction for PIPMAm/PVCL/D_2O mixture with 3/1 PIPMAm/PVCL molar ratio and 5 wt% concentration can be found in Fig. 5.19. From comparison with Fig. 5.18 it is evident that phase transitions for both polymers in the solution were detected. The lower one around 308 K corresponds to the PVCL transition while the upper one around 318 K is that of PIPMAm. Peak F corresponding to an overlap signal of both polymers shows both phase transitions. As was said earlier, in pure PIPMAm/D_2O solutions the LCST of PIPMAm does not depend

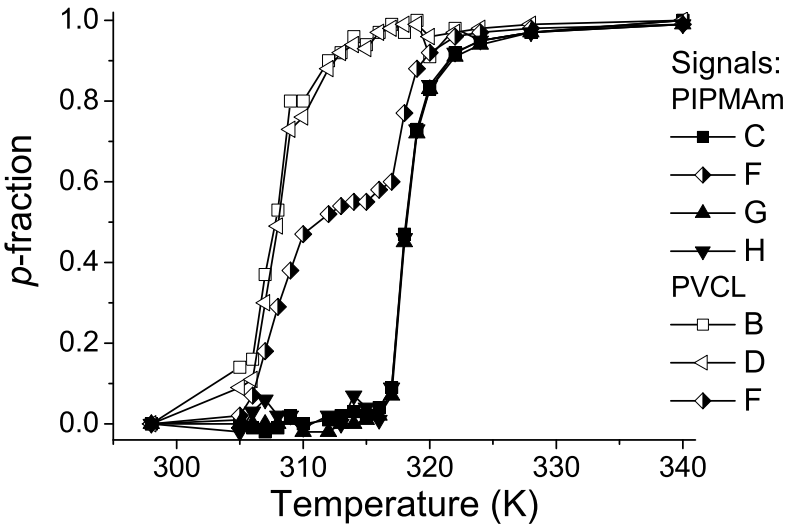

Figure 5.19: Temperature dependences of p–fraction obtained from ^{1}H NMR spectra of PIPMAm/PVCL/D_2O with 3/1 PIPMAm/PVCL molar ratio and 5 wt% polymer concentration in the solution [36]. For the peak assignment see Fig. 5.17. The lines are eye-guides only.

on polymer concentration [91], while the LCST of PVCL in PVCL/D_2O does. In polymer mixtures the polymers can mutually affect their phase transitions. For PIPMAm/PIPAAm/D_2O mixtures it was reported [90] that the PIPAAm phase transition (the one at the lower temperature, the direction of temperature change is heating) is not affected by the presence of the other polymer while the PIPMAm phase transition (the one at the higher temperature) is and depends on the solution concentration.

The LCST temperatures for all samples are summarized in Table 5.6. We measured temperature dependences of p–fraction for all these samples and it turned out that at temperatures above both the phase transitions $p_{\max} = 1$ in all cases.

PIPMAm/PVCL molar ratio	polymer concentration (wt%)	PVCL LCST (K)	PIPMAm LCST (K)
0/1	5	305.7 (305.7 - 306.0)	——
1/0	5	——	316.2 (316.2 - 316.3)
1/3	5	306.3 (306.3 - 306.6)	318.2 (318.2 - 318.8)
1/1	5	307.6 (307.6 - 308.0)	318.7 (318.7 - 318.8)
3/1	5	307.8 (307.8 - 308.2)	318.1 (318.1 - 318.2)
1/1	0.1	309.7 (309.7 - 311.7)	321.8 (318.7 - 321.8)
1/1	1	308.9 (308.9 - 309.1)	319.5 (319.5 - 319.7)
1/1	10	305.0 (305.0 - 305.7)	317.5 (317.5 - 317.6)

Table 5.6: Compositions, concentrations and LCSTs of PIPMAm/PVCL/D_2O mixtures, PVCL/D_2O and PIPMAm/D_2O. The LCST values were determined from the polymer CH peaks [36]. Since the LCST values slightly differ for other polymer groups, the whole LCST range is written down in parentheses.

Our results show that in PIPMAm/PVCL/D_2O mixtures the LCST of PVCL shifts to lower temperatures with increasing concentration – see Tab. 5.6 and Fig. 5.20. Values obtained for the less concentrated solution have a big inaccuracy.

With increasing PVCL content in the PIPMAm/PVCL/D_2O mixture the LCST of PVCL slightly decreases – see Tab. 5.6 and Fig. 5.21.

For the PIPMAm LCST, from the comparison of temperature dependences of p–fraction for samples that differ in concentration and have the same PIPMAm/-PVCL molar ratio (see Fig. 5.22) as well as from those with fixed concentration and different PIPMAm/PVCL molar ratios (see Fig. 5.23), no overall tendencies can be drawn.

Until now all temperature dependences of the phase-separated p–fraction p(T) were measured continuously without any delay between consecutive experiments at various, monotonically increasing, temperatures. We were interested if there is a difference between such "continuous" p(T) dependence and a "discontinuous" p(T) dependence, when at a certain temperature a delay is made. We measured two types of these discontinuous dependences: one with a 3-hour delay, the other with a 14-hour delay. During these delays, the temperature was kept constant at 311 K. This temperature is above the LCST of PVCL and below the LCST of PIPMAm which means that PVCL is phase-separated while PIPMAm

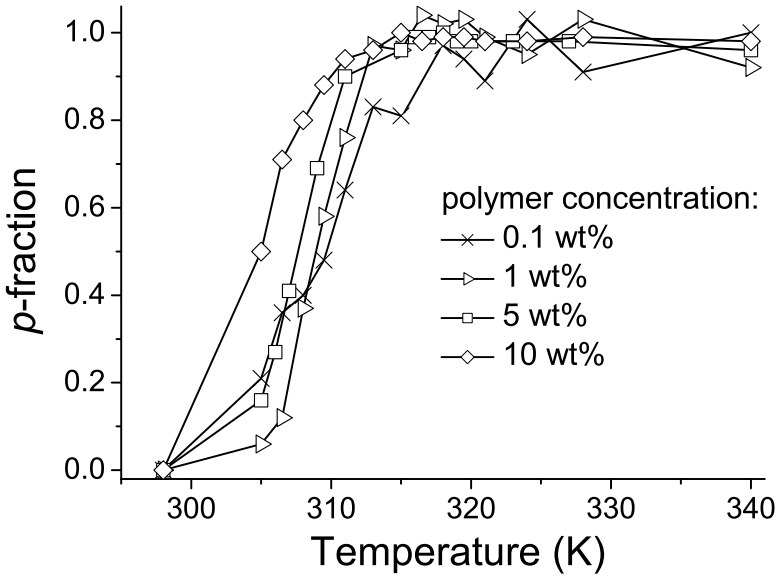

Figure 5.20: Temperature dependences of p–fraction of PIPMAm/PVCL/D_2O mixtures with PIPMAm/PVCL molar ratio 1/1 and with various concentrations in the solution [36]. The p–fraction values were determined from the CH peak of PVCL.

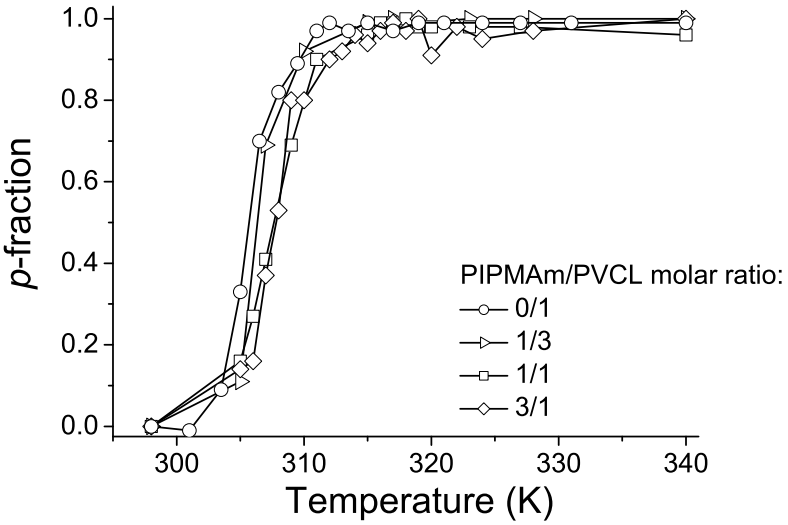

Figure 5.21: Dependence of p–fraction of PVCL CH peak in PIPMAm/PVCL/D_2O mixtures for samples with fixed polymer concentration 5 wt% and different PIPMAm/PVCL molar ratios [36].

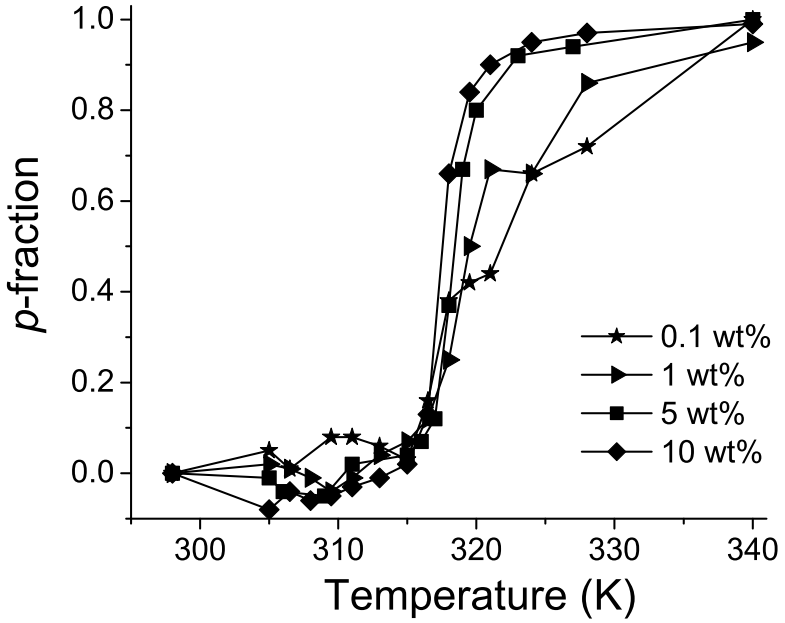

Figure 5.22: Temperature dependences of p–fraction of PIPMAm CH peak in PIPMAm/PVCL/D_2O mixtures with PIPMAm/PVCL molar ratio 1/1 and with various polymer concentrations in the solution [36].

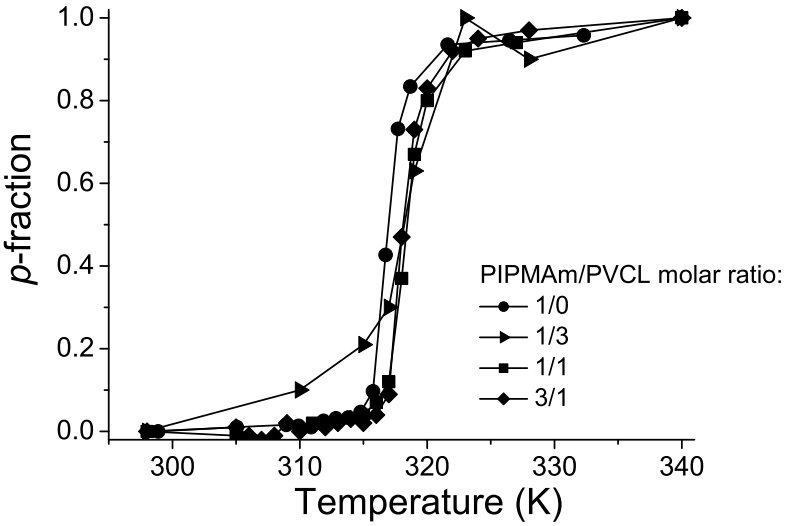

Figure 5.23: Temperature dependences of p–fraction of PIPMAm CH peak in PIPMAm/PVCL/D_2O mixtures for samples with fixed polymer concentration 5 wt% and different PIPMAm/PVCL molar ratios [36].

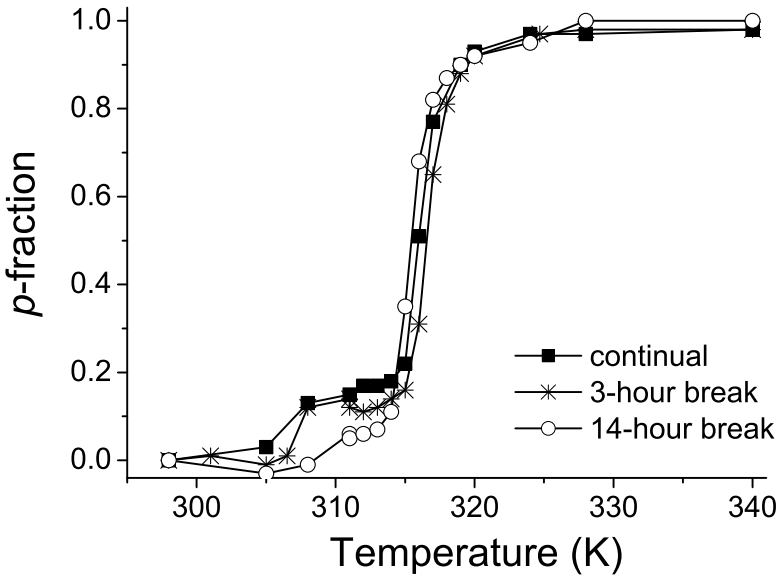

Figure 5.24: Continuous vs. discontinuous temperature dependences of p–fraction of the PIPMAm CH peak in the PIPMAm/PVCL/D_2O mixture with 10 wt% polymer concentration and 1/1 PIPMAm/PVCL molar ratio [36]. The break in the discontinuous temperature dependences was made at 311 K – the sample was kept at this temperature for 3 and 14 hours, respectively.

is dissolved. The results are shown in Fig. 5.24. All three dependences behave approximately the same way. This is different from results published in [89] where this type of experiment was done on PIPMAm/PVME mixtures with 10 wt% polymer concentration and 1/1 PIPMAm/PVME molar ratio, in the discontinuous dependence the break was done at 310 K (above the LCST of PVME and below the LCST of PIPMAm) and lasted for 12 hours. The behaviours of the continuous and discontinuous temperature dependences were reported to be different: the transition temperatures of the PIPMAm component as obtained after the 12-hour delay were ≈ 4 K lower than in the case of the continuous temperature dependence as a consequence of different arrangement of water molecules in the investigated systems.

5.3.2 Sedimentation of PVCL

The results obtained from temperature dependences above can be taken into account only qualitatively. During the experiments sedimentation of the phase-

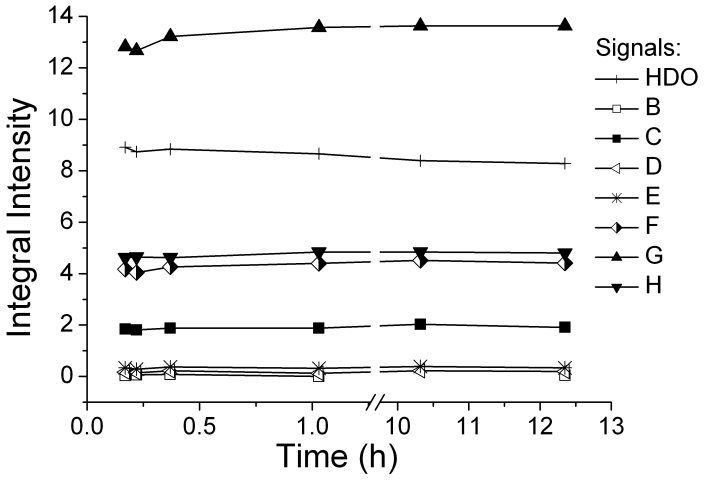

Figure 5.25: Time dependences of p–fraction of polymer bands for a PIPMAm/PVCL/D_2O sample with 10 wt% concentration and 1/1 PIPMAm/PVCL molar ratio at 311 K [36]. The sample contained an external standard DSS placed in a coaxial tube.

separated PVCL was observed. A transparent sediment appeared on the bottom of NMR tube even after one hour for samples containing higher PVCL content. (In terms of PIPMAm, which is very colloidally stable, at temperatures above its LCST, no sedimentation of the phase-separated PIPMAm was observed in our samples.)

Based on this observation we measured time dependences of p–fraction at constant temperatures. The dependence for a sample at 311 K containing 10 wt% of the polymer mixture with a PIPMAm/PVCL molar ratio 1/1 and with an external standard in a coaxial tube (for details on experiments using an external standard see Section 3.1.4) is shown in Fig. 5.25. At this temperature PVCL is phase separated, while PIPMAm is dissolved. The p–fraction values did not change even after more than 12 hours. Integrated intensity of the phase-separated polymer band is zero, so since the integrated intensities did not change with time at 311 K, it should be the already phase-separated PVCL that is sedimenting.

To confirm our conclusion that it's only PVCL in the sediment, we performed the following experiment. The PIPMAm/PVCL/D_2O sample with PIPMAm/-PVCL molar ratio 1/1 and 10 wt% polymer concentration was placed into a coaxial tube with an external standard and a ^1H spectrum was obtained. Then the sample was heated to 311 K (it's well above the PVCL LCST) and left for 1.5 hours at this temperature. Then the temperature was adjusted back

to 298 K and after the temperature equilibrated, a second ^{1}H spectrum was measured. Afterwards the sample was left at 298 K and later the solution above the sediment in the sample was taken away and placed into a new tube together with the standard in the coaxial tube that was used before. Then the third ^{1}H spectrum at 298 K was obtained. From the comparison of changes in integrated intensities of all polymer bands normalized to the intensity of the standard we confirmed that it's only PVCL that is sedimenting. PVCL bands' intensities dropped to 60% in the second measurement (after the heating and cooling back) and then to 50% of their initial value while the PIPMAm intensities remained unchanged. So after this polymer solution undergoes the PVCL phase separation, PVCL starts to sediment on the bottom of the tube and remains there when it is cooled back below the LCST of PVCL. It may be dissolving back into the solution but, due to the decrease of PVCL integrated intensities with time, this process would be much slower than the sedimentation. The results of this experiment are summarized in Tab. 5.7.

Time (hrs)	Integrated Intensities (a.u.)							
	B PVCL	C PIPMAm	D PVCL	E PVCL	F common	G PIPMAm	H PIPMAm	Standard
0.3	206	207	449	489	1960	1350	432	100
heating to 311 K and after 1.5 hours cooling back to 298 K								
2.2	122	238	277	296	1380	1630	464	100
3.9	96	219	225	236	1150	1500	461	100

Table 5.7: Integrated intensities of polymer bands in PIPMAm/PVCL/D_2O solution with 10 wt% polymer concentration and 1/1 PIPMAm/PVCL molar ratio [36]. The intensities are normalized to that of the external standard placed in a coaxial tube inside the NMR tube. All experiments were performed at 298 K. The sample was heated to 311 K and after 1.5 hours cooled back to 298 K between the first and the second measurement. The data from the third measurement (corresponding to 3.9 hours) were obtained from the nonsedimented part of the sample.

As was said earlier, the results obtained from temperature dependences of p–fraction can be taken into account only qualitatively, because they are affected by the sedimentation process. During the phase separation of PVCL, its concentration decreases due to the sedimentation and the remaining PVCL chains undergo the phase separation in the presence of a smaller amount of the phase-

separated PVCL molecules. During the phase separation of PIPMAm, a big portion of PVCL has already sedimented so PIPMAm undergoes the phase separation in a PIPMAm/PVCL/D_2O solution of significantly higher PIPMAm/PVCL ratio.

It took 4 to 6 hours to obtain a temperature dependence of p–fraction depending on the number of temperatures measured which is time sufficiently long to be affected by the sedimentation of the phase-separated PVCL.

In the next section results on relaxation behaviour of HDO molecules in these polymer mixtures are described. How does the sedimentation affect the values of HDO T_2? As was said in the previous section, at temperatures between the LCSTs of the two polymers when only PVCL is phase separated, the T_2 is short due to the PVCL phase separation. However, after the PVCL phase separates, it has tendencies to settle to the bottom of the NMR tube so the bound water molecules (with shorter T_2) get out from the measured region in the NMR tube which causes the obtained T_2 value to be higher than it should be. So when part of the mesoglobules settles, the average T_2 of the solvent rises. And it is probably also valid that the higher the temperature, the bigger the tendency to settle.

To exclude the influence of PVCL sedimentation on HDO relaxation times (for results on relaxation behaviour of HDO molecules see Section 5.3.3), the duration time of each relaxation experiment was maintained under 15 minutes and before each experiment the sample was maintained in the fridge for at least several hours at 5°C and then stirred. (To heat the sample to the desired temperature the tube was left for 15 minutes to equilibrate in the magnet before the experiment started.) We compared measurements of ^1H T_2 15 minutes (which is immediately after the temperature equilibration) and 30 minutes after the sample temperature was set. The results are discussed in the next section (5.3.3) and shown in Fig. 5.27.

The results that are affected by the sedimentation most are time dependences of HDO relaxation times. As was reported earlier [82], with time, the mesoglobules gradually release molecules of bound water into the bulk water. As these formerly bound water molecules become free, their T_2 decreases. But the sedimented bound HDO molecules with short T_2 do not contribute into the measured T_2 value thus causing it to be significantly higher than it should be. So these two effects have a similar manifestation in the time dependences and we cannot separate them.

5.3.3 Relaxation Behaviour of HDO Molecules

^{1}H T_1 of water

First we measured temperature dependences of ^{1}H T_1 of residual HDO in the PIPMAm/PVCL/D_2O mixture. Their values are summarized in the Tab. 5.8. No general conclusion can be drawn from these values. The obtained T_1 values probably lie in the range where T_1 has the extreme in its temperature dependence. As was published earlier, T_1 is not very sensitive to slow movements (movements with zero frequency $\omega(0)$), they are most sensitive to rapid motions (with correlation times $\sim \omega_H^{-1}$) [81].

T (K)	^{1}H T_1 of HDO (s)			
	1/3	1/1	3/1	PIPMAm/PVCL molar ratio
	5	5	5	Polymer concentration (wt%)
301	16.3	17.8	16.1	
308	20.1	20.1	19.2	
320	17.8	13.5	10.6	

Table 5.8: ^{1}H T_1 of residual HDO in the PIPMA/PVCL/D_2O mixture at temperatures below, between and above the phase transitions of PIPMAm and PVCL for three samples [36].

^{1}H T_2 of water

Since the temperature dependences of ^{1}H T_1 did not give us much information, we measured ^{1}H T_2 of HDO molecules. T_2 is much more sensitive to slow-motional modes than T_1 [81]. In Fig. 5.26 temperature dependences of ^{1}H T_2 of HDO in PIPMAm/PVCL/D_2O mixtures with 1/1 PIPMAm/PVCL molar ratio and various polymer concentrations in the range between 0.1 and 10 wt% are depicted. The three temperatures at which ^{1}H T_2 values were measured are 301 K (under the LCST values of both polymers), 312 K (PVCL is phase separated while PIPMAm is dissolved) and 332 K (both polymers are phase separated). At 312 K ^{1}H T_2 significantly shortens due to the formation of the PVCL mesoglobules. After further increase of the temperature to 332 K, no further decrease of ^{1}H T_2 values is observed. This behaviour is odd since one would expect further shortening of ^{1}H T_2 values due to higher number of mesoglobules which trap more water molecules leading thus to lower average HDO ^{1}H T_2. The sample

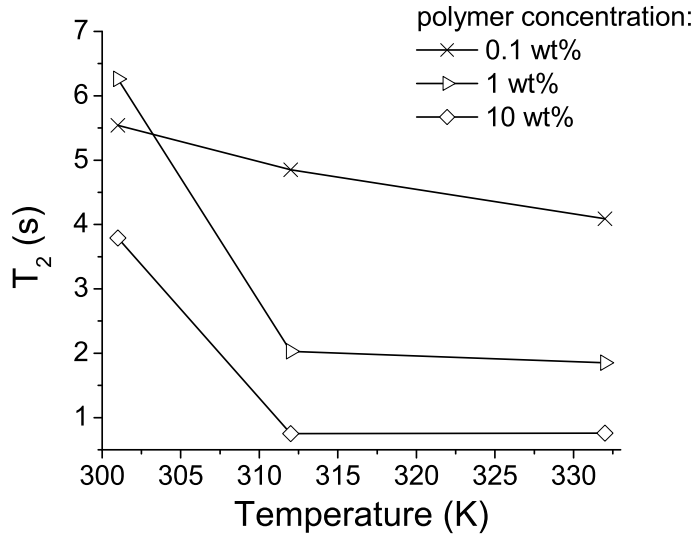

Figure 5.26: Temperature dependences of ^{1}H T_2 of HDO in PIPMAm/PVCL/D_2O mixtures with various polymer concentrations and fixed 1/1 PIPMAm/PVCL molar ratios [36].

containing the smallest portion of PVCL does show a monotonous decrease of T_2 with increasing temperature. But the bigger the content of PVCL, the greater the deviation from the expected behaviour.

To be sure to exclude the influence of sedimentation of the phase-separated PVCL on T_2 values, we made two sets of experiments for each temperature – one 15 minutes after the sample temperature was initally set (immediately after the temperature equilibration) and the other 30 minutes after the temperature was initially set. The results can be found in Fig. 5.27. We can conclude that the obtained ^{1}H T_2 values for mixtures of 5 wt% concentration with 3/1 and 1/1 PIPMAm/PVCL molar ratios are not affected by the sedimentation while the 1/3 slightly is because the ^{1}H T_2 values for the 1/3 sample obtained 15 and 30 minutes after the temperature was set differ by 20 – 25%.

In 5.28 temperature dependences of ^{1}H T_2 of HDO in PIPMAm/PVCL/D_2O mixtures measured 15 min after the sample temperature was set for samples with 5 wt% polymer concentration and various PIPMAm/PVCL molar ratios are depicted. At 301 K the T_2 values for all three samples are between 4.5 and 5.1 s. When the temperature was increased to 308 K (above the LCST of PVCL), the T_2 values significanly shorten because of the decreased mobility of water trapped in mesoglobules. As was said earlier, after further increase of temperature to the

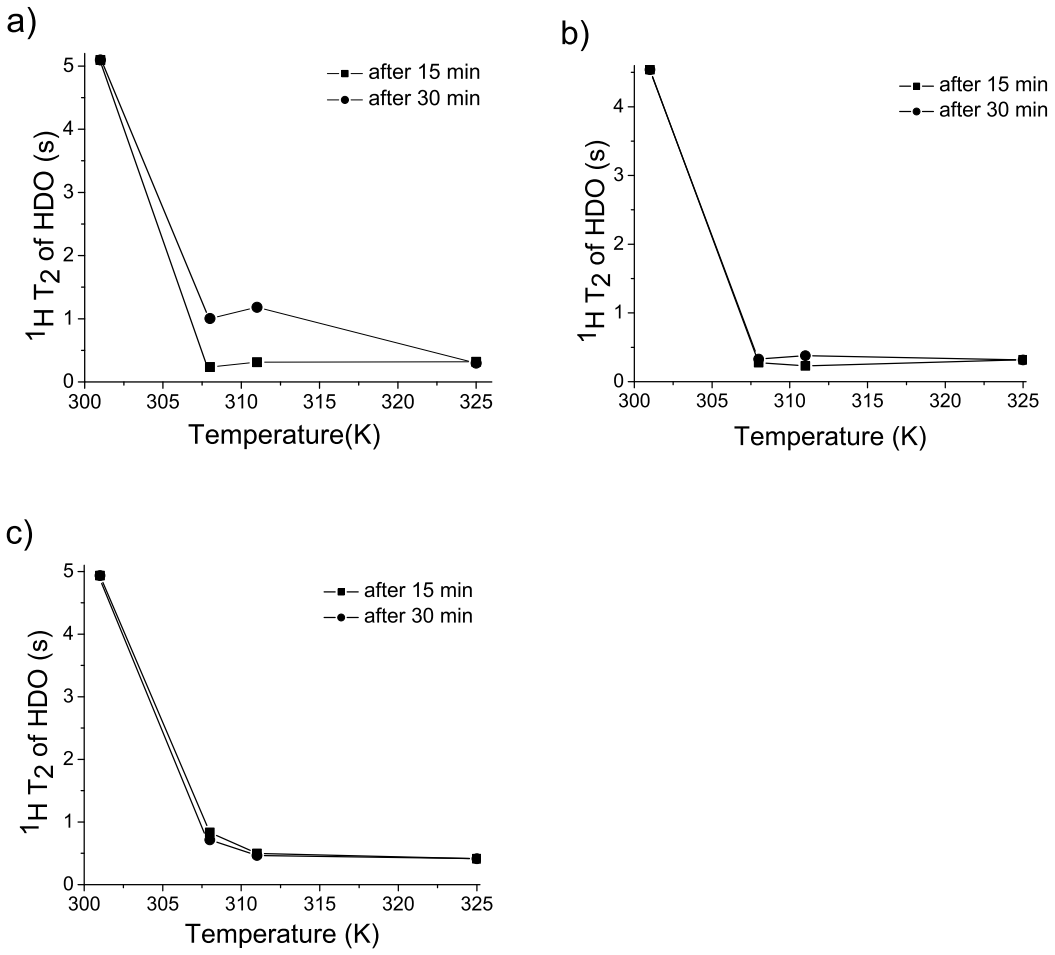

Figure 5.27: Comparison of temperature dependences of ^{1}H T_2 of HDO in PIPMAm/PVCL/D_2O mixtures measured 15 min and 30 min after the sample temperature was set [36]. All the three samples have polymer concentration 5 wt% and differ only in the PIPMAm/PVCL molar ratio which is 1/3 in a), 1/1 in b) and 3/1 in c).

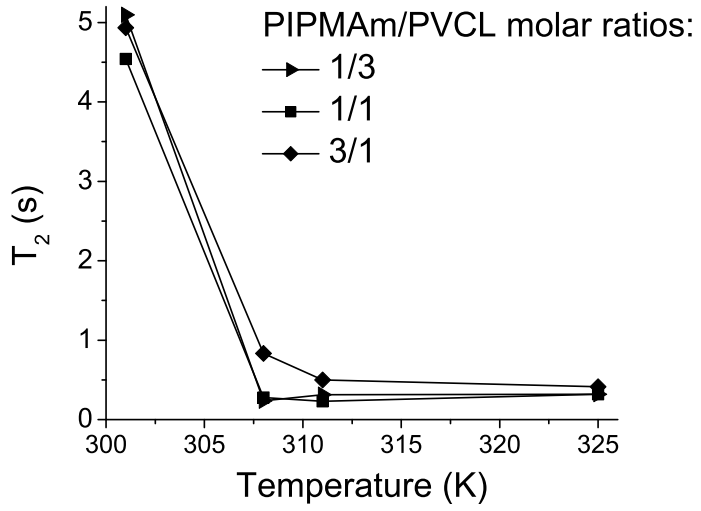

Figure 5.28: Temperature dependences of ^{1}H T_2 of HDO in PIPMAm/PVCL/D_2O mixtures measured 15 min after the sample temperature was set [36]. All the three samples have polymer concentration 5 wt% and differ only in the PIPMAm/PVCL molar ratio.

value above the LCST of PIPMAm (325 K), furter shortening of T_2 values was not observed although one would expect that.

Time dependences of water ^{1}H T_2 values

We also measured time dependences of ^{1}H T_2 of HDO. First of all we were interested in their behaviour in PIPMAm/PVCL/D_2O solutions below the LCSTs. In Fig. 5.29 such dependence at 301 K for two samples is shown. One of them with 1/3 PIPMAm/PVCL molar ratio and 5 wt% polymer concentration, the other with 1/1 PIPMAm/PVCL molar ratio and 10 wt% polymer concentration. At this temperature no sedimentation was observed and in both cases the T_2 values do not significantly change in time. A slight monotony can be observed, its values determined from a linear fit are 0.0086 for the 1/3 and 0.0045 for the 1/1 sample. Existence of this monotony is an interesting result and led us to a performance of an identical experiment on a PIPMAm/D_2O solution which is known to be colloidally stable even in the phase-separated state (it means that it doesn't precipitate in a time significantly longer than the time of the experiment, i.e. $\approx$ days). Such time dependence in PIPMAm/D_2O of 5 wt% concentration can be found in Fig. 5.30. The HDO ^{1}H T_2 value does not significantly change –

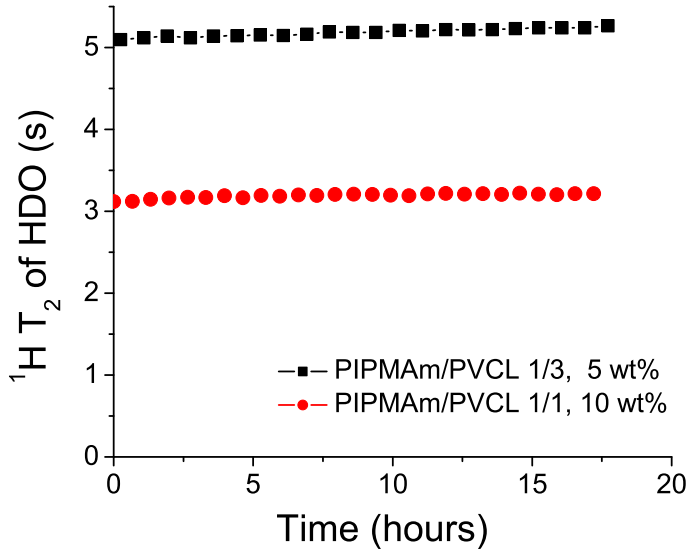

Figure 5.29: Time dependences of ^{1}H T_2 of HDO in a PIPMAm/PVCL/D_2O mixture for samples of 5 wt% polymer concentration and 1/3 PIPMAm/PVCL molar ratio (circles) and 10 wt% polymer concentration and 1/1 PIPMAm/PVCL molar ratio (squares) at 301 K.

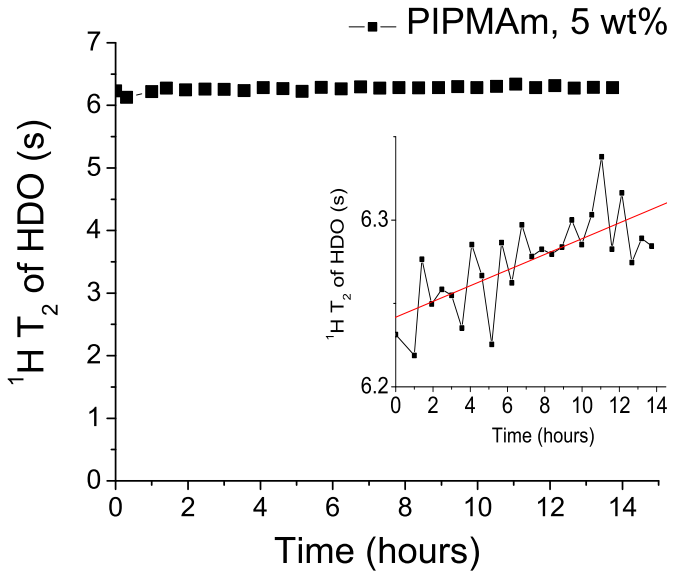

Figure 5.30: Time dependence of ^{1}H T_2 of HDO in a PIPMAm/D_2O mixture of 5 wt% polymer concentration at 301 K.

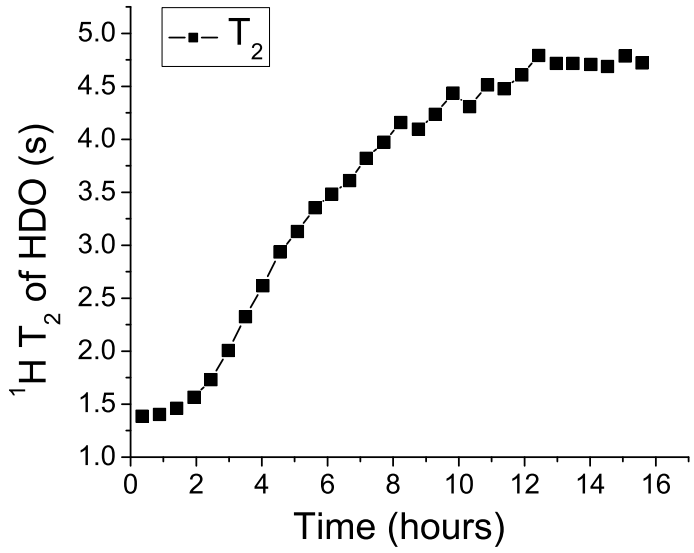

Figure 5.31: Time dependence of ^{1}H T_2 of HDO in a PIPMAm/PVCL/D_2O mixture with 5 wt% polymer concentration and 1/1 PIPMAm/PVCL molar ratio at 305 K.

it changes from the initial value 6.23 s of about 0.05 s (1 %) in 14 hours). From the indent one can clearly see that it shows some increasing monotony with a slope 0.0047 as was determined from a linear fit. To our best knowledge, this was not reported yet. This result implies that both PVCL and PIPMAm exhibit a very slow change in hydration at the room temperature. This process is much slower for PIPMAm.

For temperatures above the LCST of PVCL and/or PIPMAm the effect of time on mesoglobules should be such that water is gradually released from them becoming thus free which leads to the increase of the HDO ^{1}H T_2 values [82]. At the same time, in this (partly) phase-separated solution, the mobility of polymer chains in mesoglobules is decreased and the corresponding polymer T_2 is lower.

First we measured the time dependence at 305 K, which is the temperature where the phase separation process just begins, for a PIPMAm/PVCL/D_2O system with 5 wt% polymer concentration and 1/1 PIPMAm/PVCL molar ratio (see Fig. 5.31). The time dependence has an unusual shape in the first 3 hours. After some 13 hours a plateau is reached. The T_2 value of the plateau is around 4.7 s.

The unusual shape can be explained as a result of two effects. One of them is the sedimentation, the other is the fact that the mesoglobules are still in the

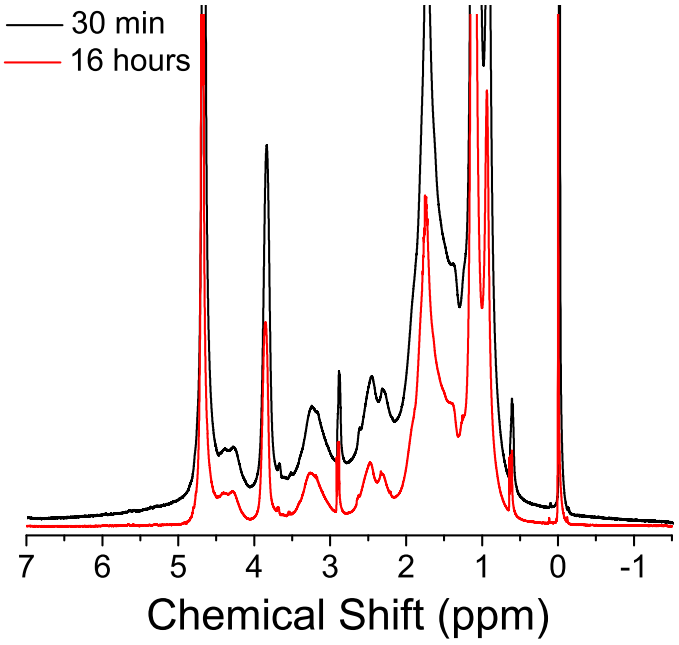

Figure 5.32: ^{1}H NMR spectra of PIPMAm/PVCL/D_2O mixture with 5 wt% polymer concentration and 1/1 PIPMAm/PVCL molar ratio at 305 K 30 minutes (black line) and 16 hours (red line) after the temperature was set.

phase-transition process (they did not reach their final conformation yet) and they are rather loose because they contain a lot of water molecules which will be later released. The latter effect can be evidenced when you compare ^{1}H NMR spectra of this mixture taken 30 minutes and 16 hours after the temperature was set to 305 K (see Fig. 5.32). The spectrum measured 30 minutes after the temperature was set corresponds to the solution where PVCL mesoglobules are still present in the whole measured region in the tube. Apart from the relatively narrow spectral lines one can clearly see a broad peak of about 6 ppm width. It indicates the presence of a rather mobile phase-separated fraction. 15.5 hours later this broad peak disappears (its integrated intensity ≈ 0) from the spectrum. The phase-separated fraction that remains mobile even in the phase separated solution and which was resolved in the spectrum was reported earlier for PVME/D_2O solutions [82]. In Spěváček's work the correlation of mobility of polymer units and solvent molecules was studied in detail.

The identical sample which we studied at 305 K (with 1/1 PIPMAm/PVCL molar ratio and 5 wt% polymer concentration) exhibits a gradual increase in

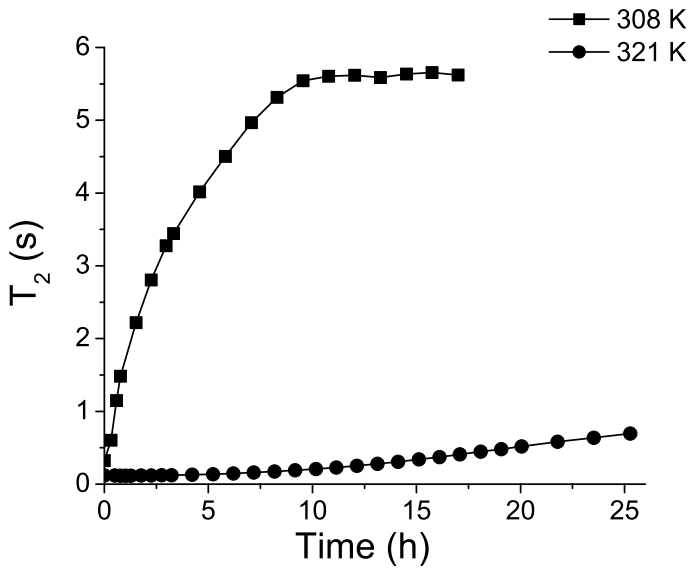

Figure 5.33: Time dependences of ^{1}H T_2 of HDO in PIPMAm/PVCL/D_2O mixtures with 1/1 PIPMAm/PVCL molar ratio and 5 wt% polymer concentration at 308 K (squares) and 10 wt% polymer concentration at 308 K (circles), respectively [36].

its time dependence at 308 K (above the LCST of PVCL). After approximately 10 hours a plateau with T_2 value around 5.6 s is reached – see Fig. 5.33. At 308 K the dependence does not show the convex shape at the beginning. It rises until a plateau at 5.5 s is reached after 9 hours.

At 321 K (above both the LCSTs) the time dependence of ^{1}H T_2 of HDO in a PIPMAm/PVCL/D_2O mixture with 10 wt% polymer concentration and 1/1 PIPMAm/PVCL molar ratio exhibits a monotony (see Fig. 5.33). In the time of duration of the experiment which was 25 hours the plateau was not reached. It ended at a T_2 value 0.7 s. The HDO T_2 time dependences for similar systems were previously reported by Starovoytova et al. [89]. In their work the time dependence for PIPMAm/D_2O was measured at 325 K for 70 hours and PIPMAm started to release water significantly from mesoglobules in 30 hours and a plateau was reached after cca 60 hours when the HDO ^{1}H T_2 value was the same as that of HDO in a non-phase separated PIPMAm/D_2O. For a more flexible polymer PVME the release started in 2 hours already. The authors stated that the shape of the time dependence is related to the glass transition temperature T_g and one can extract information about the polymer mobility out of it.

If this relation is valid, the HDO T_2 in PVCL/D_2O should be increasing in a much slower manner because the glass transition temperature values of PIPMAm and PVCL are similar (T_g of PIPMAm was reported to be 176°C [73], T_g of PVCL between 147°C [33] and 190°C [102]). Then the time dependences of T_2 for these two polymers should be similar. But from the Fig. 5.33 it follows that at 308 K it is influenced by the PVCL sedimentation which causes T_2 increase too leading thus to much faster T_2 increase. The release of water molecules from PIPMAm mesoglobules is probably not influenced by PVCL since the T_2 time dependence at 321 K has the same behaviour as that of PIPMAm/D_2O reported in [89].

Chapter 6

Conclusions

Three types of linear polymer solution systems were studied experimentally by high-resolution NMR spectroscopy. The conclusions are following:

PIPMAm/D_2O/EtOH

1. NMR integrated intensities of polymer signals revealed that the compositional range of the phase separation broadens to lower values of EtOH content in the mixed solvent with increasing temperature.

2. There is a different character of mesoglobules formed in D_2O/EtOH mixtures due to the cononsolvency and due to the temperature. This statement is supported by the following observations:

   (a) In the case of cononsolvency-induced phase separation side chains of PIPMAm do not take part in the phase separation in the same extent as polymer groups in the backbone chain suggesting thus that some side chains in phase-separated units are still in interaction with solvent molecules. In the case of temperature-induced phase separation the changes in the mobility of the side chain and the main chain polymer groups are paralell resulting thus in the same values of the phase-separated fraction p.

   (b) ^{13}C spin–spin relaxation times T_2 of EtOH carbons also depend on the type of the phase separation. ^{13}C T_2 values of EtOH are not affected by the phase separation induced by the cononsolvency, showing that virtually no EtOH is bound in respective globular-like structures. On the other hand, PIPMAm solutions heated above the LCST show a

reduction of ^{13}C T_2 values of EtOH by one order of magnitude indicating thus that a certain portion of EtOH molecules is bound in mesoglobules induced by the temperature.

(c) Introduction of negative charges into PIPMAm chains by copolymerization with MNa leads to strengthening of the polymer–solvent interactions. In the case of phase separation induced by the cononsolvency, the phase separation in the solution is prevented by the presence of the charge in the polymer chains. In the case of the temperature-induced phase separation the charge strongly suppresses the phase separation but is still detectable. In the case of the cononsolvency-induced phase separation the formed mesoglobules are more loose so the same amount of charge can prevent the phase separation totally.

P(IPMAm-*co*-AAm) Copolymers in D_2O, D_2O/EtOH and D_2O/acetone

1. The increasing fraction of hydrophilic AAm units in the copolymer significantly shifts the transition towards higher temperatures, broadens the transition interval and reduces the maximum value of the phase-separated fraction $p_{\max}$ of IPMAm units with a reduced mobility.

2. Increasing content of acetone or EtOH in mixed solvents with D_2O have an effect on the phase transition similar to that of an increasing fraction of AAm units in the copolymer.

3. AAm units extensively interact with solvent molecules, i.e. they are hydrated in D_2O even in the phase separated state. This fact results in dynamic heterogeneity of copolymer chains in mesoglobules where AAm sequences and surrounding short IPMAm sequences are hydrated and mobile, while the sufficiently long IPMAm sequences are dehydrated and their mobility is strongly reduced.

   (a) Integrated intensities revealed that the phase-separated fraction of the AAm units $p_{\mathrm{AAm}} \simeq 0$. In contrast to the IPMAm units, virtually all hydrophilic AAm units are directly detected in high-resolution NMR spectra of these systems even at temperatures above the phase transition.

4. A portion of HDO molecules is bound in mesoglobules as was revealed from temperature dependences of the spin–lattice relaxation time T_1 and

spin–spin relaxation time T_2 of HDO molecules in D_2O solutions of PIPMAm homopolymer and 95/5 and 85/15 P(IPMAm-*co*-AAm) copolymers.

5. P(IPMAm-*co*-AAm) copolymer mesoglobules are rather porous and disordered.

   (a) Relaxation experiments showed that the amount of bound HDO is probably larger in mesoglobules formed by copolymer chains than in mesoglobules formed by PIPMAm homopolymer.

PIPMAm/PVCL/D_2O mixtures

1. Both phase transitions corresponding to polymers present in the mixture were detected.

2. LCST of PVCL shifts to lower temperatures with increasing polymer concentration in the solution.

3. LCST of PVCL shifts to lower temperatures with increasing PVCL content in the PIPMAm/PVCL/D_2O mixture.

4. In terms of LCST of PIPMAm, no overall tendencies can be drawn from the comparison of temperature dependences of phase-separated fraction p for samples that differ in concentration and have the same PIPMAm/PVCL molar ratio as well as from those with fixed concentration and different PIPMAm/PVCL molar ratios.

5. Sedimentation of the phase-separated PVCL in the order of hours was observed. We shortened our experiments so that the results were not significantly affected by the sedimentation. The fact that only the already phase-separated part of PVCL units sediments is supported by these results:

   (a) Analysis of the non-sedimented part of the solution through the integrated intensities of the corresponding signals in high-resolution NMR spectra was done, integrated intensities of the PIPMAm signals in the solution at room temperature (no phase separation) and in the solution that underwent phase separation of PVCL and was cooled back to room temperature (sedimented PVCL did not dissolve again) were the same while those intensities corresponding to the PVCL signals were 50% lower.

(b) Integrated intensities of polymer signals at temperatures above the LCST of PVCL remained constant over 13 hours indicating thus that only the already phase-separated PVCL is sedimenting.

(c) Values of spin–spin relaxation times T_2 of HDO molecules at temperatures under the LCST of PVCL remained constant over 20 hours, so the non-phase-separated PVCL is colloidally stable.

6. T_2 spin–spin relaxation times of HDO molecules revealed that after the PVCL phase separation, part of solvent molecules stays bound to mesoglobules. After PIPMAm phase separation, which occurs at higher temperature,[1] no further shortening of T_2 values was observed.

[1] During the measurements of temperature dependences, the temperature is gradually increased.

Bibliography

[1] Abragam, A., The Principles of Nuclear Magnetism, Oxford University Press, London, 1961.

[2] Ageno, M., Indovina, P. L., Proceedings of the National Academy of Sciences USA, 57(5):1158–1163, 1967.

[3] Alenichev, I., Sedláková, Z., Ilavský, M., Polymer Bulletin, 58(3):191–199, 2007.

[4] Aseyev, V. O., Tenhu, H., Winnik, F. M., Advances in Polymer Science, 196:1–85, 2006.

[5] Aseyev, V., Hietala, S., Laukkanen, A., Nuopponen, M., Confortini, O., Du Prez, F. E., Tenhu, H., Polymer, 46(18):7118–7131, 2005.

[6] Atkins, P., De Paula, J., Atkins' Physical Chemistry, 8$^{\text{th}}$ Edition, Oxford University Press, Oxford, 2006.

[7] Becker, E. D., High resolution NMR: theory and chemical applications, 3$^{\text{rd}}$ Edition, Academic Press, San Diego, CA, U.S.A., 2000.

[8] Bertrand, G. L., Millero, F. J., Wu, C., Hepler, L. G., The Journal of Physical Chemistry, 70(3):699–705, 1966.

[9] Brüllová, J., Studium teplotně indukované fázová separace v kopolymerních roztocích, Master thesis, Prague, 2009.

[10] Chen, J.-H., Chen, H.-H., Chang, Y.-X., Chuang, P.-Y., Hong, P.-D., Journal of Applied Polymer Science, 107(4):2732–2742, 2008.

[11] Coccia, A., Indovina, P. L., Podo, F., Viti, V., Chemical Physics, 7(1):30–40, 1975.

[12] Costa, R. O. R., Freitas, R. F. S., Polymer, 43(22):5879–5885, 2002.

[13] Crespy, D., Golosova, A., Makhaeva, E., Khokhlov, A., Fortunato, G., Rossi, R., Polymer International, 58(11):1326–1334, 2009.

[14] Davydov, A. S., Kvantová mechanika, SPN, Prague, 1978.

[15] De Gennes, P. G., Scaling Concepts in Polymer Physics, Cornell University Press, Ithaca, NY, 1979.

[16] Djokpé, E., Vogt, W., Macromolecular Chemistry and Physics, 202(5):750–757, 2001.

[17] Dušek, K., Prins, W, Advances in Polymer Science, 6:1–102, 1969.

[18] Dušek, K., Patterson, D., Journal of Polymer Science Part A-2: Polymer Physics, 6(7):1209–1216, 1968.

[19] Eisele, M., Burchard, W., Die Makromolekulare Chemie, 191(1):169–184, 1990.

[20] Fang, L., Brown, W., Koňák, Č., Polymer, 31(10):1960–1967, 1990.

[21] Flory, P., Principles of Polymer Chemistry, Cornell University Press, Ithaca, NY, 1953.

[22] Freeman, P. I., Rowlinson J. S., Lower Critical Points in Polymer Solutions, Polymer, 1(1):20–26, 1960.

[23] Fujishige, S., Kubota, K., Ando, I., The Journal of Physical Chemistry, 93(8):3311–3313, 1989.

[24] Grosberg, A. Yu., Khokhlov, A. R., Giant Molecules: Here, There and Everywhere..., Academic Press, San Diego, CA, 1997.

[25] Guettari, M., Gomati, R., Gharbi, A., Journal of Macromolecular Science, Part B: Physics, 49(3):552–562, 2010.

[26] Gunther, H., NMR spectroscopy. Basic principles,concepts and applications in chemistry. Second edition, John Wiley & Sons Ltd, Chichester, 1995.

[27] Hanyková, L., Labuta, J., Spěváček, Polymer, 47(17):6107–16, 2006.

[28] Hanyková, L., Spěváček, J., Ilavský, M., Polymer, 42(21):8607–12, 2001.

[29] Heskins, M., Guillet, J. E., Journal of Macromolecular Science, Part A: Pure and Applied Chemistry, 2(8):1441–1455, 1968.

[30] Hirotsu, S., Okajima, T., Yamamoto, T., Macromolecules, 28(3):775–777, 1995.

[31] Hore, P. J.: Nuclear Magnetic Resonance, Oxford University Press, Oxford, 1995.

[32] Khokhlov, A. R., Polymer, 21(4):376–380, 1980.

[33] Kirsh, Yu. E., Yanul, N. A., Kalninsh, K. K., European Polymer Journal, 35(2):305–316, 1999.

[34] Kirsh, Y. E., Water soluble poly-N-vinylamides: synthesis and physicochemical properties, John Wiley and Sons, Chichester, 1998.

[35] Klíma, J., Velický, B.: Kvantová mechanika I, scriptum, Charles University, Prague, 1992.

[36] Kouřilová, H., Spěváček, J., Hanyková, L.: ^{1}H NMR Study of Temperature-Induced Phase Transitions in Aqueous Solutions of poly(N-isopropylmethacrylamide)/poly(N-vinylcaprolactam) Mixtures – to be published

[37] Kouřilová, H., Šťastná, J., Hanyková, L., Sedláková, Z., Spěváček, J., European Polymer Journal, 46(6):1299–1306, 2010.

[38] Kouřilová, H., Hanyková, L., Spěváček, J., European Polymer Journal, 45(10), 2935–2941, 2009.

[39] Kouřilová, H., Hanyková, L., WDS'07 Proceedings of Contributed Papers, Part III, 160–111, 2007.

[40] Kubota, K., Hamano, K., Kuwahara, N., Fujishige, S., Ando, I., Polymer Journal, 22(12):1051–1057, 1990.

[41] Kuenen, J. P., Robson, W. G., Philosophical Magazine, 48(5):180–203, 1899.

[42] Lau, A. C. W., Wu, C., Macromolecules, 32(3):581–584, 1999.

[43] Laukkanen, A., Valtola, L., Winnik, F. M., Tenhu, H., Polymer, 46(18):7055–7065, 2005.

[44] Laukkanen, A., Valtola, L., Winnik, F. M., Tenhu, H., Macromolecules, 37(6):2268–2274, 2004.

[45] Lebedev, V., Török, G., Cser, L., Treimer, W., Orlova, D., Sibilev, A., Journal of Applied Crystallography, 36:967–969, 2003.

[46] Lebedev, V. T., Török, Gy., Cser, L., Kali, Gy., Kirsh, Yu. E., Sibilev, A. I., Orlova, D. N., Physica B, 297(1–4):50-54, 2001.

[47] Levitt, M. H., Spin Dynamics. Basics of Nuclear Magnetic Resonance, John Wiley & Sons Ltd, The Atrium, Southern Gate, Chichester, 2001.

[48] Lifshitz, I. M., Grosberg, A. Yu., Khokhlov, A. R., Reviews of Modern Physics, 50(3):683–713, 1978.

[49] Maeda, Y., Nakamura, T., Ikeda, I., Macromolecules, 35(1):217–222, 2002.

[50] Maeda, Y., Nakamura, T., Ikeda, I., Macromolecules, 34(23):8246–8251, 2001.

[51] Maeda, Y., Nakamura, T., Ikeda, I., Macromolecules, 34(5):1391–1399, 2001.

[52] Mao, S.-Z., Zhang, X.-D., Dereppe, J.-M., Du, Y.-R., Colloid and Polymer Science, 278(3):264–269, 2000.

[53] Makhaeva, E. E., Tenhu, H., Khokhlov, A. R., Macromolecules, 35(5):1870–1876, 2002.

[54] Makhaeva, E. E., Tenhu, H., Khokhlov, A. R., Polymer, 41(26):9139–9145, 2000.

[55] Makhaeva, E. E., Tenhu, H., Khokhlov, A. R., Macromolecules, 31(18):6112–6118, 1998.

[56] Makhaeva, E. E., Thanh, Le Thi Minh, Starodoubtsev, S. G., Khokhlov, A. R., Macromolecular Chemistry and Physics, 197(6):1973–1982, 1996.

[57] Markin, G. V., Malyshkina, I. A., Gavrilova, N. D., Makhaeva, E. E., Grigor'ev, T. E., Moscow University Physics Bulletin, 63(6):410–415, 2008.

[58] McQuarrie, D. A., Simon, J. D., Physical Chemistry. A Molecular Approach, University Science Books, Sausalito, CA, 1997.

[59] Meeussen, F., Nies, E., Berghmans, H., Verbrugghe, S., Goethals, E., Du Prez, F., Polymer, 41(24):8597–8602, 2000.

[60] Meiboom, S., Gill, D., Review of Scientific Instruments, 29(8):688–691, 1958.

[61] Mikheeva, L. M., Grinberg, N. V., Mashkevich, A. Y., Grinberg, V. Y., Thanh, L. T., Makhaeva, E. E., Khokhlov, A. R., Macromolecules, 30(9):2693–2699, 1997.

[62] Mizuno, K., Miyashita, Y., Shindo, Y., Ogawa, H., The Journal of Physical Chemistry, 99(10):3225–3228, 1995.

[63] Moore, W. J., Fyzikální chemie, Nakladatelství technické literatury, Prague, 1981. Original: Physical Chemistry, Prentice-Hall, Inc.

[64] Mukae, K., Sakurai, M., Sawamura, S., Makino, K., Kim, S. W., Ueda, I., Shirahama, K., The Journal of Physical Chemistry, 97(3):737–741, 1993.

[65] Netopilík, M., Bohdanecký, M., Chytrý, V., Ulbrich, K., Macromolecular Rapid Communications, 18(2):107–11, 1997.

[66] Nishi, N., Koga, K., Ohshima, C., Yamamoto, K., Nagashima, U., Nagami, K., Journal of American Chemical Society, 110(16):5246–5255, 1988.

[67] Nose, A., Hamasaki, T., Hojo, M., Kato, R., Uehara, K., Ueda, T., Journal of Agricultural and Food Chemistry, 53(18):7074–7081, 2005.

[68] Nose, A., Hojo, M., Ueda, T., The Journal of Physical Chemistry Part B, 108(2):798–804, 2004.

[69] Prosser et al., Experimentalní metody biofyziky, Academia, Prague, 1989.

[70] Ptitsyn, O. B., Kron, A. K., Eizner, Y. Y., Journal of Polymer Science Part C: Polymer Letters, (16):3509–&, 1968.

[71] Ohta, H., Ando, I., Fujishige, S., Kubota, K., Journal of Polymer Science Part B: Polymer Physics, 29(8):963–968, 1991.

[72] Okada, Y., Tanaka, F., Macromolecules, 38(10):4465–4471, 2005.

[73] Sánchez, M. S., Hanyková, L., Ilavský, M., Polymer, 45(12):4087–4094, 2004.

[74] Schild, H. G., Progress in Polymer Science, 17(2):163–249, 1992.

[75] Schild, H. G., Muthukumar, M., Tirrell, D. A., Macromolecules, 24(4):948–952, 1991.

[76] Shushakov, O. V., Geophysics, 61(4):998–1006, 1996.

[77] Solomon, O. F., Corciovei, M., Ciută, I., Boghină, C., Journal of Applied Polymer Science, 12(8):1835–1842, 1968.

[78] Spěváček, J., Current Opinion in Colloid & Interface Science, 14(3):184–191, 2009.

[79] Spěváček, J., Starovoytova, L., Hanyková, L., Kouřilová, H., Macromolecular Symposia, 273:17–24, 2008.

[80] Spěváček, J., Macromolecular Symposia, 222:1–13, 2005.

[81] Spěváček, J., Hanyková, L., Macromolecules, 38(22): 9187-9191, 2005.

[82] Spěváček, J., Hanyková, L., Starovoytova, L., Macromolecules, 37(20):7710-7718, 2004.

[83] Spěváček, J., Hanyková, L., Macromolecular Symposia, 203:229–237, 2003.

[84] Spěváček, J., Hanyková, L., Ilavský, M., Macromolecular Symposia, 166:231-236, 2001.

[85] Spěváček, J., Hanyková, L., Ilavský, M., Macromolecular Chemistry and Physics, 202(7):1122-1129, 2001.

[86] Spěváček, J., Geschke, D., Ilavský, M., Polymer, 42(2):463–8, 2001.

[87] Spěváček, J., Schneider, B., Czechoslovak Journal of Physics, Section B, 24(6):593-604, 1974.

[88] Starovoytova, L., Spěváček, J., Trchová, M., European Polymer Journal, 43(12):5001–5009, 2007.

[89] Starovoytova, L., Spěváček, Polymer, 47(21):7329–7334, 2006.

[90] Starovoytova, L., Spěváček, J., Ilavský, M., Polymer 46(3):677–683, 2005.

[91] Starovoytova, L., Spěváček, J., Hanyková, L., Ilavský, M., Polymer, 45(17):5905–5911, 2004.

[92] Starovoytova, L., Spěváček, J., Hanyková, L., Ilavský, M., Macromolecular Symposia, 203:239–246, 2003.

[93] Stejskal, J., Gordon, M., Torkington, J. A., Polymer Bulletin, 3(11):621–625, 1980.

[94] Tager, A. A., Safronov, A. P., Sharina, S. V., Galayev, I Yu., Polymer Science U.S.S.R., 32(3):469–474, 1990.

[95] Tanaka, T., Polymer, 20(11):1404–1412, 1979.

[96] Tanaka, F., Koga T, Kojima, H., Winnik, F. M., Chinese Journal of Polymer Science, 29(1):13–21, 2011.

[97] Tanaka, F., Koga, T., Winnik, F. M., Physical Review Letters, 101(2):,028302, 2008.

[98] Tang, Y., Liu, X., Polymer, 51(4):897-901, 2010.

[99] Tang, Y., Ding, Y., Zhang, G., The Journal of Physical Chemistry B, 112(29):8447–8451, 2008.

[100] Tiktopulo, E. I., Uversky, V. N., Lushchik, V. B., Klenin, S. I., Bychkova, V. E., Ptitsyn, O. B., Macromolecules, 28(22):7519–7524, 1995.

[101] Timoshenko, E. G., Kuznetsov, Yu. A., Europhysics Letters, 53(3):322–327, 2001.

[102] Van Durme, K., Verbrugghe, S., Du Prez, F. E., Van Mele, B., Macromolecules, 37(3):1054–1061, 2004.

[103] Vihola, H., Laukkanen, A., Valtola, L., Tenhu, H., Hirvonen, J., Biomaterials, 26(16):3055–3064, 2005.

[104] Wang, X., Qiu, X., Wu, C., Macromolecules, 31(9):2972–2976, 1998.

[105] Winnik, F. M., Ottaviani, M. F., Bossmann, S. H., Garcia-Garibay, M., Turro, N. J., Macromolecules, 25(22):6007–6017, 1992.

[106] Winnik, F. M., Ringsdorf, H., Wenzmer, J., Macromolecules, 23(8):2415–2416, 1990.

[107] Wu, S., Shanks, R. A., Journal of Applied Polymer Science, 93(3):1493–1499, 2004.

[108] Wu, S., Shanks, R. A., Journal of Applied Polymer Science, 89(11):3122–3129, 2003.

[109] Yanul, N., Kirsh, Y., Verbrugghe, S., Goethals, E., Du Prez, F. E., Macromolecular Chemistry and Physics, 202(9):1700–1709, 2001.

[110] Yoshioka, H., Mori, Y., Cushman, J. A., Polymers for Advanced Technologies, 5(2):122–127, 1994.

List of Tables

List of Figures

List of Abbreviations

AAm acrylamide

CH_3OH methanol

CPMG Carr-Purcell-Meiboom-Gill (pulse sequence)

CW Continuous Wave

D_2O heavy water

DLS Dynamic Light Scattering

DSC Differential Scanning Spectroscopy

DSS Sodium 3-(Trimethylsilyl)-1-propanesulfonic acid, sodium salt, 97%

e.g. exempli gratia

EPR Electron Paramagnetic Resonance

Eq. Equation

et al. et alia

etc. et cetera

EtOH ethanol

FID Free Induction Decay

Fig. Figure

FT Fourier Transform

FTIR Fourier transform infrared (spectroscopy)

GPC Gel Permeation Chromatography

H_2O light water

HDO semi-heavy water

HMQC Heteronuclear Correlation through Multiple Quantum Coherence

i.e. id est

INEPT Insensitive Nuclei Enhanced by Polarization Transfer

IPAAm *N*-isopropylacrylamide

IPMAm *N*-isopropylmethacrylamide

LCST Lower Critical Solution Temperature

MNa sodium methacrylate

NMR Nuclear Magnetic Resonance

PAAM polyacrylamide

PDEAAm poly(*N*,*N*-diethylacrylamide)

PEO poly(ethylene oxide)

PFT Pulse Fourier Transform

PIPAAm poly(*N*-isopropylacrylamide)

PIPMAm poly(*N*-isopropylmethacrylamide)

P(IPMAm-co-AAm) poly(*N*-isopropylmethacrylamide)-*co*-acrylamide

P(IPMAm-co-MNa) poly-*N*-isopropylmethacrylamide-*co*-sodium methacrylate

PPC Pressure Perturbation Calorimetry

PVCL poly(*N*-vinylcaprolactam)

PVME poly(vinyl methyl ether)

PVP poly-*N*-vinylpyrrolidone

Tab. Table

UCST Upper Critical Solution Temperature

VCL vinylcaprolactam

vs. versus

List of Articles

Articles Related to this Thesis:

6. H. Kouřilová, J. Spěváček, L. Hanyková: ^{1}H NMR Study of Temperature-Induced Phase Transitions in Aqueous Solutions of poly(*N*-isopropylmethacrylamide)/poly(*N*-vinylcaprolactam) Mixtures
   – in preparation

5. H. Kouřilová, J. Šťastná, L. Hanyková, Z. Sedláková, J. Spěváček: ^{1}H NMR Study of Temperature-Induced Phase Separation in Solutions of poly(*N*-isopropylmethacrylamide-*co*-acrylamide) Copolymers, *European Polymer Journal*, 46(6):1299–1306, 2010.

4. H. Kouřilová, L. Hanyková, J. Spěváček: NMR Study of Phase Separation in D_2O/Ethanol Solutions of poly(*N*-isopropylmethacrylamide) Induced by Solvent Composition and Temperature; *European Polymer Journal*, 45(10):2935–2941, 2009.

3. J. Spěváček, L. Starovoytova, H. Kouřilová: Polymer-Solvent Interactions in Solutions of Thermoresponsive Polymers Studied by NMR and IR Spectroscopy, *Macromolecular Symposia*, 273:17–24, 2008.

2. H. Kouřilová, L. Hanyková: Phase Separation in Water-Ethanol Polymer Solutions Studied by NMR Methods, *WDS '07 Proceedings of Contributed Papers*, Part III, 106–111, 2007.

Other Articles:

1. P. Heřman, H. Drápalová (Kouřilová), R. Mužíková, J. Večeř: Electroporative Adjustment of pH in Living Yeast Cells: Ratiometric Fluorescence pH Imaging, *Journal of Fluorescence*, 15(5):763–768, 2005.

List of Presentations

Contributed talks:

- Ampère NMR School, Poznań/Wierzba, Poland, June 2010

  H. Kouřilová: NMR Study of Phase Separation in Solutions of Linear Polymers

- 25$^{\text{th}}$ NMR Valtice, Valtice, Czech Republic, April 2010

  H. Kouřilová, L. Hanyková, J. Spěváček: Phase Separation in Aqueous Solutions of poly(*N*-isopropylmethacrylamide)/poly(*N*-vinylcaprolactam) Mixtures

- 22$^{\text{th}}$ NMR Valtice, Valtice, Czech Republic, April 2007

  H. Kouřilová, L. Hanyková: Phase Transition in Water-Ethanol Polymer Solutions Studied by NMR Methods. Cononsolvency Effect.

- 15$^{\text{th}}$ Annual Student Conference Week of Doctoral Students, Faculty of Mathematics and Physics, Charles University in Prague, Prague, Czech Republic, June 2006

  H. Kouřilová: NMR Study of the Phase Separation in Polymer Solutions

Posters:

- Magnetic Moments in Central Europe, Tatranská Lomnica, Slovakia, March 2011

  H. Kouřilová, J. Šťastná, L. Hanyková, J. Spěváček: NMR Study of Phase Separation in Multi-Component Linear Polymer Solutions

- Euromar, Tarragona, Spain, July 2007

  H. Kouřilová, L. Hanyková: NMR Study of Phase Transition in Water-Ethanol Polymer Solutions and Cononsolvency Effect

- 16^{th} Annual Student Conference Week of Doctoral Students, Faculty of Mathematics and Physics, Charles University in Prague, Prague, Czech Republic, June 2007

  H. Kouřilová: Phase Separation in Water-Ethanol Polymer Solutions Studied by NMR Methods

Typeset by LaTeX